Studies for maximizing value of antibody drugs against tumors

Yoriko Yamashita-Kashima

Contents

General Introduction

Although the total number of cancer patients is the fifth largest in major disease, cancer is the first leading cause of death in Japan. Therefore, conquering cancer is a critical issue for modern medicine. Treatment of cancer usually involves surgery, radiation therapy, and chemotherapy. Chemotherapy is widely used in cancer therapy including adjuvant therapy, neoadjuvant therapy, and therapy for unresectable cancer. Generally, chemotherapeutic agents are carried throughout the body by the bloodstream, thereby eliciting a more systemic action, while surgical excision and radiation are regional actions. Chemotherapeutic agents are expected to be effective against blood cancer and other metastatic cancers; however, these agents can induce cytotoxicity in all cells, including normal cells. Therefore, they often produce severe side effects.

To enhance the specificity of anti-cancer drugs for cancer cells and to reduce their side effects, numerous molecular-targeted agents have been developed. Most molecular-targeted agents which are launched nowadays are small molecules and antibodies. One advantage of small molecules is that they have high stability *in vivo* and are relatively inexpensive. On the other hand, antibodies are superior to small molecules in terms of specificity. Antibody drugs against proteins that are genetically amplified or overexpressed in tumors have been developed. Especially, antibodies against epidermal growth factor receptor (EGFR), human epidermal growth factor 2 (HER2), and vascular endothelial growth factor (VEGF) have been well studied and have been launched as antibody drugs against solid tumors.

EGFR and HER2 are classified as HER family proteins. This family of receptor tyrosine kinases is composed of EGFR (HER1/ErbB1), HER2/neu (ErbB2), HER3 (ErbB3), and HER4 (ErbB4). Signal transduction via activation of these receptors regulates cell proliferation, angiogenesis, invasion, and metastasis. Aberrant expression or activity of EGFR and HER2 has been identified as an etiological factor in many human epithelial cancers, including head and neck squamous cell carcinoma (HNSCC), non-small cell lung cancer (NSCLC), colorectal cancer (CRC), and breast cancer (1).

Trastuzumab is one of the representative antibodies against the HER family of receptor tyrosine kinases. Trastuzumab is a humanized anti-HER2 monoclonal antibody that has been suggested to exert antitumor activity by

inhibiting ligand-independent HER2 signaling; enhancing antibody-dependent cellular cytotoxicity (ADCC) activity (2, 3); blocking the formation of p95HER2, a constitutively active form of HER2 (4); and suppressing tumor angiogenesis (5). Trastuzumab has demonstrated survival benefit in the treatment of HER2-overexpressing metastatic breast cancer and in the adjuvant therapy of HER2-overexpressing breast cancer (6-8). For gastric cancer, Fujimoto-Ouchi *et al.* previously showed that trastuzumab significantly inhibited tumor growth in HER2-overexpressing human gastric cancer mouse xenograft models (9), and the ToGA trial (a phase III study of trastuzumab in HER2-positive advanced and inoperable gastric cancer) showed a survival benefit when trastuzumab was added to chemotherapy in HER2-overexpressing gastric cancer patients (10)

VEGF, also referred to as VEGF-A, is known to be an essential regulator of normal and abnormal blood vessel growth. The VEGF family comprises seven secreted glycoproteins, VEGF-A, VEGF-B, VEGF-C, VEGF-D, VEGF-E, placental growth factor (PlGF), and VEGF-F (11-13). VEGF-A was first identified as a vascular permeability factor secreted by tumor cells (14). The gene encoding human VEGF-A is composed of eight exons and is differentially spliced to generate four major isoforms (VEGF121, VEGF165, VEGF189 and VEGF206) (15). VEGF165 has been reported as the predominant isoform (16, 17). VEGF-A is the most potent angiogenic factor described to date and is an important regulator of physiological angiogenesis. It induces proliferation, sprouting and tube formation of endothelial cells through interaction with VEGF receptor-1 (VEGFR-1/Flt-1) and VEGF receptor-2 (VEGFR-2/Flk-1) (11). Many solid tumors are dependent on the supply of oxygen and nourishment from tumor angiogenesis for their growth. VEGF is an important factor in tumor angiogenesis (18). Many tumors, including lung (19), breast (20), gastrointestinal tract (21), renal (22) and ovarian carcinomas (23), express VEGF. VEGF promotes increased vascular permeability in addition to angiogenesis.

Bevacizumab is a humanized anti-VEGF monoclonal antibody. Bevacizumab binds to and neutralizes all human VEGF-A isoforms and bioactive proteolytic fragments (24). Bevacizumab is thought to exert anti-tumor activity by two main mechanisms. One is by an anti-angiogenic activity. Bevacizumab inhibits the proliferation and migration of vascular endothelial cells by inhibiting VEGF, leading to anti-tumor activity. The other mechanism is through normalization of tumor vessels by promoting apoptosis of endothelial cells. Tumor vessel normalization suppresses increased vascular permeability and decreases interstitial fluid pressure, resulting in an increase in the

uptake of chemotherapeutic agents into the tumor when they are combined with bevacizumab (25, 26). Bevacizumab has been used worldwide in combination with standard chemotherapies for patients with colorectal cancer, non-small cell lung cancer, breast cancer, ovarian cancer, and malignant glioma.

Cancer treatment has been greatly improved with the advent of molecular-targeted agents, including antibody drugs such as anti-HER2 or anti-VEGF antibodies. However, cancer still often metastasizes and reoccurs. Additionally, cancer commonly shows drug resistance. Therefore, more innovative approaches to cancer treatment, including new treatment methods or personalized healthcare, should be developed. In the present study, the author has investigated: I) the treatment after disease progression during trastuzumab therapy; II) new anti-HER2 treatments for gastric cancer; III) formalin fixing conditions for HER2 testing, which determine whether trastuzumab will be a beneficial option for patients; and IV) a predictive marker for bevacizumab.

References

1. Kruser TJ, Wheeler DL. Mechanisms of resistance to HER family targeting antibodies. Experimental cell research. 2010;316:1083-100.

2. Barok M, Isola J, Palyi-Krekk Z, Nagy P, Juhasz I, Vereb G, et al. Trastuzumab causes antibody-dependent cellular cytotoxicity-mediated growth inhibition of submacroscopic JIMT-1 breast cancer xenografts despite intrinsic drug resistance. Mol Cancer Ther. 2007;6:2065-72.

3. Musolino A, Naldi N, Bortesi B, Pezzuolo D, Capelletti M, Missale G, et al. Immunoglobulin G fragment C receptor polymorphisms and clinical efficacy of trastuzumab-based therapy in patients with HER-2/neu-positive metastatic breast cancer. J Clin Oncol. 2008;26:1789-96.

4. Molina MA, Codony-Servat J, Albanell J, Rojo F, Arribas J, Baselga J. Trastuzumab (herceptin), a humanized anti-Her2 receptor monoclonal antibody, inhibits basal and activated Her2 ectodomain cleavage in breast cancer cells. Cancer Res. 2001;61:4744-9.

5. Izumi Y, Xu L, di Tomaso E, Fukumura D, Jain RK. Tumour biology: herceptin acts as an anti-angiogenic cocktail. Nature. 2002;416:279-80.

6. Buzdar AU, Valero V, Ibrahim NK, Francis D, Broglio KR, Theriault RL, et al. Neoadjuvant therapy with paclitaxel followed by 5-fluorouracil, epirubicin, and cyclophosphamide chemotherapy and concurrent trastuzumab in human epidermal growth factor receptor 2-positive operable breast cancer: an update of the initial randomized study population and data of additional patients treated with the same regimen. Clin Cancer Res. 2007;13:228-33.

7. Romond EH, Perez EA, Bryant J, Suman VJ, Geyer CE, Jr., Davidson NE, et al. Trastuzumab plus adjuvant chemotherapy for operable HER2-positive breast cancer. N Engl J Med. 2005;353:1673-84.

8. Smith I, Procter M, Gelber RD, Guillaume S, Feyereislova A, Dowsett M, et al. 2-year follow-up of trastuzumab after adjuvant chemotherapy in HER2-positive breast cancer: a randomised controlled trial. Lancet. 2007;369:29-36.

9. Fujimoto-Ouchi K, Sekiguchi F, Yasuno H, Moriya Y, Mori K, Tanaka Y. Antitumor activity of trastuzumab in combination with chemotherapy in human gastric cancer xenograft models. Cancer chemotherapy

and pharmacology. 2007;59:795-805.

10. Bang YJ, Van Cutsem E, Feyereislova A, Chung HC, Shen L, Sawaki A, et al. Trastuzumab in combination with chemotherapy versus chemotherapy alone for treatment of HER2-positive advanced gastric or gastro-oesophageal junction cancer (ToGA): a phase 3, open-label, randomised controlled trial. Lancet. 2010;376:687-97.

11. Ferrara N, Gerber HP, LeCouter J. The biology of VEGF and its receptors. Nature medicine. 2003;9:669-76.

12. Houck KA, Ferrara N, Winer J, Cachianes G, Li B, Leung DW. The vascular endothelial growth factor family: identification of a fourth molecular species and characterization of alternative splicing of RNA. Molecular endocrinology. 1991;5:1806-14.

13. Suto K, Yamazaki Y, Morita T, Mizuno H. Crystal structures of novel vascular endothelial growth factors (VEGF) from snake venoms: insight into selective VEGF binding to kinase insert domain-containing receptor but not to fms-like tyrosine kinase-1. The Journal of biological chemistry. 2005;280:2126-31.

14. Senger DR, Galli SJ, Dvorak AM, Perruzzi CA, Harvey VS, Dvorak HF. Tumor cells secrete a vascular permeability factor that promotes accumulation of ascites fluid. Science. 1983;219:983-5.

15. Tischer E, Mitchell R, Hartman T, Silva M, Gospodarowicz D, Fiddes JC, et al. The human gene for vascular endothelial growth factor. Multiple protein forms are encoded through alternative exon splicing. The Journal of biological chemistry. 1991;266:11947-54.

16. Ruhrberg C, Gerhardt H, Golding M, Watson R, Ioannidou S, Fujisawa H, et al. Spatially restricted patterning cues provided by heparin-binding VEGF-A control blood vessel branching morphogenesis. Genes & development. 2002;16:2684-98.

17. Ferrara N. Vascular endothelial growth factor: basic science and clinical progress. Endocrine reviews. 2004;25:581-611.

18. Ferrara N. VEGF and the quest for tumour angiogenesis factors. Nature reviews Cancer. 2002;2:795-803.

19. Volm M, Koomagi R, Mattern J. Prognostic value of vascular endothelial growth factor and its receptor Flt-1 in squamous cell lung cancer. International journal of cancer Journal international du cancer. 1997;74:64-8.

20. Yoshiji H, Gomez DE, Shibuya M, Thorgeirsson UP. Expression of vascular endothelial growth factor, its receptor, and other angiogenic factors in human breast cancer. Cancer research. 1996;56:2013-6.

21. Ellis LM, Takahashi Y, Fenoglio CJ, Cleary KR, Bucana CD, Evans DB. Vessel counts and vascular endothelial growth factor expression in pancreatic adenocarcinoma. European journal of cancer. 1998;34:337-40.

22. Tomisawa M, Tokunaga T, Oshika Y, Tsuchida T, Fukushima Y, Sato H, et al. Expression pattern of vascular endothelial growth factor isoform is closely correlated with tumour stage and vascularisation in renal cell carcinoma. European journal of cancer. 1999;35:133-7.

23. Sowter HM, Corps AN, Evans AL, Clark DE, Charnock-Jones DS, Smith SK. Expression and localization of the vascular endothelial growth factor family in ovarian epithelial tumors. Laboratory investigation; a journal of technical methods and pathology. 1997;77:607-14.

24. Ferrara N, Hillan KJ, Gerber HP, Novotny W. Discovery and development of bevacizumab, an anti-VEGF antibody for treating cancer. Nature reviews Drug discovery. 2004;3:391-400.

25. Gerber HP, Ferrara N. Pharmacology and pharmacodynamics of bevacizumab as monotherapy or in combination with cytotoxic therapy in preclinical studies. Cancer research. 2005;65:671-80.

26. Jain RK. Normalization of tumor vasculature: an emerging concept in antiangiogenic therapy. Science. 2005;307:58-62.

Chapter I: Preclinical study of prolonged administration of trastuzumab as combination therapy after disease progression during trastuzumab monotherapy

Introduction

HER2 overexpression is reportedly a factor of poor prognosis in clinical breast cancers (1), and thus treatments targeting HER2 are expected to show survival benefit. Trastuzumab (Herceptin®) is a humanized antibody specific to HER2, which is used in the first-line treatment for HER2-positive metastatic or early breast cancer. Clinical results have demonstrated that therapies combining trastuzumab with standard chemotherapies such as taxanes showed a survival benefit.

However, the tumors of many of these patients develop progressive disease (PD) during such therapies and often the treatment to which a patient has developed PD is discontinued and another treatment is prescribed. It has also been reported that the tumor tissues remain HER2-positive even after developing PD to trastuzumab therapies. This is in line with a recent finding that, in contrast to initial belief, trastuzumab does not down-regulate HER2 from the cell surface (2).

Taking into consideration that HER2 is a factor of poor prognosis, discontinuation of trastuzumab treatment is counterintuitive; and yet there is no adequate scientific rationale to continue the administration of trastuzumab. Here, the author examined whether trastuzumab treatment should be prolonged as a combination therapy after showing no antitumor activity as monotherapy in xenograft models. *In vitro* lines resistant to trastuzumab have been established and their mechanisms of resistance have been reported to be associated with diminished inhibition of pAKT, up-regulation of IGF-1R, and upregulation of PTEN (3-5). The mechanism of trastuzumab action, however, includes antibody-dependent cellular cytotoxicity (ADCC) in addition to the direct inhibition of cell proliferation (6) and it has become clear that the *in vivo* effects of other anticancer drugs in combination therapy differ from the *in vitro* effects (6, 7). To examine the mechanisms responsible for PD with trastuzumab, the author attempted to establish *in vivo* PD models that would show all the mechanisms of trastuzumab activity.

Using these HER2-positive xenograft models, the author investigated the combination therapies of trastuzumab

with taxanes or capecitabine, standard treatments for clinical breast cancer, after PD with trastuzumab as a single agent (8-11) to demonstrate the clinical relevance of treatment with trastuzumab after PD.

Materials and methods

Chemicals

Trastuzumab was provided by F. Hoffman-La Roche (Nutley, NJ) as a freeze-dried powder and reconstituted with distilled water and diluted with saline. Human immunoglobulin G (IgG) was purchased from MP Biomedicals, Inc. (Aurora, OH, USA) and was reconstituted with distilled water and diluted with saline. Docetaxel was synthesized by Kanto Chemical Co., Inc. (Tokyo, Japan) as a fine powder and was dissolved in saline containing 2.5% (v/v) polysorbate 80 (Sigma-Aldrich Inc., St. Louis, MO, USA) and 2.5% (v/v) ethanol. Paclitaxel was purchased from Wako Pure Chemical Industries, Ltd (Tokyo, Japan) and was dissolved in saline containing 5% (v/v) cremophol EL (Sigma-Aldrich) and 5% (v/v) ethanol. Capecitabine was provided by F. Hoffman-La Roche as a bulk powder and dissolved in 40 mM citrate buffer (pH 6.0) containing 5% (w/v) gum arabic. G-CSF (genetical recombinant lenograstim) produced by Chugai Pharmaceuticals Co., Ltd) was diluted with 0.01% of polysorbate 20 in PBS.

Animals

Female 5-week-old BALB/c-nu/nu mice (CAnN.Cg-Foxn1 < nu >/CrlCrlj nu/nu) were obtained from Charles River Japan (Yokohama, Japan). All animals were allowed to acclimatize and recover from shipping-related stress for 1 week prior to the study. The health of the mice was monitored by daily observation. Chlorinated water and irradiated food were provided ad libitum, and the animals were kept in a controlled light–dark cycle (12–12 h). All animal experiments were performed in accordance with the Guidelines for the Accommodation and Care of Laboratory Animals promulgated by Chugai Pharmaceutical Research Center.

Tumors

The HER2-positive human inflammatory breast cancer cell line KPL-4 (12, 13) was kindly provided by Dr. J. Kurebayashi (Kawasaki Medical School, Kurashiki, Japan). KPL-4 was maintained in Dulbecco's modified Eagle's medium (DMEM) supplemented with 10% fetal bovine serum (FBS). The HER2-positive human breast cancer cell line MDA-MB-361 was obtained from the American Type Culture Collection (Rockville, MD). An *in vivo* line of MDA-MB-361 was established in the laboratory of the author and maintained in BALB/c-nu/nu mice after subcutaneous (sc) inoculation of tumor pieces. Both cell lines were confirmed to be HER2 positive by IHC and FISH (14) diagnostic methods.

Establishment of the *in vivo* trastuzumab PD model

A piece of MDA-MB-361 tumor tissue was inoculated subcutaneously into the right flank of each mouse. A suspension of KPL-4 cells (5 x 10^6 cells/mouse) was orthotopically transplanted into the second mammary fat pad of female BALB/c-nu/nu mice. Several weeks after tumor inoculation, mice were randomly allocated to control and treatment groups after verification of tumor formation. Administration of trastuzumab began when tumor volumes had reached 0.2–0.3 cm^3 (designated as day 1). Trastuzumab was administered intraperitoneally (ip) once a week (qw) for 3 weeks. To evaluate the antitumor activity and tolerability of the test agents, tumor volume and body weight were measured twice a week. The tumor volumes (V) were estimated from the equation $V = ab^2/2$, where a and b are tumor length and width, respectively. The growth ratio of tumor volume was calculated to be the ratio of tumor volume on the evaluation day to that of the day of the previous measurement. The percentage of tumor growth inhibition (TGI%) was calculated as follows: TGI% = {1 − (tumor volume of treatment group on evaluation day − tumor volume of treatment group on day 1)/ (tumor volume of control group at evaluation day – tumor volume of control group on day 1)} × 100. For the tumor re-inoculation experiments, MDA-MB-361 tumor tissue was resected after 3 weeks of trastuzumab treatment and 2-mm square pieces of tumor tissue were then inoculated into BALB/c-nu/nu mice by the same method as the initial tumor inoculation.

Quantification of pAKT and IGF-1R in tumor tissues

Tumor tissues and blood were sampled at the start of treatment (group a), after 3 weeks of trastuzumab

treatment (group c), and at the time the tumor volume reached that of the trastuzumab-treated group (group b) to eliminate the effect of tumor volume on efficacy. The tumor tissues were pulverized in liquid nitrogen, lysed in cell extraction buffer (BioSource, Flynn, CA) for 30 min, and then homogenized with a potter homogenizer. The extracts were centrifuged at 150K×g for 10 min at 4°C. Aliquots of the clear lysates were dispensed and stored at −80°C until the pAKT and IGF-1R assays were carried out. ELISA of pAKT (BioSource) or IGF-1R (BioSource) was performed following the manufacturer's protocol.

Comprehensive analysis of gene expression in the tumor tissues

Tumor tissues were resected from xenograft models and immediately frozen in liquid nitrogen. Total RNA was extracted from the frozen tumor using Sepasol-RNA I (WAKO, Osaka, Japan) and was purified with an RNease column (Qiagen, Austin, TX). Total RNA (5 μg) was reverse transcribed to cDNA with a T7-(dT)24 primer. Biotin-labeled cRNA was first synthesized from cDNA using a MEGAscript *In Vitro* Transcript Kit (Ambion, Austin, TX), fragmented to an average size of 50–100 nucleotides by incubating at 95°C for 35 min in 40 mM Tris–acetate (pH 8.1) containing 100 mM potassium acetate and 30 mM magnesium acetate, and finally hybridized to murine Gene-Chip 430A 2.0 Array (Affymetrix, Santa Clara, CA). The hybridized cRNA probes were stained with streptavidin R-phycoerythrin Molecular Probes™ (Invitrogen, Carlsbad, CA) and then scanned with a confocal scanner (Affymetrix). The scanned data so obtained were normalized to correct for small differences in the levels of the cRNA probes and were processed for signal values using Affymetrix software (LIMS 5.0). The author examined gene expression profiles in four tumor tissues from each group (control, human IgG-treated, and trastuzumab-treated). Signal intensities obtained from the GeneChip analysis were transformed to logarithmic values. The author selected genes from the criteria of a minimum value >2 and more than two samples showing the present response in each group and a CV > 20% in all 12 samples from a data set of 54,613 arrays and then applied the values of the selected genes to Eisen's hierarchical clustering software (http://rana.stanford.edu/software).

Combination of trastuzumab with chemotherapy or G-CSF in the trastuzumab PD models

After the initial treatment with trastuzumab alone, mice were re-randomized and allocated to the control group,

the trastuzumab group, the chemotherapy group, or the combination of trastuzumab with chemotherapy group. Each group was, respectively, treated with human IgG and vehicle of chemotherapy, trastuzumab and vehicle of chemotherapy, human IgG and chemotherapy, or trastuzumab and chemotherapy. Trastuzumab was administered ip qw for 3 weeks similar to the initial treatment. Docetaxel was administered intravenously (iv) once in 3 weeks (q3w). Paclitaxel was administered iv qw. Capecitabine was administered orally (po) once a day for 14 consecutive days. The maximum tolerated dose (MTD) was defined as half of the minimum toxic dose causing death (one mouse out of six mice, LD17) or resulting in more than 20% of body weight loss in a separate experiment. G-CSF was administered sc once a day for 6 days.

Statistical analysis

The Mann–Whitney *U* test was used to detect the statistical differences in tumor volume ($P < 0.05$) for the *in vivo* experiments and Student's *t* test was used ($P < 0.05$) for the *in vitro* experiments. The statistical analysis was carried out using an SAS preclinical package (SAS Institute, Inc., Tokyo, Japan).

Results

Establishing a trastuzumab PD model

The HER2-positive breast cancer cell line MDA-MB-361 was inoculated into BALB/c-nu/nu mice, and trastuzumab (30 mg/kg) was administered ip qw. Up to 1 week after the start of administration, trastuzumab showed an inhibitory effect on tumor growth in all of the animals but, as the treatment continued, a decrease in growth inhibition appeared in individual animals (Fig. 1A). The rate of tumor growth inhibition also decreased during the administration of trastuzumab in these animals, and they were considered to have become unresponsive to trastuzumab. The frequency of this condition was 8 out of 16 mice during the period ranging from 2 to 3 weeks after the start of administration. After 3 weeks of initial administration, the trastuzumab group showed less tumor growth inhibition compared with the group that had been switched to treatment with HuIgG. When divided by the tumor volume ratio on day 22 (1.4), the ratio of resistant tumors was significantly higher than that of tumors

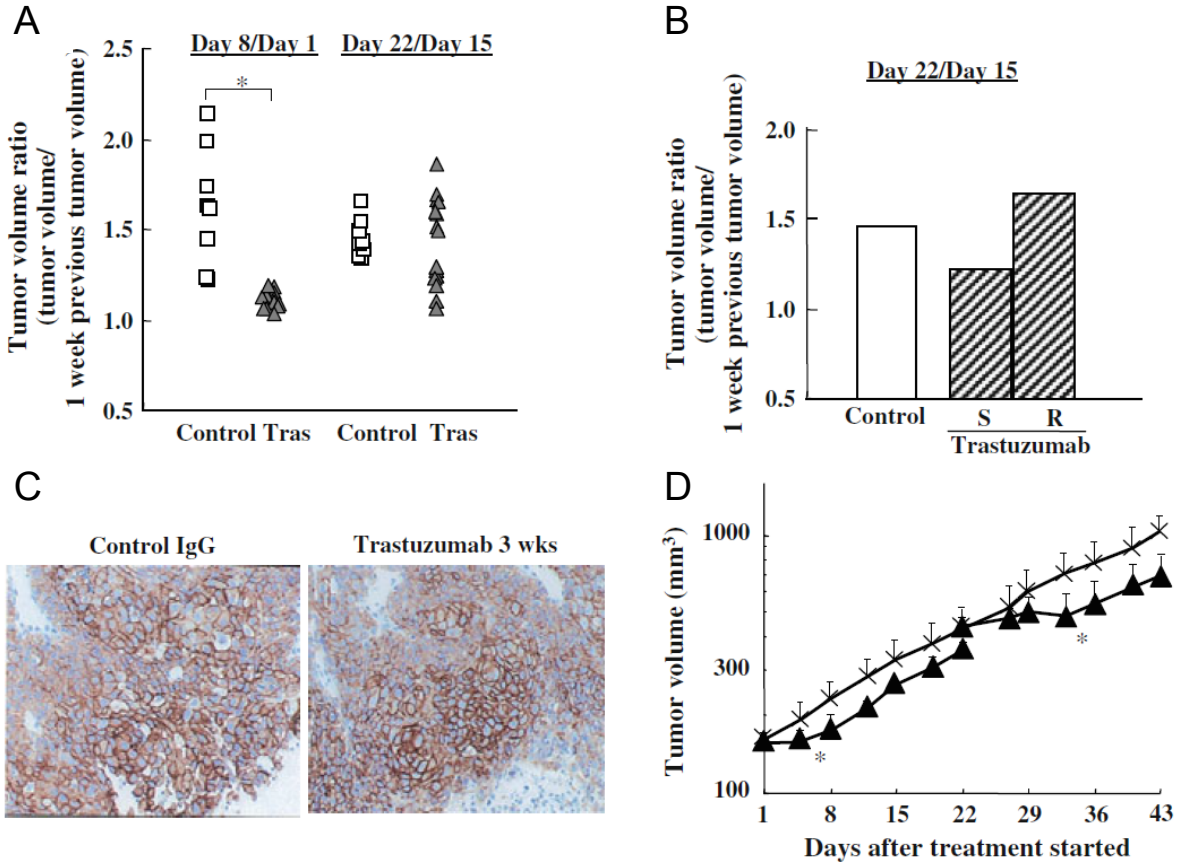

Figure 1 Establishment of the trastuzumab progressive disease model of MDA-MB-361. A, Appearance of the progressive tumor during 3 weeks of treatment with trastuzumab. Treatment with trastuzumab was started 52 days after the tumor inoculation. Mice were allocated to groups of 8 mice for control human IgG and 16 mice for trastuzumab treatment. Trastuzumab (30 mg/kg) and IgG (30 mg/kg) were administered ip qw for 3 weeks. Data points: IgG (squares), trastuzumab (triangles). Symbols represent the calculated ratio of the tumor volume versus the 1 week prior tumor volume. B, Comparison of tumor volume ratio between PD tumor and tumor sensitive to trastuzumab treatment. Mean values are shown as bars. Control IgG treatment (white bar), trastuzumab treatment (striped bar), mean of tumor with a volume ratio lower than 1.4 (S), mean of tumor with a volume ratio higher than 1.4 (R). C, Conservation of HER2 status beyond progressive disease after treatment with trastuzumab. Herceptest® (HER2 IHC) of the tumor tissues of MDA-MB-361. The method for IHC is described in the "Materials and methods". D, Comparison of the antitumor activity of trastuzumab between large and small tumor tissues. Treatment with trastuzumab against small tumors or large ones was started 47 or 69 days after the tumor inoculation. Mice were randomly allocated to groups of six mice each. Trastuzumab (30 mg/kg) and IgG (30 mg/kg) were administered ip once a week for 3 weeks. Data points: control IgG (cross marks), trastuzumab (closed triangles)

sensitive to trastuzumab (Fig. 1B). After 3 weeks of initial trastuzumab treatment, HER2 protein as determined by IHC had remained positive (Fig. 1C). In the investigation of the relationship between the size of the cancer tumor and its responsiveness to trastuzumab, the author found an inhibitory effect on tumor growth when trastuzumab was administered to a tumor having the same volume as that of a tumor that had become unresponsive at 3 weeks after initial treatment (Fig. 1D). Based on the results, the author regarded the group of individuals that had become unresponsive to trastuzumab monotherapy as trastuzumab PD models. A similar result was also observed in the

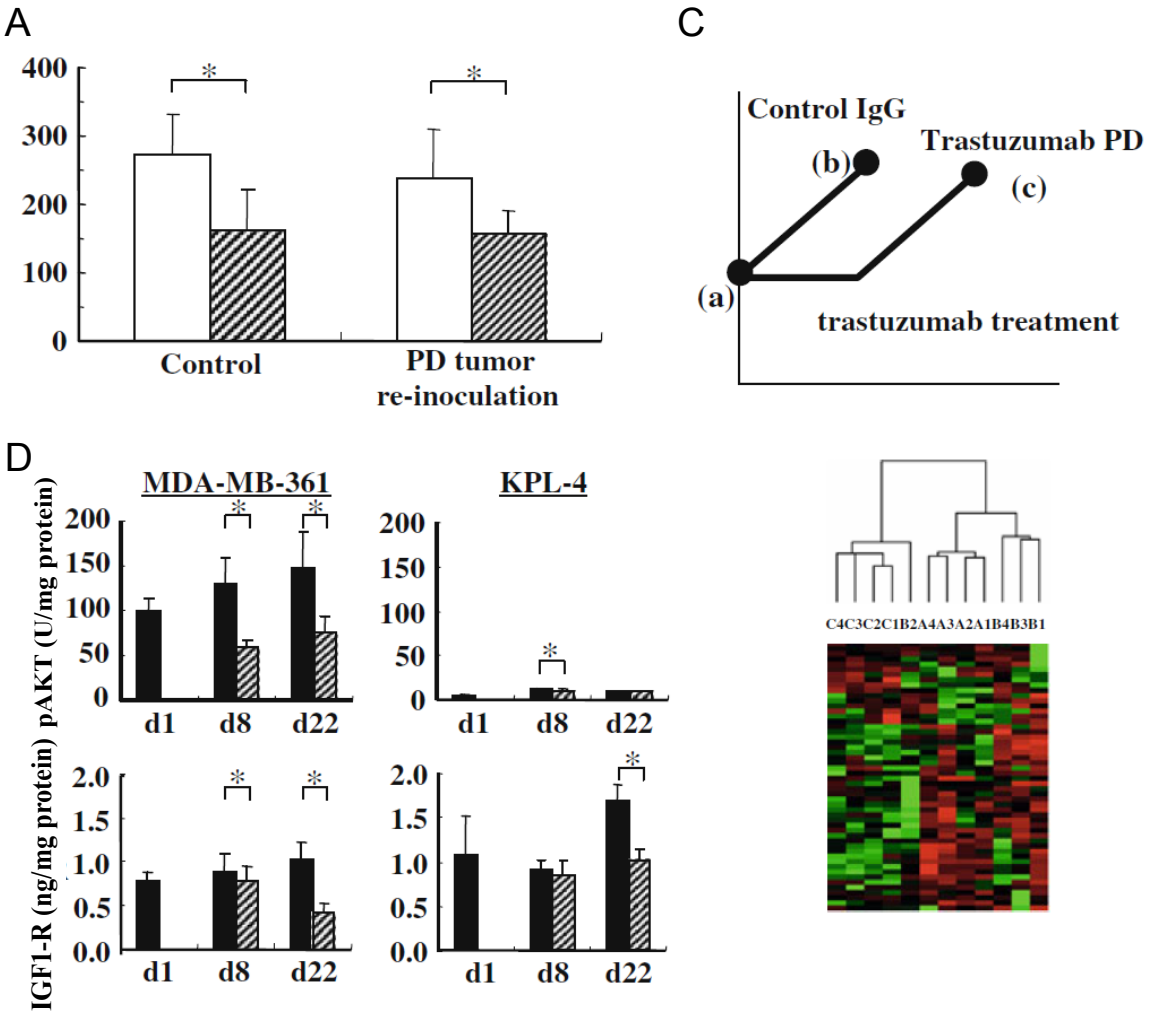

Figure 2 Changes of HER2-related growth signals in tumor tissues beyond trastuzumab progressive disease. A, Tumor volume of trastuzumab-treated mice re-inoculated with the MDA-MB-361 tumor grown under trastuzumab treatment on day 15. The original MDAMB-361 (left). Treatment with trastuzumab for original tumors or re-inoculated ones was started 53 or 59 days after the tumor inoculation. Mice were randomly allocated to groups of six mice each. Trastuzumab (30 mg/kg) and IgG (30 mg/kg) were administered ip once a week for 3 weeks. Data bars: re-inoculated MDA-MB-361 (left). Control (white), and trastuzumab (diagonal). B, Levels of pAKT and IGF1-R in the tumor tissues (n = 6), control group (white), and trastuzumab group (30 mg/kg/shot) (diagonal). C.,Comparison of the gene proWles between progressive disease tumors and control tumors. Mice were randomly allocated to groups of four mice: before treatment (a), control IgG (b), and trastuzumab treated (c). Trastuzumab or IgG were administered ip once a week for 3 weeks or 1 week. Tumor samples were collected on the 1st day (a), 8 days after (b), or 22 days after treatment (c).

KPL-4 model.

Changes in the tumor tissues of the trastuzumab PD model

To understand the mechanisms whereby tumor tissues become unresponsive to trastuzumab, MDA-MB-361 tumor tissue that had received the initial treatment with trastuzumab was re-inoculated into a different mouse. The re-inoculated tumor was found to be sensitive to be trastuzumab (Fig. 2A). Therefore, it is unlikely that the tumor A

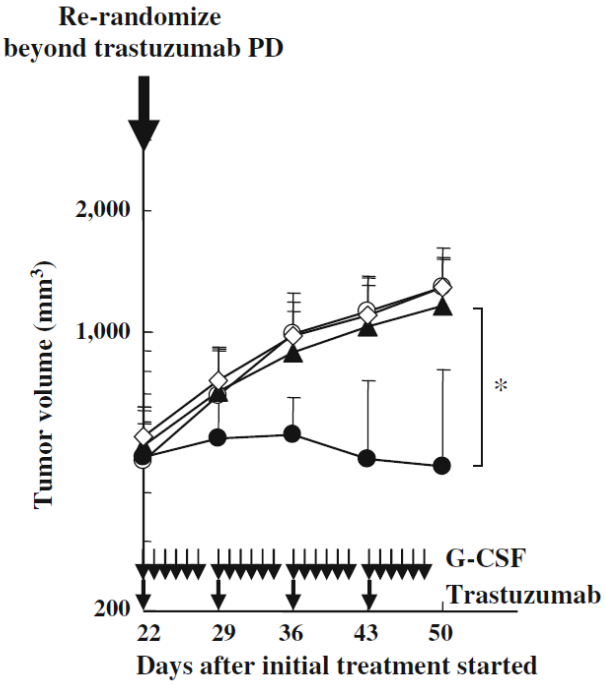

Figure 3 Antitumor activity of combinations of trastuzumab with G-CSF in the MDA-MB-361 human breast cancer model. Combination treatment was started 54 days after the tumor inoculation and 3 weeks of treatment with trastuzumab. Mice were randomly allocated to groups of ten mice each. G-CSF (300 mg/kg, po) was administered six times a week for 4 weeks. Trastuzumab (30 mg/kg) and IgG (30 mg/ kg) were administered ip once a week for 3 weeks. Data points: mean value + SD of tumor volume. Control IgG and vehicle (diamonds), trastuzumab and vehicle (triangles), control IgG and G-CSF (open circles), and combination with trastuzumab and G-CSF (closed circles)

tissue itself had been replaced with cells that had acquired resistance to trastuzumab, or that irreversible changes had occurred in the tumor tissues such as mutations of HER2-related signals. The author confirmed that the sensitivity to trastuzumab monotherapy was similar in both the tumor before treatment (group a) and the control tumor tissue (group b) having the same volume as the tumor that had become unresponsive to trastuzumab. The author then investigated the changes in the tumor tissues among groups sensitive to trastuzumab (groups a and b) and a refractory group (group c). The levels of pAKT in tumor were decreased in the trastuzumab PD tumors (group c), compared with the levels in the control groups a and b; and the levels of IGF-1R in PD tumors did not increase compared with the control groups a and b (Fig. 2B). Comprehensive GeneChip analyses (Fig. 2C) revealed differences in the gene expression of the (groups a, b, and c. Unsupervised hierarchical clustering analysis was carried out using 55 genes selected from microarray data according to the criteria described in “Materials and methods”. Groups a, b, and c were clustered into each subgroup with the exception of one mouse. The gene expression patterns of groups a and b were relatively similar in comparison with group c, indicating that the gene expression profiles of tumor tissues were associated with trastuzumab sensitivity in MDA-MB-361.

Involvement of the immune system in the trastuzumab PD model

The mechanism of the activity of trastuzumab involves FCγ-mediated ADCC (6). Based on a report that G-CSF enhances the appearance of FCγ in nude mice (15), the author considered that G-CSF might enhance ADCC activity. After 3 weeks of trastuzumab monotherapy in the MDA-MB-361 model, mice were randomly reallocated and trastuzumab was administered in combination with G-CSF. The results showed that even though trastuzumab or G-CSF monotherapy showed no antitumor effect, tumor growth was significantly inhibited by the combination therapy (Fig. 3).

Study of combining taxane anticancer drugs in the trastuzumab PD model

After 3 weeks of trastuzumab monotherapy in the MDA-MB-361 model, mice were randomly reallocated and trastuzumab was administered in combination with either paclitaxel or docetaxel. The results showed that even though trastuzumab monotherapy showed no tumor inhibitory effect, the combination groups showed significant antitumor effects with paclitaxel (Fig. 4A) and with docetaxel (Fig. 4B). In the KPL-4 model, the same results were found (Table 1). The author investigated the combination of trastuzumab with capecitabine in the KPL-4 trastuzumab PD model. Capecitabine combination therapy was significantly more effective than capecitabine alone, even in the PD model. Therefore, even if the tumor becomes unresponsive to trastuzumab monotherapy, an added effect can be gained by a regimen of trastuzumab in combination chemotherapy.

Discussion

Trastuzumab is an anticancer drug widely used for treating HER2-positive metastatic breast cancers. Recently, it has been suggested that prolonged administration of trastuzumab as a combination therapy beyond PD would be of clinical relevance. In the present study, the author demonstrated in xenograft models that, even after showing a loss of antitumor activity as a monotherapy, trastuzumab in combination chemotherapy is an effective anticancer agent.

In the present study, the author used *in vivo* murine xenograft models of HER2 + breast cancer as the experimental model. BT-474, KPL-4, and MDA-MB-361 have been reported to be natural HER2-overexpressing

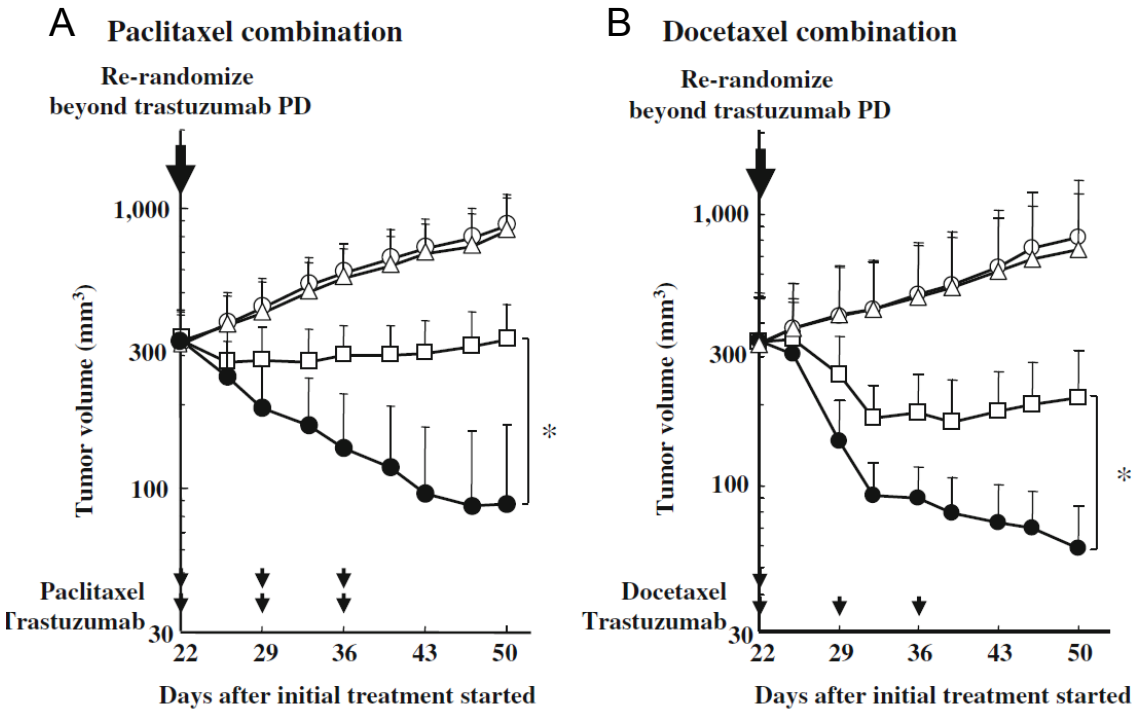

Figure 4 Antitumor activity of combinations of trastuzumab with taxanes in the MDA-MB-361 human breast cancer model. Combination of trastuzumab with paclitaxel (A) or docetaxel (B). Previous treatments with trastuzumab were started 52 and 48 days after the tumor inoculation, respectively. After 3 weeks of treatment, mice were randomly allocated to groups of ten mice each. Paclitaxel (60 mg/kg, iv) was administered once in 3 weeks. Trastuzumab (30 mg/kg) and IgG (30 mg/kg) were administered ip once a week for 3 weeks. Data points: mean value + SD of tumor volume. Control IgG and vehicle (circles), trastuzumab and vehicle (open triangles), control IgG and taxane (open squares), and combination with trastuzumab and taxane (closed squares)

breast cancer xenograft models (12, 14, 16). To eliminate the influence of the hormone receptors, the PgR-positive BT-474 model was not used and hormone receptor-negative KPL-4 and MDA-MB-361 models were used. Although in clinical practice trastuzumab is usually administered in combination with chemotherapies as the initial treatment, the author established a trastuzumab monotherapy PD model to avoid the development of resistance to chemotherapy in this study and to clarify whether trastuzumab administration should be maintained in combination therapy after PD has developed with trastuzumab monotherapy.

Trastuzumab alone was initially effective in both of the HER2-positive models; however, 3 weeks after the start of administration, trastuzumab showed no significant antitumor activity in spite of the fact that HER2 continued to be overexpressed on the cell surface in the tumor tissues. Ritter et al. (17) also reported of HER2-positive expression remaining in their trastuzumab-resistant model. A possible mechanism for the development of resistance to trastuzumab is a weakening of antitumor activity by a reduced ability of trastuzumab

Table 1 Antitumor activity of combination of trastuzumab with capecitabine in the KPL-4 human breast cancer model

	n	Day 1	Day 22
Tumor volume at day 22 beyond trastuzumab progression disease			
Control	8	567 ± 73	879 ± 89
Trastuzumab	7	565 ± 52	836 ± 52
Capecitabine	8	545 ± 63	642 ± 86[a]
Combination	8	551 ± 61	531 ± 91[a,b]

Treatment was started 17 days after the tumor inoculation. After 3 weeks of treatment with trastuzumab, mice were randomly allocated to groups of eight mice each. Capecitabine (90 mg/kg, po), was administered consecutively once a day for 14 days. Trastuzumab (40 mg/kg) and IgG (40 mg/kg) were administered ip qw for 3 weeks. Data points: mean value § SD of tumor volume

[a] Significantly different from the control group

[b] Significantly different from the capecitabine group

to penetrate into tumors that have grown larger during the initial treatment. In the present study, however, trastuzumab initially showed antitumor activity in large tumors, thereby contradicting the explanation that large tumor volume as a mechanism of the PD that occurs after initial treatment.

Another possible mechanism for the development of resistance to trastuzumab in the preclinical models of the author is the reversible change in the tumor tissue together with decreased ADCC activity in the host. Reversible changes in PD tumors were indicated by the fact that the antitumor activity of trastuzumab was restored when tumor tissue that had become resistant to trastuzumab monotherapy was reinoculated into another mouse, suggesting that the author's model for *in vivo* PD was different from the resistant cell line established *in vitro*. In the author's models, PD with trastuzumab could not be explained by the selection of a population of resistant cells or an irreversible gene mutation. Furthermore, the author observed neither attenuation of pAKT inhibition nor up-regulation of IGF-1R in tumor tissue, both of which have been reported as mechanisms of trastuzumab resistance (4). The gene expression profiles in the tumors with PD, differed from the profiles in the tumor before PD had developed. Therefore, changes other than pAKT or IGF-1R might be involved in the PD mechanisms.

ADCC has been reported to play an important role in the antitumor activity of trastuzumab(4, 6, 18). Therefore, an increase in ADCC activity would be expected to improve the efficacy of trastuzumab. G-CSF is used as a supportive treatment to improve neutropenia caused by chemotherapy in cancer patients, and it has been reported to increase FcγR expression in peripheral blood mononuclear cells (15, 19). Because FcγR is important for ADCC, the

author examined the combination effect of G-CSF with trastuzumab. Although, neither G-CSF nor trastuzumab monotherapy alone showed any antitumor effects in this model, the combination of trastuzumab + G-CSF showed significantly stronger tumor growth inhibition than even the initial trastuzumab monotherapy. These results suggest that G-CSF restored ADCC activity and augmented the antitumor activity of trastuzumab in the PD model. G-CSF would be useful not only as supportive care in clinical but also to potentiate the antitumor activity of trastuzumab in combination therapy.

In the trastuzumab PD model, trastuzumab was compared with chemotherapy alone, even though trastuzumab showed no antitumor activity. The results suggested that the trastuzumab combination therapy for HER-2 positive patients continued even after the development of PD. The mechanisms accounting for the combination effects of trastuzumab and chemotherapy treatments in this model are not yet clear. The antitumor activity of trastuzumab is possibly enhanced by ADCC activity because it has been reported that taxanes increase the TNF in macrophages and cancer cells by means of an inflammatory effect (20, 21). Capecitabine has not been reported to augment ADCC activity, however, and thus further investigations are needed to clarify the mechanisms of the effects in combination with trastuzumab.

The present results indicate that trastuzumab is able to potentiate the antitumor activity of taxanes or capecitabine even after it no longer shows antitumor activity as a monotherapy in xenograft models, thus suggesting a clinical relevance for cancer treatment with trastuzumab in combination therapy beyond PD.

References

1. Slamon DJ, Clark GM, Wong SG, Levin WJ, Ullrich A, McGuire WL. Human breast cancer: correlation of relapse and survival with amplification of the HER-2/neu oncogene. Science. 1987;235:177-82.

2. Austin CD, De Maziere AM, Pisacane PI, van Dijk SM, Eigenbrot C, Sliwkowski MX, et al. Endocytosis and sorting of ErbB2 and the site of action of cancer therapeutics trastuzumab and geldanamycin. Molecular biology of the cell. 2004;15:5268-82.

3. Yakes FM, Chinratanalab W, Ritter CA, King W, Seelig S, Arteaga CL. Herceptin-induced inhibition of phosphatidylinositol-3 kinase and Akt Is required for antibody-mediated effects on p27, cyclin D1, and antitumor action. Cancer research. 2002;62:4132-41.

4. Nagata Y, Lan KH, Zhou X, Tan M, Esteva FJ, Sahin AA, et al. PTEN activation contributes to tumor inhibition by trastuzumab, and loss of PTEN predicts trastuzumab resistance in patients. Cancer cell. 2004;6:117-27.

5. Nahta R, Yuan LX, Zhang B, Kobayashi R, Esteva FJ. Insulin-like growth factor-I receptor/human epidermal growth factor receptor 2 heterodimerization contributes to trastuzumab resistance of breast cancer cells. Cancer research. 2005;65:11118-28.

6. Clynes RA, Towers TL, Presta LG, Ravetch JV. Inhibitory Fc receptors modulate *f* cytotoxicity against tumor targets. Nature medicine. 2000;6:443-6.

7. Fujimoto-Ouchi K, Sekiguchi F, Tanaka Y. Antitumor activity of combinations of anti-HER-2 antibody trastuzumab and oral fluoropyrimidines capecitabine/5'-dFUrd in human breast cancer models. Cancer chemotherapy and pharmacology. 2002;49:211-6.

8. Seidman AD, Berry D, Cirrincione C, Harris L, Muss H, Marcom PK, et al. Randomized phase III trial of weekly compared with every-3-weeks paclitaxel for metastatic breast cancer, with trastuzumab for all HER-2 overexpressors and random assignment to trastuzumab or not in HER-2 nonoverexpressors: final results of Cancer and Leukemia Group B protocol 9840. Journal of clinical oncology : official journal of the American Society of Clinical Oncology. 2008;26:1642-9.

9. Schaller G, Fuchs I, Gonsch T, Weber J, Kleine-Tebbe A, Klare P, et al. Phase II study of capecitabine plus trastuzumab in human epidermal growth factor receptor 2 overexpressing metastatic breast cancer pretreated with anthracyclines or taxanes. Journal of clinical oncology : official journal of the American Society of Clinical Oncology. 2007;25:3246-50.

10. Cobleigh MA, Vogel CL, Tripathy D, Robert NJ, Scholl S, Fehrenbacher L, et al. Multinational study of the efficacy and safety of humanized anti-HER2 monoclonal antibody in women who have HER2-overexpressing metastatic breast cancer that has progressed after chemotherapy for metastatic disease. Journal of clinical oncology : official journal of the American Society of Clinical Oncology. 1999;17:2639-48.

11. Marty M, Cognetti F, Maraninchi D, Snyder R, Mauriac L, Tubiana-Hulin M, et al. Randomized phase II trial of the efficacy and safety of trastuzumab combined with docetaxel in patients with human epidermal growth factor receptor 2-positive metastatic breast cancer administered as first-line treatment: the M77001 study group. Journal of clinical oncology : official journal of the American Society of Clinical Oncology. 2005;23:4265-74.

12. Kurebayashi J, Otsuki T, Tang CK, Kurosumi M, Yamamoto S, Tanaka K, et al. Isolation and characterization of a new human breast cancer cell line, KPL-4, expressing the Erb B family receptors and interleukin-6. British journal of cancer. 1999;79:707-17.

13. Kunisue H, Kurebayashi J, Otsuki T, Tang CK, Kurosumi M, Yamamoto S, et al. Anti-HER2 antibody enhances the growth inhibitory effect of anti-oestrogen on breast cancer cells expressing both oestrogen receptors and HER2. British journal of cancer. 2000;82:46-51.

14. Fujimoto-Ouchi K, Sekiguchi F, Yasuno H, Moriya Y, Mori K, Tanaka Y. Antitumor activity of trastuzumab in combination with chemotherapy in human gastric cancer xenograft models. Cancer chemotherapy and pharmacology. 2007;59:795-805.

15. van der Kolk LE, de Haas M, Grillo-Lopez AJ, Baars JW, van Oers MH. Analysis of CD20-dependent cellular cytotoxicity by G-CSF-stimulated neutrophils. Leukemia. 2002;16:693-9.

16. Baselga J, Norton L, Albanell J, Kim YM, Mendelsohn J. Recombinant humanized anti-HER2 antibody (Herceptin) enhances the antitumor activity of paclitaxel and doxorubicin against HER2/neu overexpressing human breast cancer xenografts. Cancer research. 1998;58:2825-31.

17. Ritter CA, Perez-Torres M, Rinehart C, Guix M, Dugger T, Engelman JA, et al. Human breast cancer cells selected for resistance to trastuzumab *in vivo* overexpress epidermal growth factor receptor and ErbB ligands and remain dependent on the ErbB receptor network. Clinical cancer research : an official journal of the American Association for Cancer Research. 2007;13:4909-19.

18. Barok M, Isola J, Palyi-Krekk Z, Nagy P, Juhasz I, Vereb G, et al. Trastuzumab causes antibody-dependent cellular cytotoxicity-mediated growth inhibition of submacroscopic JIMT-1 breast cancer xenografts despite intrinsic drug resistance. Molecular cancer therapeutics. 2007;6:2065-72.

19. Kakinoki Y, Kubota H, Yamamoto Y. CD64 surface expression on neutrophils and monocytes is significantly up-regulated after stimulation with granulocyte colony-stimulating factor during CHOP chemotherapy for patients with non-Hodgkin's lymphoma. International journal of hematology. 2004;79:55-62.

20. Bogdan C, Ding A. Taxol, a microtubule-stabilizing antineoplastic agent, induces expression of tumor necrosis factor alpha and interleukin-1 in macrophages. Journal of leukocyte biology. 1992;52:119-21.

21. Sawada N, Ishikawa T, Fukase Y, Nishida M, Yoshikubo T, Ishitsuka H. Induction of thymidine phosphorylase activity and enhancement of capecitabine efficacy by taxol/taxotere in human cancer xenografts. Clinical cancer research : an official journal of the American Association for Cancer Research. 1998;4:1013-9.

Chapter II: Investigation of new anti-HER2 therapy for HER2-positive gastric cancer

1. Pertuzumab in combination with trastuzumab shows significantly enhanced antitumor activity in HER2-positive human gastric cancer xenograft models.

Introduction

Gastric cancer is the fourth frequently diagnosed tumors in the world with 989,000 cases estimated to have occurred (47) and is the second leading cause of cancer death worldwide (738,000 deaths, 9.7% of all cancers) as of 2008 (47). Although fluoropyrimidine- or platinum-based combination chemotherapy are the most widely accepted regimens for advanced gastric cancer in the world at present, their benefit has not necessarily been translated into higher overall survival rates. Therefore, more effective therapies for gastric cancer are required.

The human epidermal growth factor receptor (HER) family is composed of EGFR, HER2, HER3, and HER4. They regulate cell proliferation, differentiation, and apoptosis through the activation of their signal transduction by forming homodimers or heterodimers (48). The over-expression of HER family protein is often related to tumor malignancy. In gastric cancer, EGFR, HER2, and HER3 overexpression has been identified and a relationship with prognosis is suggested (49-53). Therefore, inhibiting the signal transduction through heterodimers including HER2 possibly provides more benefit to patients with gastric cancer. Recently, the ToGA trial (a phase III study of trastuzumab (Herceptin®) in HER2-positive advanced and inoperable gastric cancer) showed a survival benefit when trastuzumab was added to chemotherapy in HER2-overexpressing gastric cancer patients (10) and the FDA has approved trastuzumab for HER2-positive metastatic gastric and gastroesophageal junction cancer. Thus, anti-HER2 therapy has been identified to be of clinical significance.

Pertuzumab, which is a new humanized anti-HER2 antibody, is thought to exert antitumor activity in a different manner from trastuzumab. Pertuzumab binds to domain II of HER2, the region of dimer formation, whereas trastuzumab binds to domain IV of HER2. Thus, pertuzumab could inhibit the dimerization of HER2 with other HER family proteins and prevent ligand-dependent HER2 signaling (54). In HER2-positive breast cancer, the

usefulness of pertuzumab and trastuzumab was shown in preclinical and clinical reports (55, 56). To investigate the effect of pertuzumab and trastuzumab for patients with previously untreated HER2-positive metastatic breast cancer, a phase III trial of pertuzumab in combination with trastuzumab and docetaxel (CLEOPATRA) was underway (57). Clinical benefit of combination therapy of pertuzumab and trastuzumab was expected. Pertuzumab and trastuzumab in combination might provide more effective antitumor activity than either single agent for HER2-positive tumors including gastric cancer, because of their different mechanisms of HER2-signal inhibition. This combination therapy could provide clinical benefit for HER2-positive gastric cancer patients. In the present study, the author investigated the antitumor efficacy of pertuzumab in combination with trastuzumab as well as its mechanism of action as a new therapy for gastric cancer by using HER2-overexpressing human gastric cancer mouse xenograft models.

Materials and Methods

Molecular modeling of trastuzumab/pertuzumab/HER2 ternary complex

The binding position of the Fab of pertuzumab or trastuzumab to HER2 was assigned using the crystallographic structure of the Fab (pertuzumab)/HER2 complex (Protein Data Bank (PDB) ID: 1s78) (54) or the Fab (Trastuzumab)/HER2 complex (PDB ID: 1n8z) (58). The author used the 3D structure of IgG1 monoclonal antibody (PDB ID: 1IGY) (59) as a surrogate for that of each whole antibody because the 3D structures of the whole antibodies are not known. The position of pertuzumab or trastuzumab whole antibody was estimated by superposing the 3D structure of IgG1 (PDB ID: 1IGY) onto that of the Fab (pertuzumab or trastuzumab)/HER2 complex (PDB ID: 1s78 or 1n8z respectively). The superposition of the Fab of IgG1 and the Fab of pertuzumab or trastuzumab was done using the software PyMOL (The PyMOL Molecular Graphics System, Schrödinger, LLC, New York, NY, USA). Finally the pertuzumab whole antibody/HER2 complex model and trastuzumab whole antibody/HER2 complex model were merged by superposing the 3D structures of HER2 of the two models.

Construction of the transfectants of NK-92 expressed human FcγRIIIa-158V allotypes

CD16-negative NK-92 tumor line was purchased from the American Type Culture Collection (ATCC, Manassas, VA, USA).The cDNA encoding FcgRIIIa was amplified by PCR from the fetal spleen cDNA Library (Clontech, Mountain View, CA, USA) using a specific primer set (CD16F1: TAA GAA TTC CCA CCA TGT GGC AGC TGC TCC TCC C, CD16F2: TAA GCG GCC GCT TAT CAT TTG TCT TGA GGG TCC TTT CTC C). The cDNA encoding FcγRIIIa was subcloned into pGEM® T-Easy vector (Promega, Madison, WI, USA). Since cDNA sequencing revealed that the obtained FcγRIIIa were all 158F allotype, the FcγRIIIa-158V allotype sequence was generated by site-directed mutagenesis (Quick change®: Stratagene, La Jolla, CA, USA). The cDNA encoding FcγRIIIa-158V allotype was cloned at the EcoRI and NotI sites of the pCXND3 expression vector, which is a derivative of pCXN (60) containing a CAG promoter and a neomycin-resistant gene. The resulting plasmid was designated pCXND3/CD16(V). To establish transfectants of NK-92 cells that produce human FcγRIIIa-158V allotype, pCXND3/CD16(V) was transfected by the electroporation method using GENE-PULSER II (BioRad Laboratories, Hercules, CA, USA) under the conditions of 1.5 kV and 25 μFD. Flow cytometry-based screening was performed using αCD16-FITC (Beckman Coulter, Brea, CA, USA), and ^{51}Cr-release assay was performed to confirm the ADCC activity in pCXND3/CD16(V)-transfected NK-92 cells. The resulting FcγRIIIa-158V-positive NK-92 cells exerting ADCC activity were designated CD16(158V)/NK-92 cells.

Test agents

Trastuzumab and pertuzumab were provided by F. Hoffmann-La Roche (Basel, Switzerland) as a fine powder and a liquid, respectively. Trastuzumab was dissolved in purified water. Both antibodies were diluted with saline or culture medium in *in vivo* or *in vitro* experiments. Human immunoglobulin G (HuIgG) was purchased from MP Biomedicals, Inc. (Aurora, OH, USA) and was reconstituted with water and diluted with saline.

Animals

Male, 5-week-old BALB-nu/nu mice (CAnN.Cg-Foxn1<nu>/CrlCrlj nu/nu) were obtained from Charles River Japan (Yokohama, Japan). All animals were allowed to acclimatize and recover from shipping-related stress for

1 week prior to the study. The health of the mice was monitored by daily observation. Chlorinated water and irradiated food were provided ad libitum, and the animals were kept under a controlled light-dark cycle (12h-12h). All the animal experiments were conducted in accordance with the Institutional Animal Care and Use Committee.

Cell lines and culture

Three human gastric cancer cell lines were used in the present study. NCI-N87 cells were purchased from ATCC. MKN-28 cells were purchased from immuno-Biochemical Laboratories Co., Ltd. (Fujioka, Japan). NCI-N87 and MKN-28 were maintained in RPMI-1640 (Sigma-Aldrich, St. Louis, MO, USA) supplemented with 10% FBS at 37°C under 5% CO_2. 4-1ST cells were purchased from the Central Institute for Experimental Animals (Yokohama, Japan) and maintained in BALB-nu/nu mice by subcutaneous (sc) inoculation of pieces of tumor. CD16(158V)/NK-92 was maintained in MEMα (Wako, Osaka, Japan) supplemented with 12.5% FBS, 12.5% horse serum, 0.02 mM folic acid, 0.1 mM 2-mercaptoethanol, 0.2 mM inositol, and 0.5 mg/mL G418, and 20 ng/mL recombinant human IL-2 at 37°C under 5% CO_2.

Immunohistochemistry of EGFR and HER2

Tumor xenograft tissues were resected and processed as formalin-fixed, paraffin-embedded specimen sections. These were examined for the expression of EGFR or HER2 protein by immunohistochemistry (IHC) using EGFR pharmDx kit™ and HercepTest®.

***In vivo* tumor growth inhibition studies**

Each mouse was inoculated sc into the right flank with either 5×10^6 cells/mouse of human gastric cancer cell lines MKN-28 or NCI-N87, or an 8-mm^3 piece of 4-1ST tumor tissue. Several weeks after tumor inoculation, mice were randomly allocated to control and treatment groups. The administration of anticancer agents was started when the tumor volumes reached approximately 0.2 to 0.3 cm^3. To evaluate the antitumor activity of the test agents, tumor volume was measured twice a week. The tumor volumes (V) were estimated and the percentage of tumor growth inhibition (TGI%) was calculated as described previously (33). Trastuzumab and pertuzumab were

administered intraperitoneally once a week for three weeks.

***In vitro* anti-proliferation assays**

NCI-N87 cells were seeded on 96-well plates at 5×10^3 cells/well and pre-cultured for 24 hours. The cells were treated with pertuzumab, trastuzumab or both and cultured for three days. The cells were fixed with 10% formalin neutral buffer solution. Crystal violet staining and extraction were performed as described previously (9). Their absorbance was measured at 595 nm. The cells after 24 hours pre-culture were also detected by crystal violet staining as the absorbance of the pre-cultured well. The percentage of cell proliferation inhibition (% Inhibition) was calculated as follows: % Inhibition = {1 – (absorbance of treatment well – absorbance of pre-cultured well) / (absorbance of non-treatment well – absorbance of pre-cultured well)} × 100. In case of ligand-dependent proliferation, cells were pre-cultured in RPMI-1640 with 0.1% FBS and treated with pertuzumab, trastuzumab or both 30 min before EGF or HRGα stimulation. The percentage of cell proliferation (% Proliferation) was calculated as follows: % Proliferation = (absorbance of treatment well – absorbance of pre-cultured well) / (absorbance of unstimulated well – absorbance of pre-cultured well) × 100.

Apoptosis assay

NCI-N87 cells were seeded on 96-well plates at 1×10^4 cells/well and cultured in the same way as the ligand-dependent anti-proliferation assay (see above). Twenty-four hours after treatment, Caspase-Glo™ 3/7 Assay (Promega) was used to measure caspase 3/7 activity. Caspase 3/7 activity was calculated as follows: Caspase 3/7 activity = (luminescent unit of treatment well – luminescent unit of blank well) / (mean luminescent unit of control well).

Cell stimulations

Cells were precultured for 1 day after seeding. After that the cells were starved in RPMI-1640 supplemented with 0.1% FBS for 20-24 hours and treated with pertuzumab, trastuzumab or both. After 3.5 hours incubation, cells were exposed to EGF or heregulin (HRG) α for 5 min.

Western blotting

Cells were washed with ice-cold PBS and lysed with Cell Lysis Buffer (Cell Signaling Technology, Beverly, MA, USA) with 10 mM NaF, 1 μg/mL aprotinin and 1 mM PMSF. After centrifugation (4°C, 14,000g, 5 min.), the resultant supernatant was used for the assays. Protein concentration of the supernatant was quantified using the DC protein assay kit (BioRad). Cell lysates (20 μg protein/lane) were electrophoresed on SDS-PAGE and transferred to a polyvinylidene difluoride membrane (Millipore, Bedford, MA, USA). The membrane was blocked in SuperBlock® T20 (TBS) Blocking Buffer (Thermo Scientific, Waltham, MA, USA) and probed with each antibody against HER2 (sc-31153), HER3 (sc-285), (Santa Cruz Biotechnology, Santa Cruz, CA, USA), EGFR (#2963), pEGFR (Tyr1068) (#2236), pHER2 (Tyr1248) (#2247), pHER3 (Tyr1289) (#4791), Akt (#2920), pAkt (Ser473) (#4058), ERK1/2 (#9102), pERK1/2 (Thr202/Tyr204) (#9106) (Cell Signaling) and actin (A2228) (Sigma-Aldrich, St. Louis, MO, USA) as the first antibodies. These proteins were detected by horseradish peroxidase-conjugated secondary antibodies (Santa Cruz Biotechnology). The bands were visualized using ECL plus (GE Healthcare Life Sciences, Buckinghamshire, UK).

ELISA

Tumor samples were taken when the tumors had reached a volume of approximately 0.3 to 0.5 cm^3 and were immediately frozen in liquid nitrogen and stored at -80°C. Tumor samples were homogenized in PBS containing 0.05% Tween 20 and centrifuged (4°C, 10,000 × g, 20 min.). The resultant supernatant was used for the assays. The author used Duo Set® IC (R&D Systems, Minneapolis, MN, USA) to detect human total EGFR, HER2, and HER3. Quantikine® (R&D systems) was used to detect human VEGF. Total protein levels in the tumor tissue samples using a DC protein assay kit (BioRad Laboratories).

***in situ* proximity ligation assay**

in situ proximity ligation assay (PLA) was done to detect EGFR-HER2 heterodimer. The author used Duolink® *in situ* PLA™ (Olink Bioscience, Uppsala, Sweden). In the assay, oligonucleotide-conjugated 'PLA probe' antibodies are directed against primary antibodies for EGFR or HER2. Annealing of the 'PLA probes' occurs when

EGFR and HER2 are in close proximity, which initiates the amplification of repeat sequences recognized by the fluorescently-labeled oligonucleotide probe. Cells were seeded on 8-well chamber slides at 1×10^4 cells/well and stimulated as described above. Cells were washed with ice-cold PBS and fixed with 4% (w/v) paraformaldehyde PBS 30 min at RT. The cells were then washed with ice-cold PBS and permeabilized with 0.2% Triton X-100 PBS 5 min at RT. After that the cells were washed with ice-cold PBS and assayed with Duolink® *in situ* PLA™. Anti-HER2 Ab (OP15, Calbiochem, Darmstadt, Germany) and Anti-EGFR Ab (sc-03, Santa Cruz Biotechnology) were used as primary antibodies. PLA™ probe anti-Mouse MINUS and PLA™ probe anti-Rabbit PLUS were used as two PLA™ probes. In a negative control, primary antibodies were not included. For detection, Duolink® detection kit 563 was used. ProLong Gold Antifade Reagent with DAPI (Molecular Probes, Eugene, OR, USA) was used as the mounting medium. The specimens were observed using a fluorescence microscope (BX50: Olympus, Center Valley, PA, USA).

Immunoprecipitation

Streptavidin-coupled magnetic beads (Invitrogen, Carlsbad, CA, USA) were incubated with biotinylated HER2 antibody (ab79205, Abcam, Cambridge, MA, USA) at 4℃ 1 h. Cell lysates (1 mg) were add for 2 h at 4℃. Beads were washed 3 times with lysis buffer (20 mM HEPES, 15 mM NaCl, 2 mM EDTA, 10 mM NaF, 0.5% NP-40 and 0.1 mM Na_3VO_4 supplemented with protease inhibitor cocktail and phosphatase inhibitor cocktail (Sigma-Aldrich)), resuspended in SDS sample buffer, and boiled. The supernatant was used for western blotting.

ADCC assays

The author used RTCA (Real-time Cell Analyzer) (xCELLigence, Roche Diagnostics K. K., Tokyo, Japan) to monitor ADCC activities in real time. The system measures electrical impedance on the bottom of the tissue culture E-Plates, which contain interdigitated electrodes, as the Cell Index. NCI-N87 cells were seeded on E-plates at 5×10^3 cells/well and were precultured for 24 hours. CD16(158V)/NK-92 were added as the effector at a target ratio of 1:1. Cells were treated with pertuzumab, trastuzumab or both at the same time. The Cell Index was measured for three days after treatment. The Normalized Cell Index was calculated as follows: (Cell Index at each point) / (Cell

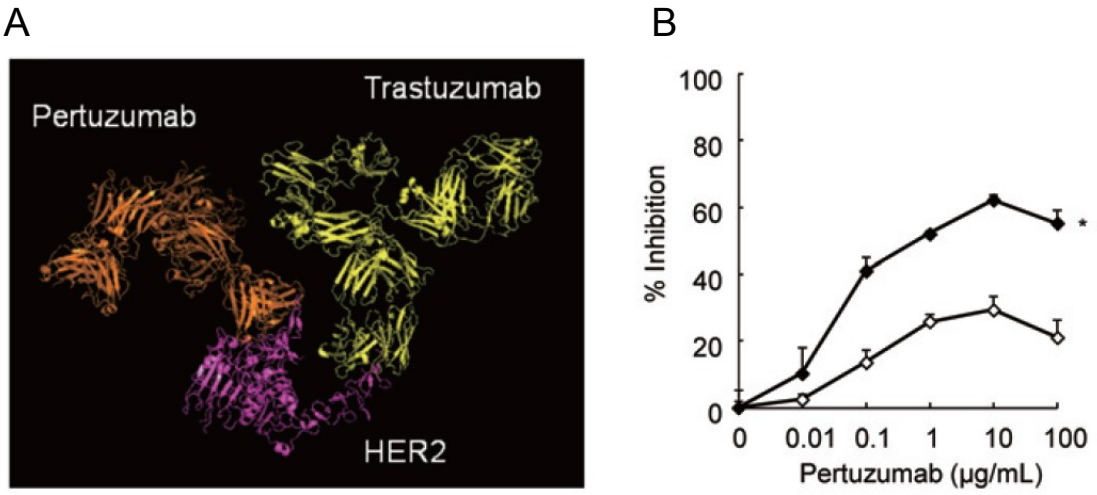

Figure 1 A, 3D structure of the trastuzumab/pertuzumab/HER2 ternary complex. B, anti-proliferative activity of pertuzumab in combination with trastuzumab. Cells were treated with pertuzumab (0.1–100 μg/mL), with or without trastuzumab (20 μg/mL), for three days in the culture medium. Open rhombus: without trastuzumab; and filled rhombus: with trastuzumab. Data points are mean + SD (n = 3). The 0% point was defined as the point of 0 μg/mL of pertuzumab of both open and filled rhombuses. Statistically significant differences are shown as *: $P < 0.05$ by the two-way analysis of variance.

Index at the point of pertuzumab and trastuzumab treatment).

Measurement of microvessel density in tumor tissues

Microvessel density (MVD) in tumor tissue was evaluated with immunohistochemical staining of CD31. Tumor samples were collected 96 hours after administration of trastuzumab, pertuzumab or both. Immunohistochemical staining was performed as described previously (61). MVD (%) was calculated from the ratio of the CD31-positive staining area to the total observation area in the viable region. Three to six fields per section (0.4856 mm^2 each) were randomly analyzed, excluding necrotic areas. Positive staining areas were calculated using imaging analysis software (WinROOF; Mitani Corporation, Fukui, Japan).

Results

Pertuzumab in combination with trastuzumab inhibits tumor cell growth more than each does as a single agent.

Pertuzumab has a different binding site from trastuzumab and could bind to HER2 without competing with

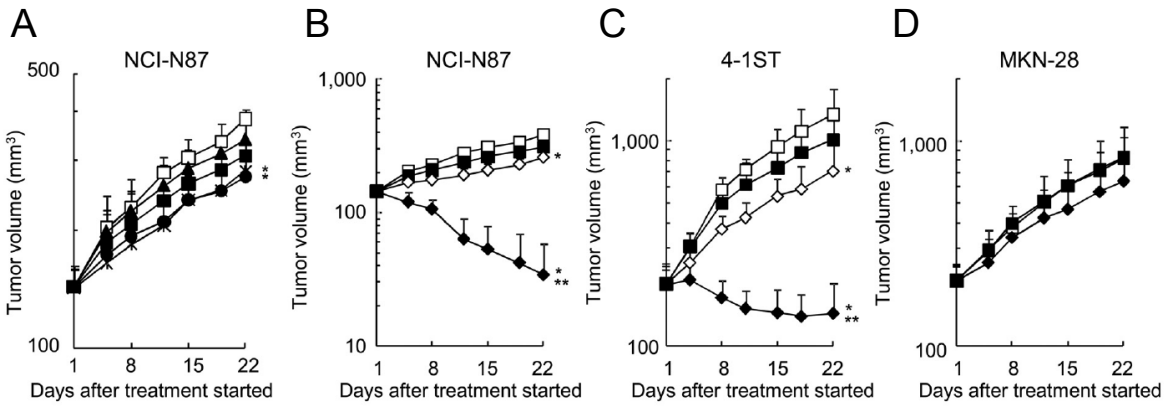

Figure 2 Antitumor activity of pertuzumab as a single agent and in combination with trastuzumab. A, mice bearing NCI-N87 tumors were randomly divided into 5 groups (n = 6/group) and treated with HuIgG or pertuzumab once a week for 3 weeks. Open square: HuIgG; filled triangle: Pertuzumab 10 mg/kg; filled square: Pertuzumab 20 mg/kg; filled circle: Pertuzumab 40 mg/kg and asterisk: Pertuzumab 80 mg/kg. B, C, D, tumor-bearing mice were randomly divided into 4 groups (B,C) or 2 groups (D) (n = 6/group) and treated with HuIgG, pertuzumab, trastuzumab or both pertuzumab and trastuzumab once a week for 3 weeks. B: NCI-N87 tumors (HER2 positive); C: 4-1ST tumors (HER2 positive) and D: MKN-28 tumors (HER2-negative). Open square: HuIgG; filled square: Pertuzumab at 20 mg/kg (B) or 40 mg/kg (C, D); open rhombus: Trastuzumab at 20 mg/kg and filled rhombus: Combination of pertuzumab and trastuzumab at 20 mg/kg and 20 mg/kg (B) or 40 mg/kg and 20 mg/kg (C, D respectively). Data points are mean + SD of the tumor volume (mm^3). Statistically significant differences are shown as *: $P < 0.05$ vs. the control group, **: $P < 0.05$ vs. the singe agent groups by the Wilcoxon test.

trastuzumab (Fig. 1A). Therefore the author hypothesized that pertuzumab would show significant antitumor activity in combination with trastuzumab. To examine whether pertuzumab could provide efficacy in combination with trastuzumab, the author first analyzed tumor cell growth inhibition of pertuzumab in combination with trastuzumab *in vitro*. Pertuzumab alone inhibited the growth of NCI-N87, the HER2-positive human gastric cancer cell line (Fig. 1B open rhombus). In combination with trastuzumab, pertuzumab could potentiate its anti-proliferation activity (Fig. 1B filled rhombus). Trastuzumab alone at 20 μg/mL inhibited the growth of the cells to 55.2 ± 1.3% (mean ± SD, n = 3).

Pertuzumab has antitumor activity as a single agent in a mouse xenograft model.

The author examined the efficacy of pertuzumab in NCI-N87 tumor xenograft. On day 22 (21 days after starting treatment), tumor growth inhibition rates (TGI%) were 18%, 31%, 46% and 41% at doses of 10, 20, 40 and 80 mg/kg, respectively. Pertuzumab showed significant antitumor activity at 40 and 80 mg/kg (Fig. 2A). The maximum effective dose was 40 mg/kg.

Table 1. HER family protein expression levels in human gastric tumor tissues.

Xenograft	ELISA (ng/mg protein) †			IHC‡	
	EGFR	HER2	HER3	EGFR	HER2
NCI-N87	9.0 ± 1.2	180 ± 76	0.88 ± 0.084	+	+
4-1ST	0.94 ± 0.10	330 ± 72	1.9 ± 0.49	+	+
MKN-28	3.5 ± 0.37	1.7 ± 0.39	0.70 ± 0.20	+	?

†Means ± SD (n = 4)
‡IHC was according to clinical diagnosis (EGFR pharmDx kit™ and HercepTest®)

Pertuzumab in combination with trastuzumab enhances antitumor activity.

Next, the author investigated the antitumor activity of pertuzumab in combination with trastuzumab in NCI-N87 tumor xenograft. The combination of pertuzumab and trastuzumab dramatically enhanced the antitumor activity (TGI% was 145%) compared with pertuzumab or trastuzumab alone (TGI% was 31% and 52% respectively.) (Fig. 2B). The author also examined the efficacy of pertuzumab and trastuzumab in two other human gastric cancer xenografts, HER2-positive 4-1ST and HER2-negative MKN-28. The antitumor activity of pertuzumab in combination with trastuzumab in 4-1ST was also significantly higher than either pertuzumab and trastuzumab as single agents (TGI% was 22%, 57% and 109% respectively) (Fig. 2C). On the other hand, no combined effect was seen in MKN-28, (TGI% was -2%, and 27% in the pertuzumab treatment group and the combination treatment group, respectively) (Fig. 2D). MKN-28 was insensitive for trastuzumab in a separate experiment (9). The author examined the expression levels of HER family protein in these gastric tumor tissues of mice xenograft models by ELISA and IHC (Table1). All cell lines expressed EGFR and HER3 by ELISA. All cell lines were also identified as EGFR-positive cells by IHC according to clinical diagnosis. The author also stained HER3 immunohistochemically; however HER3 was only slightly detected on the plasma membrane in all examined cell lines (data not shown). The expression level of HER2, but not EGFR or HER3, was considered to be a key factor of the efficacy.

Pertuzumab in combination with trastuzumab strongly reduces EGFR-HER2 signaling.

To examine the mechanism of combination efficacy of pertuzumab and trastuzumab, the author next analyzed HER2 signal transduction. The author focused on the EGFR-HER2 signaling because HER3 expression level was

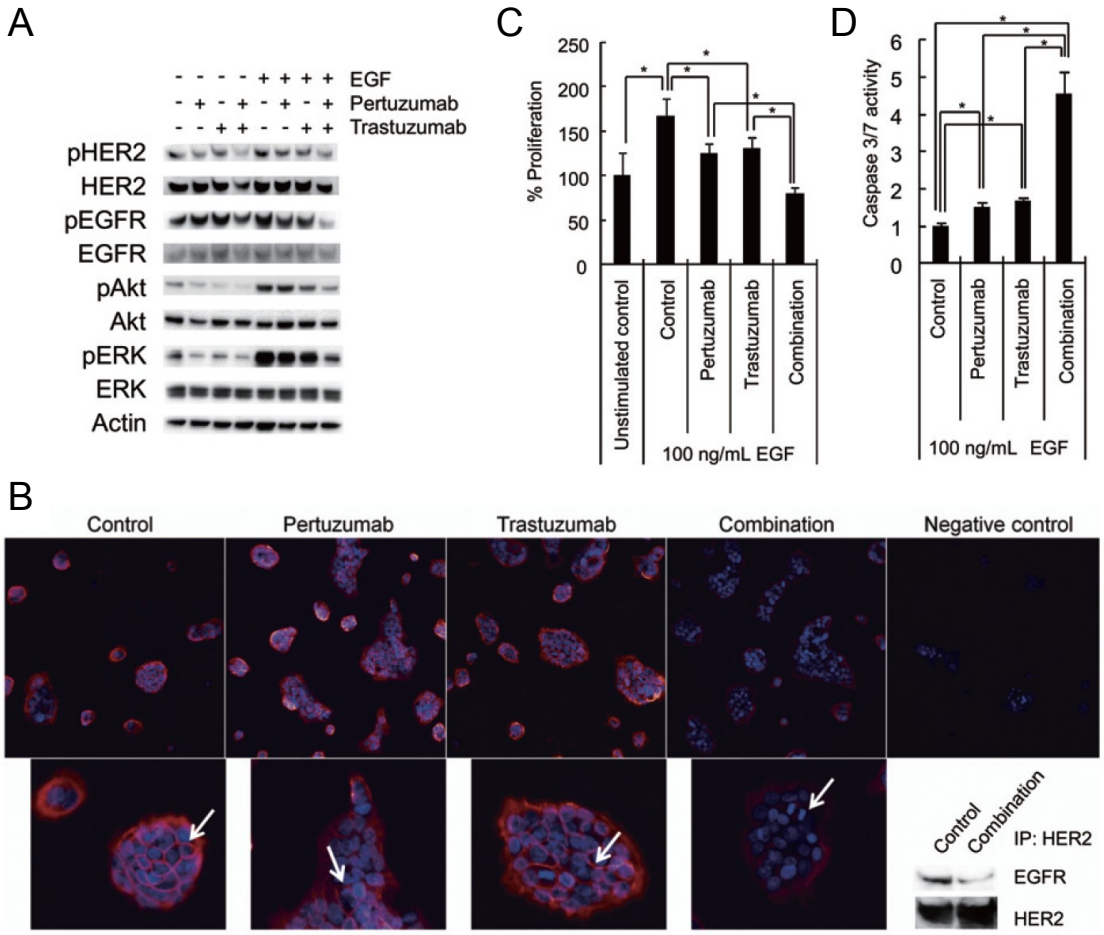

Figure 3 Effect of pertuzumab in combination with trastuzumab on the signal transduction of HER family proteins. A, NCI-N87 cells were treated with pertuzumab (40 μg/mL), trastuzumab (40 μg/mL) or both for 3.5 h followed by EGF (100 ng/mL) stimulation for 5 min. The pHER2, HER2, pEGFR, EGFR, pAkt, Akt, pERK1/2, ERK1/2 and actin were detected by western blotting. B, EGFR-HER2 heterodimer was detected by Duolink® in situ PLA™ and immunoprecipitation. Red: EGFR/HER2 heterodimer; Blue: Nuclear. EGFR/HER2 heterodimers were slightly decreased by pertuzumab and strongly decreased by the combination of pertuzumab and trastuzumab (white arrows). Objective ×20. C, the cell growth inhibition in the presence of EGF was examined. NCI-N87 cells were treated with pertuzumab (20 μg/mL), trastuzumab (20 μg/mL) or both 30 min before the addition of EGF (100 ng/mL). Control was untreated cells. The cell proliferation was examined three days after the treatment. Data points are mean + SD (n = 3). Statistically significant differences are shown as *: $P < 0.05$ by the t-test. D, the caspase 3/7 activity of pertuzumab and trastuzumab combination was measured. NCI-N87 cells were treated with pertuzumab (20 μg/mL), trastuzumab (20 μg/mL) or both 30 min before the addition of EGF (100 ng/mL). Control was untreated cells. The caspase 3/7 activity was measured 24 h after treatment. Data points are mean + SD (n = 5). Statistically significant differences are shown as *: $P < 0.05$ by the t-test.

very low in the gastric cancer models the author used. First, the author examined the phosphorylation of HER2 under serum starvation or under EGFR stimulation to evaluate ligand-independent or ligand-dependent signals, respectively. In the absence of EGF, phosphorylation of HER2 and the down-stream factor Akt and ERK1/2 were strongly reduced by combination of pertuzumab and trastuzumab. In the presence of EGF, pHER2 was also more attenuated by the combination than by either antibody alone. Phosphorylation of EGFR, Akt and ERK1/2 were

increased by EGF stimulation and the combination of pertuzumab and trastuzumab strongly reduced these phosphorylations (Fig. 3A). Next, the author examined whether pertuzumab in combination with trastuzumab down-regulated the phosphorylation of EGFR and HER2 by inhibiting their heterodimerization. The author evaluated the dimerization level of EGFR-HER2 induced by EGF in the presence of pertuzumab, trastuzumab or both by *in situ* PLA. EGFR-HER2 heterodimers were slightly decreased by pertuzumab. However pertuzumab and trastuzumab in combination remarkably reduced the EGFR-HER2 heterodimers on the plasma membrane (Fig. 3B). The inhibition of EGFR-HER2 heterodimerization by the combination was also detected by immunoprecipitation (Fig. 3B). The author also examined the cell proliferation and apoptosis activity under EGF-stimulation. The cells proliferated EGF-dependently and both pertuzumab and trastuzumab inhibited this EGF-dependent cell growth. The combination of pertuzumab and trastuzumab significantly enhanced the cell growth inhibition (Fig. 3C). Additionally, the combination of pertuzumab and trastuzumab significantly enhanced apoptosis activity (Fig. 3D). These results suggest that pertuzumab in combination with trastuzumab inhibits EGFR-HER2 dimerization and its down-stream signaling, although neither pertuzumab nor trastuzumab does it sufficiently alone.

Pertuzumab in combination with trastuzumab enhances the ADCC activity.

Both pertuzumab and trastuzumab are reported to have ADCC activity. The author investigated the ADCC activity induced by pertuzumab and trastuzumab as another mechanism of the combined effect by using RTCA. The author observed the Cell Index of NCI-N87 for three days after the addition of pertuzumab, trastuzumab and CD16(158V)/NK-92 cells. The Cell Index was normalized at the point of pertuzumab and trastuzumab addition. Normalized Cell Index after NK cells were added was significantly reduced by the addition of pertuzumab and trastuzumab compared with the addition of each single agent alone. No reduction of the Normalized Cell Index was seen after the addition of pertuzumab and trastuzumab without NK cells (Fig. 4A). These results suggest that combination therapy of pertuzumab and trastuzumab has more potent antitumor activity through the enhancement of ADCC activity.

Pertuzumab in combination with trastuzumab shows anti-angiogenic activity.

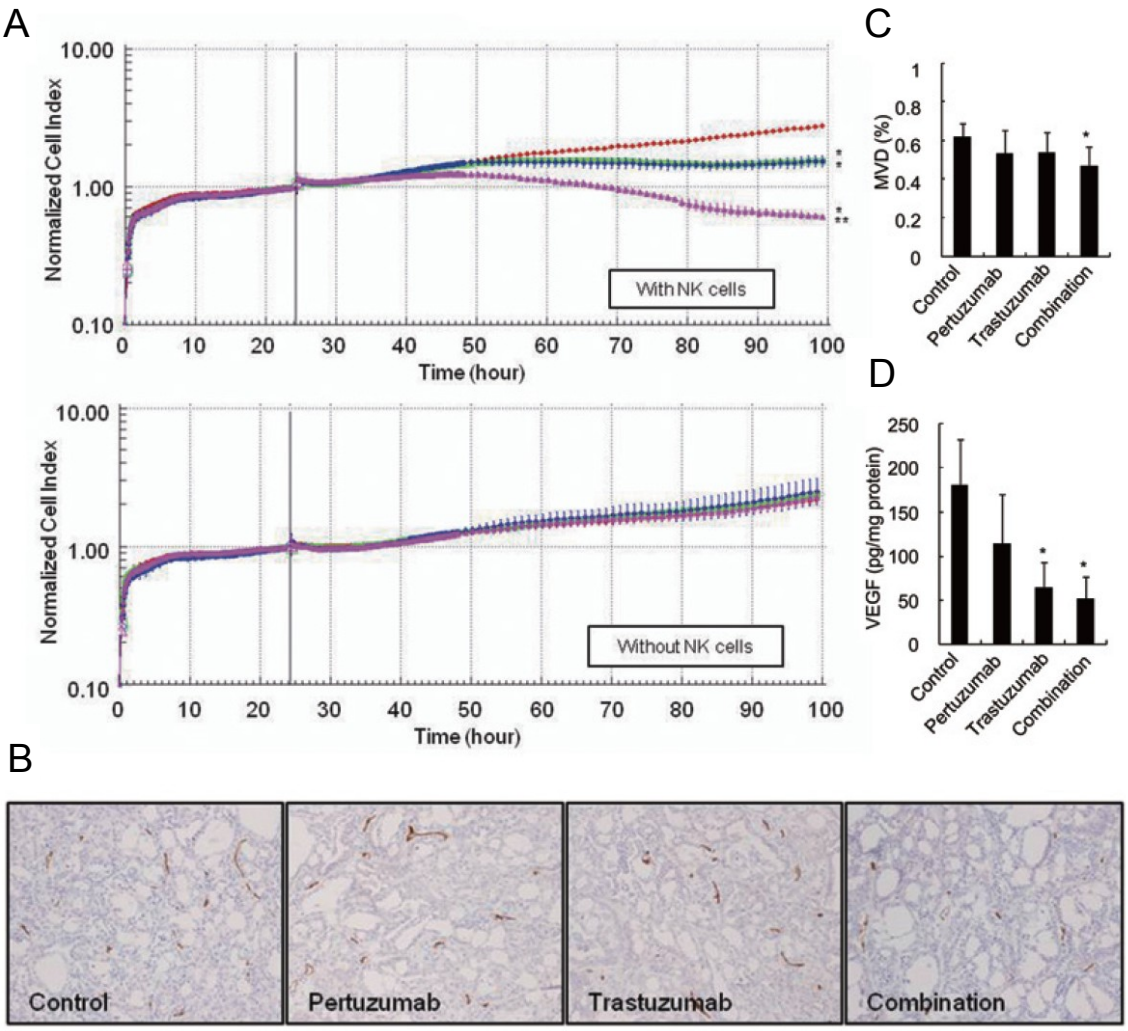

Figure 4 Effect of pertuzumab in combination with trastuzumab on ADCC activity and anti-angiogenic activity. A, ADCC activity was examined with RTCA. NCI-N87 cells were pre-cultured in the culture medium for 24 h and treated with pertuzumab (10 ng/mL), trastuzumab (2 ng/mL) or both. NK cells were added as the effector at target ratios of 1:1 simultaneously. Cell Indices were measured every 5 min for the first 4 h, every 15 min for the next 44 h, and every hour thereafter. Cell Indices were normalized at the treatment point. Red: Control (non-treatment) group; Green: Pertuzumab group; Blue: Trastuzumab group; Magenta: Combination group. Data points are mean ± SD (n = 3). Statistically significant differences are shown as *: $P < 0.05$ vs. the control group, **: $P < 0.05$ vs. the singe agent groups by the t-test. B, tumor microvissel was stained immunohistochemically with anti-CD31 antibody at 96 h after the treatment with HuIgG (40 mg/kg) (as a control), pertuzumab (20 mg/kg), trastuzumab (20 mg/kg) or both (n = 5-6/group). C, the MVD of NCI-N87 was determined as described above. D, the VEGF protein levels of each treatment groups at 96 h were quantified by ELISA (n = 5-6/group). Data points are mean + SD of tumor volume (mm^3). Statistically significant differences are shown as *: $P < 0.05$ vs. control group by the Wilcoxon test.

There are some reports on the anti-angiogenic activity of trastuzumab (5, 62). As another combination mechanism, the author examined whether pertuzumab enhances the anti-angiogenic activity of trastuzumab. In this study, neither pertuzumab nor trastuzumab could significantly decrease MVD. However a significant reduction in MVD was seen if the tumor tissue was treated with pertuzumab in combination with trastuzumab (Fig. 4B, C). The author also quantified the VEGF protein levels in those tumor tissues. Trastuzumab reduced VEGF levels in tumor

tissues significantly. Pertuzumab also tended to reduce the VEGF levels, although it was not significant. When mice were treated with pertuzumab in combination with trastuzumab, the VEGF levels decreased more than they did with pertuzumab alone or trastuzumab alone (Fig. 4D). These results show that pertuzumab in combination with trastuzumab has an effect not only by inhibition of EGFR-HER2 signaling and enhancement of ADCC activity, but also by inhibition of tumor angiogenesis.

Pertuzumab in combination with trastuzumab strongly reduces HER2-HER3 signaling.

Finally, the author also examined the signal transduction of HER2-HER3 in NCI-N87. Although NCI-N87 showed low expression levels of HER3 by ELISA and IHC assay, it has been reported that HER3 triggered strong signal transduction by dimer formation with HER2. Therefore it is possible that a few HER3 proteins in NCI-N87 still play a role as mediators of the growth signal. The author examined the phosphorylation levels of HER2, HER3, Akt and ERK1/2 under HRGα stimulation after treatment with pertuzumab and trastuzumab. HRGα increased pHER3 and pAkt, and the combination of trastuzumab and pertuzumab reduced them as well as pHER2 (Fig. 5A). The author also examined the contribution of HRGα to cell proliferation. The cells proliferated HRGα-dependently and both pertuzumab and trastuzumab inhibited the HRGα-dependent cell growth. The combination of pertuzumab and trastuzumab significantly enhanced the cell growth inhibition. (Fig. 5B). The apoptosis activity of pertuzumab and trastuzumab in combination also significantly increased compared to that of pertuzumab or trastuzumab alone (Fig. 5C). Therefore, HER3 would also play a role in showing the efficacy of the combination even though the HER3 protein expression is low.

Discussion

It is reported that pertuzumab and trastuzumab bind to different domains of HER2. A previous study showed that pertuzumab and trastuzumab were oriented at different angles with respect to HER2 after binding to HER2, by using a 3D-structure model of the Fab region of pertuzumab and trastuzumab and p185HER2 (63). As shown in Fig.1A, binding of whole IgG to HER2 ECD protein, pertuzumab would not interfere with the binding of

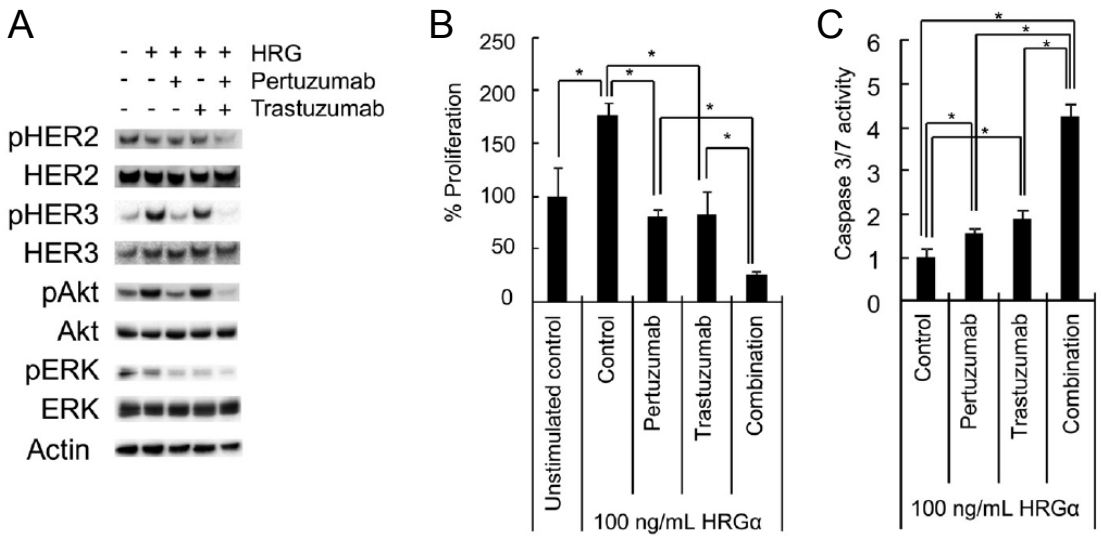

Figure 5 Effect of pertuzumab in combination with trastuzumab on the signal transduction of HER2 and HER3. A, NCI-N87 cells were treated with pertuzumab (20 μg/mL), trastuzumab (20 μg/mL) or both for 3.5 h followed by HRGα (100 ng/mL) stimulation for 5 min. The phosphorylation levels of HER2 and HER3 in the cell lysates were detected by western blotting. B, the cell growth inhibition in the presence of HRGα was examined. NCI-N87 cells were treated with pertuzumab (20 μg/mL), trastuzumab (20 μg/mL) or both 30 min before the addition of HRGα (100 ng/mL). Control was untreated cells. The cell proliferation was examined three days after treatment. Data points are mean + SD (n = 3). Statistically significant differences are shown as *: $P < 0.05$ by the t-test. C, the caspase 3/7 activity of pertuzumab and trastuzumab combination was measured. NCI-N87 cells were treated with pertuzumab (20 μg/mL), trastuzumab (20 μg/mL) or both 30 min before the addition of HRGα (100 ng/mL). Control was untreated cells. The caspase 3/7 activity was measured 24 h after treatment. Data points are mean + SD (n = 5). Statistically significant differences are shown as *: $P < 0.05$ by the t-test.

trastuzumab on HER2, even though both antibodies are displayed in their whole IgG conformation. This result indicates that pertuzumab and trastuzumab could have combination effects on antitumor activity.

The author examined the efficacy of pertuzumab and trastuzumab *in vivo*. The reason for *in vivo* study is that the *in vivo* models indicate the efficacy of this antitumor activity more accurately, because trastuzumab or pertuzumab have a mechanism through ADCC activity. The author used NCI-N87 and 4-1ST as HER2-positive models. NCI-N87 and 4-1ST were determined as HER2 2+ and 3+ respectively by IHC (HercepTest®) and FISH (Pathvysion®) in the previous study of Fujimoto-Ouchi *et al*. (9). MKN-28 was determined to be a HER2-negative cell line (9), so the author used it as a negative control model. At first, the author examined the dose dependent activity of pertuzumab on tumor growth in the xenograft model to determine the combination dose. In the NCI-N87 model, 3-week treatment with pertuzumab showed a significant antitumor activity at 40 and 80 mg/kg. The maximum effective dose of pertuzumab was determined as 40 mg/kg, because the efficacy of 40 mg/kg of pertuzumab was the same as that of 80 mg/kg (TGI% was 46% and 41%, respectively). Next, the author examined

the antitumor activity of pertuzumab in combination with trastuzumab. In the NCI-N87 HER2-positive xenograft model, remarkable tumor regression was observed. The antitumor activity of the combination group was more potent than that of the maximum effective dose of both antibodies as single agents (the TGI% of the current combinational study was 145% and the maximum TGI% of pertuzumab and trastuzumab were 46% in the current study and 89% in a separate experiment (9) respectively.). Another HER2-positive model 4-1ST also showed a potent effect of the pertuzumab and trastuzumab combination. Meanwhile, in MKN-28, a HER2-negative tumor model expressing HER1 or HER3, an effect of the combination was not shown. Therefore, the usefulness of this combination would only be observed in HER2-positive tumors. The author could not examine the safety profile except for body weight in the present study because of species difference. No significant loss of body weight was observed. In the present study, the author used subcutaneous xenograft models. However, orthotopic models might reflect actual tumors better and it would be interesting to know if the same efficacy would be shown in the orthotopic models.

In order to explain the strongly enhanced antitumor efficacy of pertuzumab and trastuzumab combination treatment, the author hypothesized two mechanisms, direct action on tumor cells and a specific mechanism caused by the tumor environment. Actually, pertuzumab showed more potent cell-growth inhibition and apoptosis activity in combination with trastuzumab than either pertuzumab or trastuzumab monotherapy showed *in vitro*, and the efficacy of the combination in mouse xenograft models was more remarkable than *in vitro*. As the direct action on tumor cells, the author examined whether pertuzumab in combination with trastuzumab enhanced the inhibition of HER2 signal transduction. In the analysis of inhibition of the signaling pathways through HER1 and HER2, down-regulation of pHER1, pHER2, pAkt and pERK1/2 was observed in the combination group compared to the single agents. The author also showed that pertuzumab in combination with trastuzumab reduced EGFR-HER2 heterodimers with Duolink® *in situ* PLA™, which was reported to detect heterodimers (64, 65). Others reported that pertuzumab could enhance the endocytic down-regulation of EGFR by counteracting the EGFR-HER2 heterodimerization (66). In the HER2-positive gastric cancer model that the author used, only a little decrease in EGFR-HER2 heterodimers was detected by pertuzumab alone. Anyway, the author considers that one mechanism of the effect of the combination of pertuzumab and trastuzumab is the reduction of EGFR-HER2 heterodimers and

their signal transduction. In NCI-N87, HER3 expression was low and the author considered that EGFR and HER2 were mainly functional. However, HER2-HER3 heterodimer is considered the most active HER signaling dimer (57, 67) and there are some reports suggesting that pertuzumab show antitumor activity through HER2-HER3 signal inhibition in non-small cell lung cancer and breast cancer (68, 69). In fact, HRGα induced the phosphorylation of HER3 and Akt in NCI-N87, and pertuzumab in combination with trastuzumab reduced them strongly; therefore, it is possible that low expression of HER3 was functional in this model and that pertuzumab in combination with trastuzumab also showed antitumor activity by inhibiting HER2-HER3 signaling as well as EGFR-HER2 signaling. In this study, total HER2 level of the combination was decreased. It is reported that anti-HER2 antibodies like trastuzumab led to degradation through the c-Cbl-regulated proteolytic pathway (70, 71). The author could not examine the signal inhibition in 4-1ST model because it was an *in vivo*-maintained cell line. In this study, it was suggested that both the EGFR-HER2 and the HER2-HER3 signaling were involved in the tumor growth inhibition of the combination of pertuzumab and trastuzumab. Comparing the degree of cell growth, the HER3-dependent cell growth was inhibited more strongly than the EGFR-dependent cell growth. However, it should not be concluded that HER3 is more important than EGFR for the clinical therapy of HER2-positive gastric cancer, and the contributing rate of EGFR and HER3 to HER-signaling might be different between types of cancer (e.g. gastric cancer and breast cancer). In a HER2-positive breast cancer cell line, KPL-4, where pertuzumab in combination with trastuzumab showed strongly enhanced antitumor activity (56), EGF did not stimulate phosphorylation of EGFR, but HRGα did phosphorylate HER3 (data not shown). It is necessary to examine exhaustively whether EGFR or HER3 is valuable as a secondary biomarker in clinical research from many points of view, such as the expression level of ligands or HER family proteins.

As an *in vivo*-specific mechanism caused by the tumor environment, the author considered the potentiation of ADCC activity and anti-angiogenic activity. ADCC activity is one of the key mechanisms of the antitumor activity of trastuzumab (72). Moreover, recent reports showed that pertuzumab also had ADCC activity (56, 73). Anti-angiogenic activity is also shown as the mechanism of antitumor activity of trastuzumab (5). The author examined the potentiation of ADCC, because both trastuzumab and pertuzumab showed antitumor activity through ADCC activity. ADCC was measured using RTCA, reported as a new method by which it is possible to observe cell

adhesion areas according to time (74). The degree of ADCC measured with RTCA was equivalent to that of measured with ^{51}Cr-release assay. The author tried to use CD16-transfected NK-92 as the effector cell. The ADCC of trastuzumab was reported using the NK-92 cell, a human NK cell line (75). However, the NK-92 cell used in the study did not show ADCC activity to the target cell NCI-N87. Using this CD16-transfected cell line, the ADCC activity of pertuzumab or trastuzumab on NCI-N87 was observed, and that of the combination group was significantly more potent. In a breast cancer model, another report showed that pertuzumab in combination with trastuzumab did not enhance ADCC activity of either antibody alone (56). This difference may be due to the different materials and methods. Secondly, the author tried to clarify the anti-angiogenic activity of these antibodies. In the combination group, a significant decrease in MVD and the VEGF protein in tumor tissue was observed. VEGF has been reported as a key angiogenic factor in tumors (76). Therefore, it was considered that pertuzumab in combination with trastuzumab decreased MVD by reduction of VEGF as a result of HER2 signal inhibition. Based on these results, the potent activity of the combination was due to enhancement of the ADCC activity and anti-angiogenic activity in addition to direct cell growth inhibition through HER2 signal inhibition.

In conclusion, compared to single agent treatment, pertuzumab in combination with trastuzumab showed significantly stronger antitumor activity in HER2-positive human gastric cancer mouse xenograft models through the enhancement of direct cell growth inhibition, ADCC activity, and anti-angiogenesis activity. The combination therapy of pertuzumab and trastuzumab is worth examining as a new therapy for HER2 positive gastric cancer.

References

1. Ferlay J, Shin HR, Bray F, Forman D, Mathers C, Parkin DM. Estimates of worldwide burden of cancer in 2008: GLOBOCAN 2008. Int J Cancer. 2010; 127: 2893-917.

2. Yarden Y, Sliwkowski MX. Untangling the ErbB signalling network. Nat Rev Mol Cell Biol 2001; 2:127-37.

3. Garcia I, Vizoso F, Martin A, Sanz L, Abdel-Lah O, Raigoso P, et al. Clinical significance of the epidermal growth factor receptor and HER2 receptor in resectable gastric cancer. Ann Surg Oncol 2003; 10:234-41.

4. Yonemura Y, Ninomiya I, Yamaguchi A, Fushida S, Kimura H, Ohoyama S, et al. Evaluation of immunoreactivity for erbB-2 protein as a marker of poor short term prognosis in gastric cancer. Cancer Res 1991; 51:1034-8.

5. Tanner M, Hollmen M, Junttila TT, Kapanen AI, Tommola S, Soini Y, et al. Amplification of HER-2 in gastric carcinoma: association with Topoisomerase IIalpha gene amplification, intestinal type, poor prognosis and sensitivity to trastuzumab. Ann Oncol 2005; 16:273-8.

6. Nicholson RI, Gee JM, Harper ME. EGFR and cancer prognosis. Eur J Cancer 2001; 37 Suppl 4:S9-15.

7. Hayashi M, Inokuchi M, Takagi Y, Yamada H, Kojima K, Kumagai J, et al. High expression of HER3 is associated with a decreased survival in gastric cancer. Clin Cancer Res 2008; 14:7843-9.

8. Bang YJ, Van Cutsem E, Feyereislova A, Chung HC, Shen L, Sawaki A, et al. Trastuzumab in combination with chemotherapy versus chemotherapy alone for treatment of HER2-positive advanced gastric or gastro-oesophageal junction cancer (ToGA): a phase 3, open-label, randomised controlled trial. Lancet 2010; 376:687-97.

9. Barok M, Isola J, Palyi-Krekk Z, Nagy P, Juhasz I, Vereb G, et al. Trastuzumab causes antibody-dependent cellular cytotoxicity-mediated growth inhibition of submacroscopic JIMT-1 breast cancer xenografts despite intrinsic drug resistance. Mol Cancer Ther 2007; 6:2065-72.

10. Musolino A, Naldi N, Bortesi B, Pezzuolo D, Capelletti M, Missale G, et al. Immunoglobulin G fragment C receptor polymorphisms and clinical efficacy of trastuzumab-based therapy in patients with HER-2/neu-positive

metastatic breast cancer. J Clin Oncol 2008; 26:1789-96.

11. Molina MA, Codony-Servat J, Albanell J, Rojo F, Arribas J, Baselga J. Trastuzumab (herceptin), a humanized anti-Her2 receptor monoclonal antibody, inhibits basal and activated Her2 ectodomain cleavage in breast cancer cells. Cancer Res 2001; 61:4744-9.

12. Izumi Y, Xu L, di Tomaso E, Fukumura D, Jain RK. Tumour biology: herceptin acts as an anti-angiogenic cocktail. Nature 2002; 416:279-80.

13. Buzdar AU, Valero V, Ibrahim NK, Francis D, Broglio KR, Theriault RL, et al. Neoadjuvant therapy with paclitaxel followed by 5-fluorouracil, epirubicin, and cyclophosphamide chemotherapy and concurrent trastuzumab in human epidermal growth factor receptor 2-positive operable breast cancer: an update of the initial randomized study population and data of additional patients treated with the same regimen. Clin Cancer Res 2007; 13:228-33.

14. Romond EH, Perez EA, Bryant J, Suman VJ, Geyer CE, Jr., Davidson NE, et al. Trastuzumab plus adjuvant chemotherapy for operable HER2-positive breast cancer. N Engl J Med 2005; 353:1673-84.

15. Smith I, Procter M, Gelber RD, Guillaume S, Feyereislova A, Dowsett M, et al. 2-year follow-up of trastuzumab after adjuvant chemotherapy in HER2-positive breast cancer: a randomised controlled trial. Lancet 2007; 369:29-36.

16. Fujimoto-Ouchi K, Sekiguchi F, Yasuno H, Moriya Y, Mori K, Tanaka Y. Antitumor activity of trastuzumab in combination with chemotherapy in human gastric cancer xenograft models. Cancer Chemother Pharmacol 2007; 59:795-805.

17. Franklin MC, Carey KD, Vajdos FF, Leahy DJ, de Vos AM, Sliwkowski MX. Insights into ErbB signaling from the structure of the ErbB2-pertuzumab complex. Cancer Cell 2004; 5:317-28.

18. Baselga J, Gelmon KA, Verma S, Wardley A, Conte P, Miles D, et al. Phase II trial of pertuzumab and trastuzumab in patients with human epidermal growth factor receptor 2-positive metastatic breast cancer that progressed during prior trastuzumab therapy. J Clin Oncol 2010; 28:1138-44.

19. Scheuer W, Friess T, Burtscher H, Bossenmaier B, Endl J, Hasmann M. Strongly enhanced antitumor activity of trastuzumab and pertuzumab combination treatment on HER2-positive human xenograft tumor models. Cancer Res 2009; 69:9330-6.

20. Baselga J, Swain SM. Novel anticancer targets: revisiting ERBB2 and discovering ERBB3. Nat Rev Cancer 2009; 9:463-75.

21. Cho HS, Mason K, Ramyar KX, Stanley AM, Gabelli SB, Denney DW, Jr., et al. Structure of the extracellular region of HER2 alone and in complex with the Herceptin Fab. Nature 2003; 421:756-60.

22. Harris LJ, Skaletsky E, McPherson A. Crystallographic structure of an intact IgG1 monoclonal antibody. J Mol Biol 1998; 275:861-72.

23. Niwa H, Yamamura K, Miyazaki J. Efficient selection for high-expression transfectants with a novel eukaryotic vector. Gene 1991; 108:193-9.

24. Fujimoto-Ouchi K, Sekiguchi F, Tanaka Y. Antitumor activity of combinations of anti-HER-2 antibody trastuzumab and oral fluoropyrimidines capecitabine/5'-dFUrd in human breast cancer models. Cancer Chemother Pharmacol 2002; 49:211-6.

25. Yanagisawa M, Yorozu K, Kurasawa M, Nakano K, Furugaki K, Yamashita Y, et al. Bevacizumab improves the delivery and efficacy of paclitaxel. Anticancer Drugs 2010; 21:687-94.

26. Klos KS, Zhou X, Lee S, Zhang L, Yang W, Nagata Y, et al. Combined trastuzumab and paclitaxel treatment better inhibits ErbB-2-mediated angiogenesis in breast carcinoma through a more effective inhibition of Akt than either treatment alone. Cancer 2003; 98:1377-85.

27. Cai Z, Zhang G, Zhou Z, Bembas K, Drebin JA, Greene MI, et al. Differential binding patterns of monoclonal antibody 2C4 to the ErbB3-p185her2/neu and the EGFR-p185her2/neu complexes. Oncogene 2008; 27:3870-4.

28. Nilsson I, Bahram F, Li X, Gualandi L, Koch S, Jarvius M, et al. VEGF receptor 2/-3 heterodimers detected *in situ* by proximity ligation on angiogenic sprouts. EMBO J 2010; 29:1377-88.

29. Greenberg JI, Shields DJ, Barillas SG, Acevedo LM, Murphy E, Huang J, et al. A role for VEGF as a negative regulator of pericyte function and vessel maturation. Nature 2008; 456:809-13.

30. Hughes JB, Berger C, Rodland MS, Hasmann M, Stang E, Madshus IH. Pertuzumab increases epidermal growth factor receptor down-regulation by counteracting epidermal growth factor receptor-ErbB2 heterodimerization. Mol Cancer Ther 2009; 8:1885-92.

31. Olayioye MA, Neve RM, Lane HA, Hynes NE. The ErbB signaling network: receptor heterodimerization in development and cancer. EMBO J 2000; 19:3159-67.

32. Sakai K, Yokote H, Murakami-Murofushi K, Tamura T, Saijo N, Nishio K. Pertuzumab, a novel HER dimerization inhibitor, inhibits the growth of human lung cancer cells mediated by the HER3 signaling pathway. Cancer Sci 2007; 98:1498-503.

33. Lee-Hoeflich ST, Crocker L, Yao E, Pham T, Munroe X, Hoeflich KP, et al. A central role for HER3 in HER2-amplified breast cancer: implications for targeted therapy. Cancer Res 2008; 68:5878-87.

34. Yarden Y. Biology of HER2 and its importance in breast cancer. Oncology 2001; 61 Suppl 2:1-13.

35. Ohta T, Fukuda M. Ubiquitin and breast cancer. Oncogene 2004; 23:2079-88.

36. Spector NL, Blackwell KL. Understanding the mechanisms behind trastuzumab therapy for human epidermal growth factor receptor 2-positive breast cancer. J Clin Oncol 2009; 27:5838-47.

37. El-Sahwi K, Bellone S, Cocco E, Cargnelutti M, Casagrande F, Bellone M, et al. *In vitro* activity of pertuzumab in combination with trastuzumab in uterine serous papillary adenocarcinoma. Br J Cancer 2010; 102:134-43.

38. Glamann J, Hansen AJ. Dynamic detection of natural killer cell-mediated cytotoxicity and cell adhesion by electrical impedance measurements. Assay Drug Dev Technol 2006; 4:555-63.

39. Kute TE, Savage L, Stehle JR, Jr., Kim-Shapiro JW, Blanks MJ, Wood J, et al. Breast tumor cells isolated from *in vitro* resistance to trastuzumab remain sensitive to trastuzumab anti-tumor effects *in vivo* and to ADCC killing. Cancer Immunol Immunother 2009; 58:1887-96.

40. Ferrara N. Vascular endothelial growth factor. Arterioscler Thromb Vasc Biol 2009; 29:789-91.

2. Enhanced antitumor activity of trastuzumab emtansine (T-DM1) in combination with pertuzumab in a HER2-positive gastric cancer model

Introduction

Trastuzumab emtansine (T-DM1) is a HER2-targeted antibody-drug conjugate (ADC), composed of microtubule polymerization inhibitor DM1 (a derivative of maytansine) linked to trastuzumab. T-DM1 is designed to deliver DM1 into HER2-overexpressing tumor cells. Namely, T-DM1 binds to HER2 on tumor cells, followed by internalization and degradation in lysosomes. As a consequence, active DM1 is liberated intracellularly from T-DM1 (77-79) and inhibits microtubule assembly causing cell apoptosis/death (80, 81). In addition, T-DM1 has been shown to retain the mechanism of action of trastuzumab as an antibody, including antibody-dependent cellular cytotoxicity (ADCC), inhibition of cell signaling through the phosphatidylinositol 3-kinase (PI3K)/AKT pathway, and inhibition of HER2 shedding (82, 83). To investigate the clinical effectiveness of T-DM1, two phase III trials, EMILIA (evaluating T-DM1 compared with lapatinib plus capecitabine for patients with HER2-positive metastatic breast cancer previously treated with trastuzumab and a taxane) and MARIANNE (evaluating T-DM1 plus placebo versus T-DM1 plus pertuzumab versus trastuzumab plus a taxane for patients with previously untreated HER2-positive metastatic breast cancer) (84) are under way.

Thus, therapies containing anti-HER2 antibodies are expected to be of great clinical significance. In a previous study, the author showed an enhanced antitumor activity of trastuzumab in combination with pertuzumab and described its mechanism of action in a HER2-positive gastric cancer model (85). In this context, the author believes that the combination of T-DM1 with pertuzumab could be a new potential therapy for advanced gastric cancer. Therefore, in the present study, the author investigated the combination effects of T-DM1 and pertuzumab on antitumor activities in vitro and in vivo using HER2-positive human gastric cancers.

Materials and methods

Test agents

T-DM1 and pertuzumab were provided by F. Hoffmann-La Roche (Basel, Switzerland). Both antibodies were diluted with saline or culture medium in *in vivo* or *in vitro* experiments, respectively. Human immunoglobulin G (IgG) was purchased from MP Biomedicals, Inc. (Aurora, OH, USA) and reconstituted with water and diluted with saline.

Animals

Five-week-old male BALB-nu/nu mice (CAnN.Cg-Foxn1<nu>/CrlCrlj nu/nu) were obtained from Charles River Laboratories Japan (Yokohama, Japan). All animals were acclimatized for 1 week prior to the study. The health of the mice was monitored daily. Chlorinated water and irradiated food were provided ad libitum, and the animals were maintained under a controlled light–dark cycle (12 h–12 h). All animal experiments were conducted in accordance with the Institutional Animal Care and Use Committee.

Cell lines and culture

Five human gastric cancer cell lines were used in the present study: NCI-N87; SNU-16; SCH; MKN-28; and 4-1ST. NCI-N87 and SNU-16 cells were purchased from ATCC. SCH cells were purchased from Japan Health Science Foundation (Osaka, Japan). MKN-28 cells were purchased from Immuno-Biological Laboratories Co., Ltd. (Fujioka, Japan). NCI-N87, SNU-16, SCH, and MKN-28 were maintained in RPMI-1640 (Sigma-Aldrich, St. Louis, MO, USA), supplemented with 10% FBS at 37°C under 5% CO_2. 4-1ST cells were purchased from the Central Institute for Experimental Animals (Yokohama, Japan) and maintained in BALB-nu/nu mice by subcutaneous (sc) inoculation of pieces of tumor. CD16(158V)/NK-92 cells were constructed as described previously (85) and were maintained in MEMα (Wako Pure Chemical Industries, Osaka, Japan) supplemented with 12.5% FBS, 12.5% horse serum, 0.02 mM folic acid, 0.1 mM 2-mercaptoethanol, 0.2 mM inositol, 0.5 mg/mL G418, and 20 ng/mL recombinant human IL-2 at 37°C under 5% CO_2.

Immunohistochemistry and fluorescent *in situ* hybridization

As previously described, HER2 protein expression and HER2 gene amplification in tumors were examined by immunohistochemistry (IHC) using HercepTest™ (Dako Japan, Tokyo, Japan) and fluorescent *in situ* hybridization (FISH) using Path Vysion® (Abbott Japan, Tokyo, Japan), respectively (9).

***In vivo* tumor growth inhibition studies**

Each mouse was inoculated subcutaneously in the right flank with either 5×10^6 cells of human gastric cancer cell lines NCI-N87, SCH, SNU-16 or MKN-28, or with an approximately 8 mm^3 piece of 4-1ST tumor tissue. Several weeks after tumor inoculation, mice were randomly allocated to control and treatment groups.

The administration of anticancer agents was started when the tumor volumes reached approximately 150 to 350 mm^3. T-DM1 was administered intravenously once every 3 weeks and pertuzumab was administered intraperitoneally once a week for 6 weeks. To evaluate the antitumor activity of the test agents, tumor volume was measured twice a week and the percentage of tumor growth inhibition (TGI%) was calculated as described previously (33).

***In vitro* anti-proliferation assays**

NCI-N87 cells were seeded on 96-well plates at 1×10^4 cells/well and pre-cultured for 24 h. Afterwards, the cells were starved in serum-free RPMI-1640 for 24 h and treated with pertuzumab, T-DM1, or both. Following 30 min of incubation, cells were exposed to 100 ng/mL of EGF or heregulin (HRG) α and incubated for 2 days. Cells were fixed with 10% formalin neutral buffer solution. Crystal violet staining and extraction were performed as described previously (9) and absorbance was measured at 595 nm. Cells pre-cultured for 24 h were also detected by crystal violet staining as the absorbance of the pre-cultured well. The percentage of cell proliferation (% proliferation) was calculated as follows: % proliferation = (absorbance of treatment well – absorbance of pre-cultured well)/(absorbance of unstimulated well – absorbance of pre-cultured well) × 100.

Apoptosis assay

NCI-N87 cells were seeded on 96-well plates at 1×10^4 cells/well and cultured in 0.1% FBS medium with 100

ng/mL of EGF or HRG α added for 24 h. After that, cells were treated with pertuzumab, T-DM1, or both. Twenty-four hours after treatment, Caspase-Glo® 3/7 Assay (Promega, Madison, WI, USA) was used to measure caspase 3/7 activity, which was calculated as follows: caspase 3/7 activity = (luminescent unit of treatment well – luminescent unit of blank well)/(mean luminescent unit of control well).

Western blotting

NCI-N87 cells were seeded in 0.1% FBS RPMI-1640 for 24 h and then treated with IgG as the control or with 40 μg/ml pertuzumab, 5 μg/ml T-DM1, or both. Following incubation for 1 h, cells were exposed to EGF or HRG α for 1 or 5 min, respectively. Cells were washed with ice-cold PBS and then lysed with Cell Lysis Buffer (Cell Signaling Technology, Beverly, MA, USA) with 10 mM NaF, 1 μg/mL aprotinin, and 1 mM PMSF. After centrifugation (4°C, 14,000 × *g*, 5 min), the resultant supernatants were used for the Western blotting assays.

To prepare *in vivo* samples, tumor samples were taken on day 5 (4 days after treatment) and immediately frozen in liquid nitrogen and stored at -80°C. Tumor samples were homogenized in Cell Lysis Buffer, and centrifuged (4°C, 10,000 × *g*, 20 min.). The resultant supernatants were used for the Western blotting assays.

The protein concentration of the supernatant was quantified using the DC protein assay kit (Bio-Rad Laboratories, Hercules, CA, USA). The supernatants were denatured for 5 min at 95°C, electrophoresed on SDS-PAGE and transferred to a polyvinylidene difluoride membrane (Millipore, Bedford, MA, USA). The membrane was blocked in SuperBlock® T20 (TBS) Blocking Buffer (Thermo Scientific, Waltham, MA, USA) and probed with each antibody against HER3 (sc-285), (Santa Cruz Biotechnology, Santa Cruz, CA, USA), HER2 (#2248), EGFR (#2963), pEGFR (Tyr1068) (#3777), pHER2 (Tyr1248) (#2247), pHER3 (Tyr1289) (#4791), AKT (#9272), pAkt (Ser473) (#9271), ERK1/2 (#9102), pERK1/2 (Thr202/Tyr204) (#9106) (Cell Signaling Technology), and actin (A2228) (Sigma-Aldrich) as primary antibodies. These proteins were detected by horseradish peroxidase-conjugated secondary antibodies. The bands were visualized using Chemi-Lumi One Super (Nacalai Tesque, Kyoto, Japan).

Table 1 Antitumor activity of T-DM1 as a single agent in human gastric cancer mouse xenograft models

Tumor name	HER2 IHC score	HER2/CEP17 ratio (FISH)	Tumor volume (mm^3)			TGI%
			Treatment	Day 1	Day 22	
NCI-N87	3+	8.4[b]	Control	174±25	667±152	133
			T-DM1	174±24	11±9[a]	
4-1ST	3+	16.5	Control	283±75	1320±396	126
			T-DM1	283±72	12±18[a]	
SCH	2+	2.1	Control	240±51	1565±223	109
			T-DM1	241±63	121±25[a]	
SNU-16	1+	1.4[b]	Control	185±23	485±116	39
			T-DM1	184±16	369±47	
MKN-28	0	1.0[b]	Control	271±50	1662±286	27
			T-DM1	269±52	1290±507	

$n = 5\sim6$, mean ± SD, a: $P < 0.05$ by the Wilcoxon test, Day 1: first day of treatment, Day 22: 21 days after starting treatment, TGI%: % of tumor growth inhibition, b: citation data from [19].

ADCC assays

The author used Real-time Cell Analyzer (xCELLigence, Roche Diagnostics, Tokyo, Japan) to monitor ADCC activity in real time. The system detects electrical impedance on the bottom of the tissue culture E-Plates, which contain interdigitated electrodes as the Cell Index. NCI-N87 cells were seeded on E-plates at 5×10^3 cells/well and pre-cultured for 24 h. CD16(158V)/NK-92 cells were added as effector cells at a target ratio of 1:1. Cells were treated with pertuzumab, T-DM1, or both concurrently. The Cell Index was measured every 5 min for the first 4 h and every 10 min thereafter. The Normalized Cell Index was calculated as follows: (Cell Index at each point)/(Cell Index at the point when pertuzumab and T-DM1 treatment started).

Statistical analysis

The Wilcoxon test was used to detect differences in tumor volume for *in vivo* experiments and Student's *t*-test was used for *in vitro* experiments, with $P < 0.05$ considered statistically significant. Statistical analyses were carried out using the SAS preclinical package (SAS Institute, Tokyo, Japan).

Results

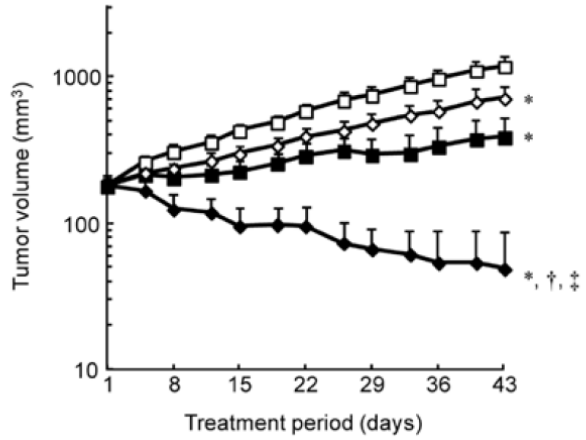

Figure 1. *In vivo* efficacy of T-DM1 in combination with pertuzumab. Mice bearing NCI-N87 tumors were randomly divided into 4 groups (n = 6/group) and treated with 40 mg/kg of HuIgG as a control (open square), 5 mg/kg of T-DM1 (filled square), 40 mg/kg of pertuzumab (open rhombus) or 5 mg/kg of T-DM1 and 40 mg/kg of pertuzumab (filled rhombus). Data points are mean + SD of the tumor volume (mm^3). Statistically significant differences are shown as *: $P < 0.05$ vs. the control group; †: $P < 0.05$ vs. the T-DM1 group; ‡: $P < 0.05$ vs. the pertuzumab group using the Wilcoxon test.

Antitumor activity of T-DM1 as a single agent in human gastric cancer mouse xenograft models

Antitumor activity of T-DM1 was evaluated in 5 gastric tumor models with various HER2 statuses. NCI-N87, 4-1ST and SCH xenografted tumors exhibited high HER2 expression with IHC scores of 3+ or 2+ and a FISH HER2/CEP17 ratio >2.0. SNU-16 and MKN-28 showed low HER2 expression with IHC scores of 1+ or 0 and a <2.0 FISH ratio. On day 22 (21 days after treatment), T-DM1 (20 mg/kg) showed significant antitumor activity in the xenograft models with high HER2 expression and decreasing tumor volumes. However, T-DM1 did not show significant efficacy for tumors with low HER2 expression (Table 1).

Antitumor activity of T-DM1 in combination with pertuzumab in a HER2-positive gastric cancer mouse xenograft model

The author assessed the combined efficacy of T-DM1 with pertuzumab using a NCI-N87 xenograft model which expressed high levels of HER2 and was sensitive to T-DM1 treatment. Compared to each antibody alone, T-DM1 in combination with pertuzumab showed significantly enhanced antitumor activity (Fig. 1).

Combination effect of T-DM1 and pertuzumab on proliferation and apoptosis in a HER2-positive human gastric cancer cell line

To investigate the mechanism of action of T-DM1 in combination with pertuzumab, the author examined the growth inhibitory effect of T-DM1 and pertuzumab in NCI-N87 cells. These cells have been previously shown to be

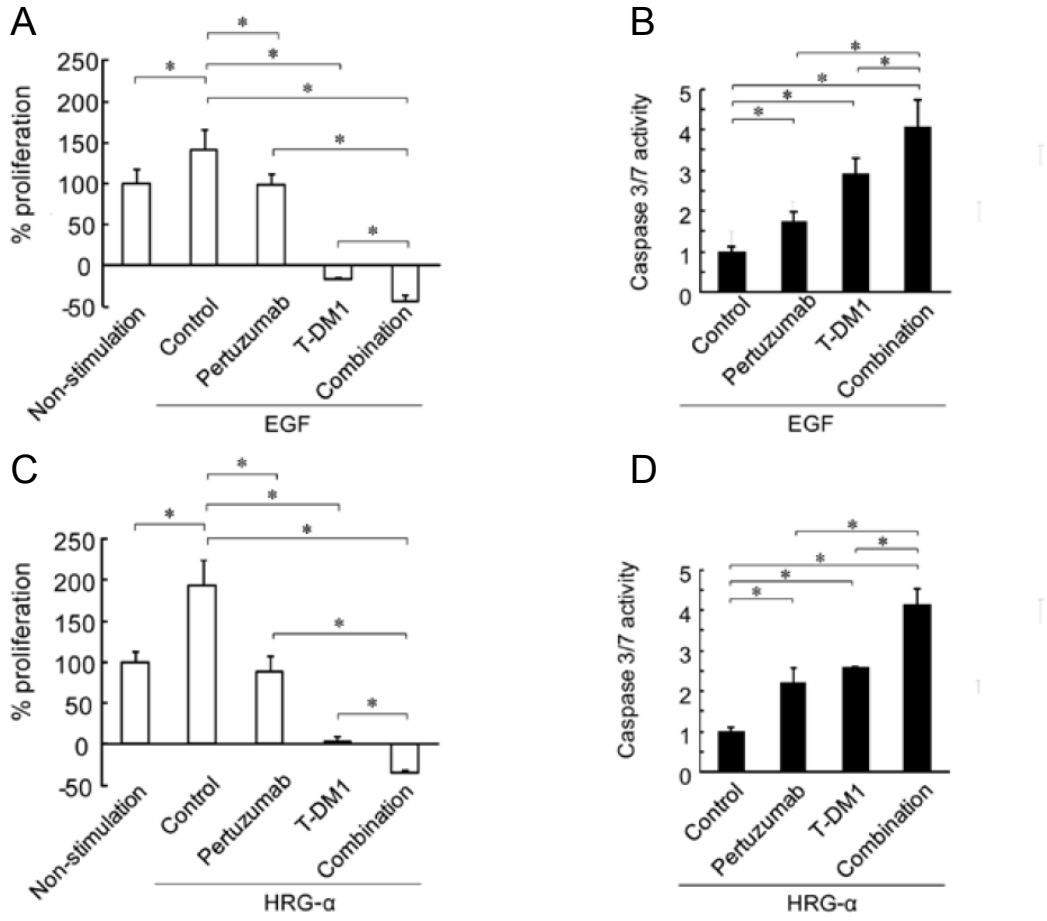

Figure 2. ***In vitro*** **efficacy of T-DM1 combined with pertuzumab on cell proliferation and apoptosis.** A, C, Inhibition of cell growth induced by pertuzumab (40 μg/mL), T-DM1 (5 μg/mL), or both in the presence of EGF (A) or HRG α (C) was examined in NCI-N87 cells. Control cells were treated with human IgG. Cell proliferation was examined 2 days after treatment. Data points are mean + SD (n = 5). B, D, Caspase 3/7 activity in cells treated with pertuzumab and trastuzumab combination was measured in the presence of EGF (B) or HRG α (D). Caspase 3/7 activity in NCI-N87 cells was measured 24 h after treatment with pertuzumab (20 μg/mL), T-DM1 (10 μg/mL), or both. Data points are mean + SD (n = 5). Statistically significant differences are shown as *: $P < 0.05$ using the t-test.

positive for both HER2 and EGFR and also express low levels of HER3 (85). Pertuzumab completely blocked EGF-stimulated cell proliferation, and T-DM1 stopped cell growth at the initial cell number. In the presence of EGF, T-DM1 combined with pertuzumab significantly enhanced the inhibition of cell proliferation compared to T-DM1 alone (Fig. 2A). The author also examined the apoptotic activity of these agents by measuring caspase 3/7 activity. Treatment with both pertuzumab and T-DM1 significantly induced caspase 3/7 activity compared to treatment with either single agent, indicating that pertuzumab in combination with T-DM1 significantly enhanced the apoptosis-inducing activity of T-DM1 (Fig. 2B). Then, the author evaluated the growth inhibition and apoptotic activity induced by T-DM1 in combination with pertuzumab in NCI-N87 cells when stimulated with HRG α.

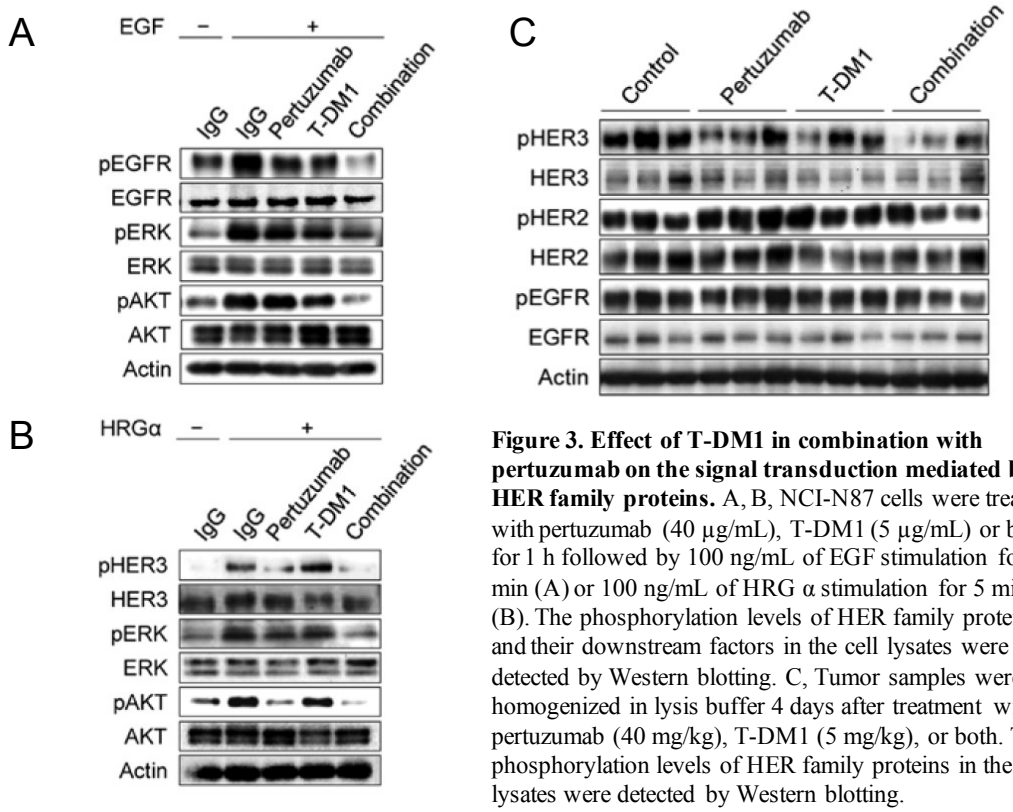

Figure 3. Effect of T-DM1 in combination with pertuzumab on the signal transduction mediated by HER family proteins. A, B, NCI-N87 cells were treated with pertuzumab (40 μg/mL), T-DM1 (5 μg/mL) or both for 1 h followed by 100 ng/mL of EGF stimulation for 1 min (A) or 100 ng/mL of HRG α stimulation for 5 min (B). The phosphorylation levels of HER family proteins and their downstream factors in the cell lysates were detected by Western blotting. C, Tumor samples were homogenized in lysis buffer 4 days after treatment with pertuzumab (40 mg/kg), T-DM1 (5 mg/kg), or both. The phosphorylation levels of HER family proteins in the cell lysates were detected by Western blotting.

Similar to the stimulation with EGF, combining pertuzumab and T-DM1 significantly enhanced the anti-proliferative activity in HRG α-stimulated cells. Likewise, the increased caspase 3/7 activity seen with pertuzumab and T-DM1 as single agents was further enhanced by their combination under HRG α (Fig. 2C, D). These results suggest that T-DM1 in combination with pertuzumab has the potential to suppress ligand-dependent cell growth by inducing apoptosis.

Effect of T-DM1 in combination with pertuzumab on HER2 signal transduction

To examine whether pertuzumab and T-DM1 could inhibit HER2 signal transduction, the author examined the phosphorylation status of the molecules in HER2-EGFR or HER2-HER3 signaling pathways. Under EGF stimulation, only T-DM1 combined with pertuzumab strongly suppressed phosphor(p)-EGFR, pERK, and pAKT (Fig. 3A). Under HRG α stimulation, pertuzumab alone strongly inhibited pHER3 and, in combination with T-DM1, almost completely suppressed pHER3 and downstream pAKT. T-DM1 in combination with pertuzumab further reduced pERK in comparison with pertuzumab or T-DM1 alone (Fig. 3B). To confirm whether the HER family signaling pathway was also inhibited by this therapy in xenografted tumors, tumor specimens collected 4 days after

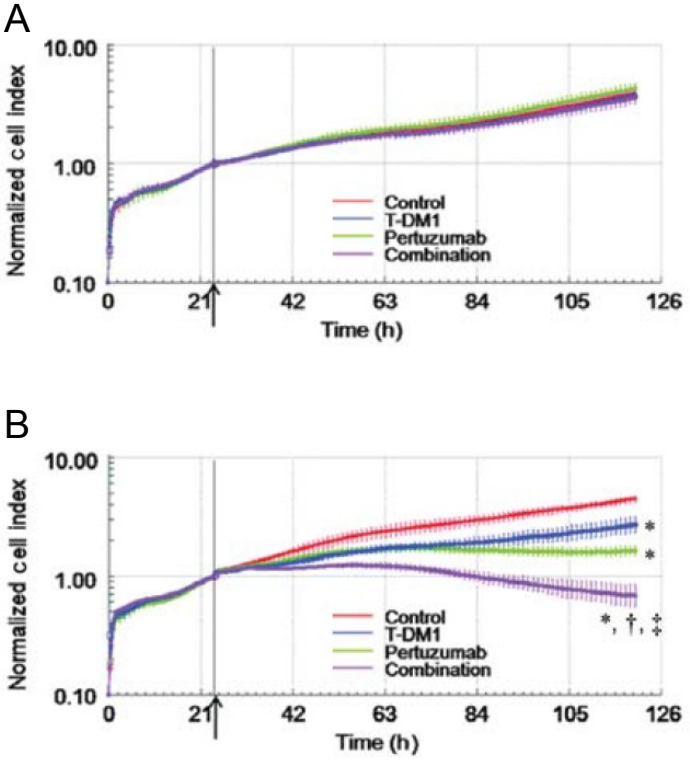

Figure 4. Effect of T-DM1 in combination with pertuzumab on ADCC activity. A, B, ADCC activity was examined using RTCA (A) without or (B) with NK cells. NCI-N87 cells were treated with T-DM1 (1 ng/mL), pertuzumab (10 ng/mL), or both. Cell Indices were normalized at the treatment point (at the point of arrows). Red: Control (HuIgG-treatment) group; Blue: T-DM1 group; Green: Pertuzumab group; and Magenta: Combination group. Data points are mean ± SD (n = 3). Statistically significant differences are shown as *: $P <$ 0.05 vs. the control group; †: $P <$ 0.05 vs. the T-DM1 group; and ‡: $P <$ 0.05 vs. the pertuzumab group using the t-test.

treatment were tested for the phosphorylation level of HER family receptors: pHER2, pEGFR, and pHER3. pHER2 and pEGFR were slightly reduced whereas pHER3 was clearly reduced by the combination of T-DM1 with pertuzumab compared to either T-DM1 or pertuzumab alone (Fig. 3C).

ADCC activity of T-DM1 in combination with pertuzumab

One way to interpret the different antitumor potency observed *in vitro* and *in vivo* is to consider an immune effector-mediated activity, such as ADCC. Hence, the author examined whether T-DM1-induced ADCC activity in NCI-N87 cells was further enhanced by pertuzumab, using a real-time cell analyzer. In the wells without effector cells, the addition of pertuzumab and T-DM1 did not reduce the Normalized Cell Index (Fig. 4A). With effector cells, however, the Normalized Cell Index was significantly reduced by the addition of each single agent. Furthermore, T-DM1 in combination with pertuzumab significantly enhanced the reduction of the Normalized Cell Index induced by either T-DM1 or pertuzumab (Fig. 4B), indicating that the combination treatment of T-DM1 and pertuzumab enhanced ADCC activity in *in vitro* experiments.

Discussion

First, the author clarified whether the relationship between HER2 expression level and T-DM1 efficacy in a gastric cancer model was comparable to that of trastuzumab. In breast cancer cells, it is known that T-DM1 shows great antitumor potency to cancer cells with high HER2 expression but less efficacy to those with low HER2 status (78). This study using gastric cancer xenograft models similarly showed that T-DM1 demonstrated significant antitumor activity only in cancers in which HER2 status was positive (the IHC score was 3+ or 2+, and the FISH ratio was >2.0), suggesting that, as with trastuzumab, efficacy of T-DM1 is associated with HER2 status. On the other hand, antitumor potency of T-DM1 for NCI-N87 (TGI% was 133%) was much higher than that of trastuzumab administered at the maximum effective dose in the previous study (TGI% was 89%) (9). Even in SCH, in which trastuzumab did not show significant antitumor activity, T-DM1 showed clear antitumor efficacy (TGI% was 109%). Also T-DM1 was efficacious to trastuzumab-insensitive xenograft tumors which expressed HER2 (78). These results confirmed that T-DM1 has more potent antitumor activity than trastuzumab. Further research both in clinical and preclinical studies, however, is required to examine the efficacy of T-DM1 for tumors expressing low levels of HER2 or that are trastuzumab-refractory.

There were some clinical reports that the combination of pertuzumab and trastuzumab was active and well tolerated in patients with metastatic HER2-positive breast cancer (55). In addition, the CLEOPATRA trial showed that pertuzumab significantly improved PFS of breast cancer patients in combination with trastuzumab plus docetaxel (86) and the combination was thus approved by the FDA. Meanwhile, T-DM1 was reported to have significantly improved the PFS of the combination of trastuzumab and docetaxel (87). In addition, the potency of T-DM1 and pertuzumab in combination as a first line treatment in HER2-positive metastatic breast cancers is currently being investigated in the MARIANNE trial. Also, in the ToGA trial investigating gastric cancer, patients with HER2-positive gastric cancer who received trastuzumab in addition to chemotherapy achieved a significant improvement in overall survival compared to treatment with chemotherapy alone (10). From these lines of clinical evidence, next, the author studied the combined efficacy of T-DM1 and pertuzumab in HER2-positive gastric cancers. In this *in vivo* study, the combination treatment of T-DM1 with pertuzumab showed significantly stronger

antitumor activity compared to either single agent in the HER2-positive NCI-N87 model, similarly to trastuzumab in combination with pertuzumab (85). T-DM1 in combination with pertuzumab may show strong efficacy in HER2-positive gastric cancer.

The present study demonstrated that the combination of two different anti-HER2 antibodies with different HER2-binding sites enhanced the inhibition of HER2 signal transduction in cultured NCI-N87 cells. Under EGF stimulation, the combination strongly reduced the phosphorylation of EGFR and its downstream factors, ERK and AKT compared to either single agent. Similar results were shown in the author's previous study in which the combination of trastuzumab and pertuzumab suppressed pEGFR and pHER2 and their downstream pERK and pAKT by inhibiting the EGFR-HER2 heterodimerization more strongly than either single agent (85). These results suggest that T-DM1 in combination with pertuzumab also suppressed heterodimer formation of EGFR-HER2.

In the NCI-N87 cells stimulated with HRG α, concomitant treatment of T-DM1 and pertuzumab almost completely reduced the phosphorylation of HER3 and AKT, and more potently inhibited cell growth and increased apoptotic cells. Furthermore, in the xenografted NCI-N87 tumors, Western blot analysis revealed that the combination suppressed the phosphorylation of HER3 not but EGFR. Considering the studies that HER2-HER3 heterodimer is the most active signal transducer among HER family complexes (57, 67), it is possible that disruption of the signal of HER3 rather than EGFR may play an important role in the antitumor efficacy of the combination treatment, even though HER3 expression levels were low in NCI-N87 tumors. Although further study is required to elucidate the mechanism of action, suppression of AKT signal followed by apoptosis induction in tumor may contribute to the enhanced antitumor efficacy by pertuzumab combined with T-DM1.

T-DM1 retains the ADCC that is reported as a key mechanism of trastuzumab (72), and pertuzumab also had ADCC (56, 73). The results of the present study, which are consistent with the enhanced ADCC activity of pertuzumab combined with trastuzumab in the author's previous study (85), demonstrate that in the combination treatment using T-DM1 with pertuzumab the ADCC activity was significantly enhanced compared to either single agent alone. On the other hand, a report has shown that the simultaneous binding of trastuzumab and pertuzumab onto target cells did not mediate a synergistic effect on ADCC when they were used at maximum effective doses (56). The authors showed that the level of ADCC of the combination of trastuzumab and pertuzumab was the same

as those of the single antibodies, when the final total antibody concentration was identical. The difference may arise from the difference in materials and methods; that is, the author used a real-time cell analyzer to measure ADCC and the sum of the concentration of each antibody was used as the combinational concentration. The results of the present study confirm that, in addition to enhanced inhibition of HER2 signaling, ADCC may be another mechanism of action that explains the increased efficacy of the combination.

In conclusion, T-DM1 in combination with pertuzumab achieved significant antitumor activity by enhancing HER family signal inhibition and ADCC activity in a HER2-positive human gastric cancer model. These findings suggest that T-DM1 in combination with pertuzumab is a rational and promising treatment option for HER2-positive gastric cancer.

References

1. Kovtun YV, Goldmacher VS. Cell killing by antibody-drug conjugates. Cancer Lett. 2007;255:232-40.

2. Lewis Phillips GD, Li G, Dugger DL, Crocker LM, Parsons KL, Mai E, et al. Targeting HER2-positive breast cancer with trastuzumab-DM1, an antibody-cytotoxic drug conjugate. Cancer Res. 2008;68:9280-90.

3. Erickson HK, Lewis Phillips GD, Leipold DD, Provenzano CA, Mai E, Johnson HA, et al. The effect of different linkers on target cell catabolism and pharmacokinetics/pharmacodynamics of trastuzumab maytansinoid conjugates. Mol Cancer Ther. 2012;11:1133-42.

4. Oroudjev E, Lopus M, Wilson L, Audette C, Provenzano C, Erickson H, et al. Maytansinoid-antibody conjugates induce mitotic arrest by suppressing microtubule dynamic instability. Mol Cancer Ther. 2010;9:2700-13.

5. Lopus M, Oroudjev E, Wilson L, Wilhelm S, Widdison W, Chari R, et al. Maytansine and cellular metabolites of antibody-maytansinoid conjugates strongly suppress microtubule dynamics by binding to microtubules. Mol Cancer Ther. 2010;9:2689-99.

6. Junttila TT, Li G, Parsons K, Phillips GL, Sliwkowski MX. Trastuzumab-DM1 (T-DM1) retains all the mechanisms of action of trastuzumab and efficiently inhibits growth of lapatinib insensitive breast cancer. Breast Cancer Res Treat. 2011;128:347-56.

7. Barok M, Tanner M, Koninki K, Isola J. Trastuzumab-DM1 is highly effective in preclinical models of HER2-positive gastric cancer. Cancer Lett. 2011;306:171-9.

8. LoRusso PM, Weiss D, Guardino E, Girish S, Sliwkowski MX. Trastuzumab emtansine: a unique antibody-drug conjugate in development for human epidermal growth factor receptor 2-positive cancer. Clin Cancer Res. 2011;17:6437-47.

9. Yamashita-Kashima Y, Iijima S, Yorozu K, Furugaki K, Kurasawa M, Ohta M, et al. Pertuzumab in combination with trastuzumab shows significantly enhanced antitumor activity in HER2-positive human gastric cancer xenograft models. Clin Cancer Res. 2011;17:5060-70.

10. Fujimoto-Ouchi K, Sekiguchi F, Yasuno H, Moriya Y, Mori K, Tanaka Y. Antitumor activity of trastuzumab in combination with chemotherapy in human gastric cancer xenograft models. Cancer chemotherapy

and pharmacology. 2007;59:795-805.

11. Fujimoto-Ouchi K, Sekiguchi F, Tanaka Y. Antitumor activity of combinations of anti-HER-2 antibody trastuzumab and oral fluoropyrimidines capecitabine/5'-dFUrd in human breast cancer models. Cancer chemotherapy and pharmacology. 2002;49:211-6.

12. Baselga J, Gelmon KA, Verma S, Wardley A, Conte P, Miles D, et al. Phase II trial of pertuzumab and trastuzumab in patients with human epidermal growth factor receptor 2-positive metastatic breast cancer that progressed during prior trastuzumab therapy. J Clin Oncol. 2010;28:1138-44.

13. Baselga J, Cortes J, Kim SB, Im SA, Hegg R, Im YH, et al. Pertuzumab plus trastuzumab plus docetaxel for metastatic breast cancer. N Engl J Med. 2012;366:109-19.

14. Hurvitz SA DL, Kocsis J, Gianni L, Lu MJ, Vinholes J, Song C, Tong B, Chu Y-W, Perez EA. Trastuzumab emtansine (T-DM1) vs trastuzumab plus docetaxel (H+T) in previously untreated HER2-positive metastatic breast cancer (MBC): primary results of a randomized, multicenter, open-label phase II study (TDM4450g/BO21976). European Multidisciplinary Cancer Congress. 2011:Abstract.5001.

15. Bang YJ, Van Cutsem E, Feyereislova A, Chung HC, Shen L, Sawaki A, et al. Trastuzumab in combination with chemotherapy versus chemotherapy alone for treatment of HER2-positive advanced gastric or gastro-oesophageal junction cancer (ToGA): a phase 3, open-label, randomised controlled trial. Lancet. 2010;376:687-97.

16. Baselga J, Swain SM. Novel anticancer targets: revisiting ERBB2 and discovering ERBB3. Nat Rev Cancer. 2009;9:463-75.

17. Olayioye MA, Neve RM, Lane HA, Hynes NE. The ErbB signaling network: receptor heterodimerization in development and cancer. EMBO J. 2000;19:3159-67.

18. Spector NL, Blackwell KL. Understanding the mechanisms behind trastuzumab therapy for human epidermal growth factor receptor 2-positive breast cancer. J Clin Oncol. 2009;27:5838-47.

19. Scheuer W, Friess T, Burtscher H, Bossenmaier B, Endl J, Hasmann M. Strongly enhanced antitumor activity of trastuzumab and pertuzumab combination treatment on HER2-positive human xenograft tumor models. Cancer Res. 2009;69:9330-6.

20. El-Sahwi K, Bellone S, Cocco E, Cargnelutti M, Casagrande F, Bellone M, et al. In vitro activity of pertuzumab in combination with trastuzumab in uterine serous papillary adenocarcinoma. Br J Cancer. 2010;102:134-43.

Chapter III: Importance of formalin fixing conditions for HER2 testing in gastric cancer: immunohistochemical staining and fluorescence *in situ* hybridization

Introduction

The addition of the HER2-targeted agent trastuzumab to these standard chemotherapy regimens has been investigated for patient with HER2-positive disease. HER2, a member of the HER family proteins, regulates cell proliferation, differentiation, and apoptosis. These functions are triggered by the formation of HER2 homodimers or heterodimers with other HER family proteins (1) and subsequent activation of downstream signaling. In breast cancer, HER2 overexpression is a prognostic factor (2-4) and an important predictive marker for determining which patients are likely to benefit from treatment with trastuzumab. In gastric cancer, there is controversy around whether HER2 status provides prognostic information (5). However, it is necessary to determine HER2 status in order to determine whether trastuzumab will be a beneficial option for patients.

The ToGA trial, an open-label, international, phase III, randomized controlled trial, demonstrated that patients with HER2-positive gastric cancer assigned to receive trastuzumab plus standard chemotherapy had significantly longer overall survival (OS) (hazard ratio: HR 0.74, 95% CI 0.60-0.91) compared with patients with HER2-positive gastric cancer assigned to receive chemotherapy alone (6). The improvement in OS in the trastuzumab arm was more apparent in patients whose tumors had high HER2 expression (IHC 3+, or IHC 2+ and FISH positive), with a HR of 0.65 (95% CI 0.51-0.83). Based on the results of the ToGA study, regimen that include trastuzumab plus chemotherapy became a new standard treatment modality for HER2-positive gastric cancer.

IHC analysis which evaluates protein expression and FISH analysis which evaluates gene amplification are major methods for HER2 testing. Although assessing HER2 status accurately and reliably is of great importance to determine whether patients have HER2-positive breast or gastric cancer, there is variability of sample preparation for HER2 testing (7). A number of reports show discordance in HER2 testing results between laboratories (8, 9). Perez et al have shown the importance of using high-volume, experienced laboratories for HER2 testing to improve the process of selecting patients likely to benefit from trastuzumab therapy(10). To ensure accurate evaluation, the

American Society of Clinical Oncology (ASCO) and College of American Pathologists (CAP) implemented guidelines for HER2 evaluation in breast cancer in 2007 (11).

By virtue of the ASCO/CAP guidelines, the method of preparing specimens has been standardized in breast cancer. In Japan, HER2 testing guidelines for gastric cancer were defined by the Trastuzumab pathological advisory board for gastric cancer in line with ASCO/CAP guidelines. Paraffin sections are prepared, and the IHC scoring system is used according to these criteria which aimed to develop a validated HER2 scoring system for gastric cancer (12). However, inter-laboratory differences in the results of HER2 testing are still a big problem in gastric cancer. One cause of this may be inappropriate preparation of formalin-fixed paraffin-embedded tissues. In the present study, the author investigated the effect of formalin fixing conditions, including time to fixation, fixation time and composition of fixatives, on IHC and FISH for HER2 using human gastric cancer cell line xenografted tumor tissues with different HER2 status.

Materials and methods

Animals

Five-week-old male BALB-nu/nu mice (CAnN.Cg-Foxn1<nu>/CrlCrlj nu/nu) were obtained from Charles River Laboratories Japan (Yokohama, Japan). All animals were housed in a pathogen-free environment under controlled conditions (temperature 20-26°C, humidity 40-70%, light/dark 12h/12h). Chlorinated water and irradiated food were provided ad libitum. All animals were allowed to acclimatize and recover from shipping-related stress for 1 week prior to the study. The health of the mice was monitored by daily observation. All animal experiments were conducted in accordance with the Guidelines for the Accommodation and Care of Laboratory Animals promulgated in Chugai Pharmaceutical Co., Ltd.

Cell lines and culture conditions

Three human gastric cancer cell lines were used in the present study. NCI-N87 and SNU-16 cells were purchased from American Type Culture Collection (ATCC) (Rockville, MD, USA). SCH cells were purchased

Table 1 Histological type and HER2 status of three gastric tumor tissues

Tumor name	Histological type *	HER2 IHC score	HER2/CEP17 ratio (FISH)
NCI-N87	Differentiated / intestinal type epithelial carcinoma	3+	8.4 (13)
SCH	Undifferentiated / diffuse type choriocarcinoma	2+	2.3
SNU-16	Undifferentiated / diffuse type epithelial carcinoma	1+	1.4 (13)

*: The histological type was described according to the information of each cell line distributor.

from Japan Health Sciences Foundation (Osaka, Japan). NCI-N87, SNU-16 and SCH were maintained in RPMI-1640 (Sigma-Aldrich, St. Louis, MO, USA) supplemented with 10% (v/v) fetal bovine serum at 37°C under 5% CO_2. The histological type of each cell line was shown in Table 1.

Preparation of specimens

Each mouse was inoculated subcutaneously into the right flank with either 5×10^6 cells/mouse of human gastric cancer cell lines NCI-N87, SCH or SNU-16. Tumor xenograft tissues were collected and allowed to stand at room temperature for 0, 6, or 24 hours before being fixed with 10% NBF for 24 hours, 5, 7, or 10 days and then embedded in paraffin. To compare the effect of fixing solution on HER2 IHC, 10% NBF, 20% NBF, 10% non-buffered formalin and 20% non-buffered formalin were used. Specimens were prepared from two separate tumors from NCI-N87 and SNU-16 inoculated mice and three tumors from SCH inoculated mice.

IHC, gene amplification of HER2, and histological assessment

HER2 protein expression and HER2 gene amplification in tumors were examined by IHC using HercepTest™ (DAKO, Glostrup, Denmark) and by FISH using PathVysion® HER2 DNA Probe (Abbott Molecular, Abott Park, IL), respectively, at SRL Inc. (Tokyo, Japan) as described previously (13). Histological assessment was performed under light microscope.

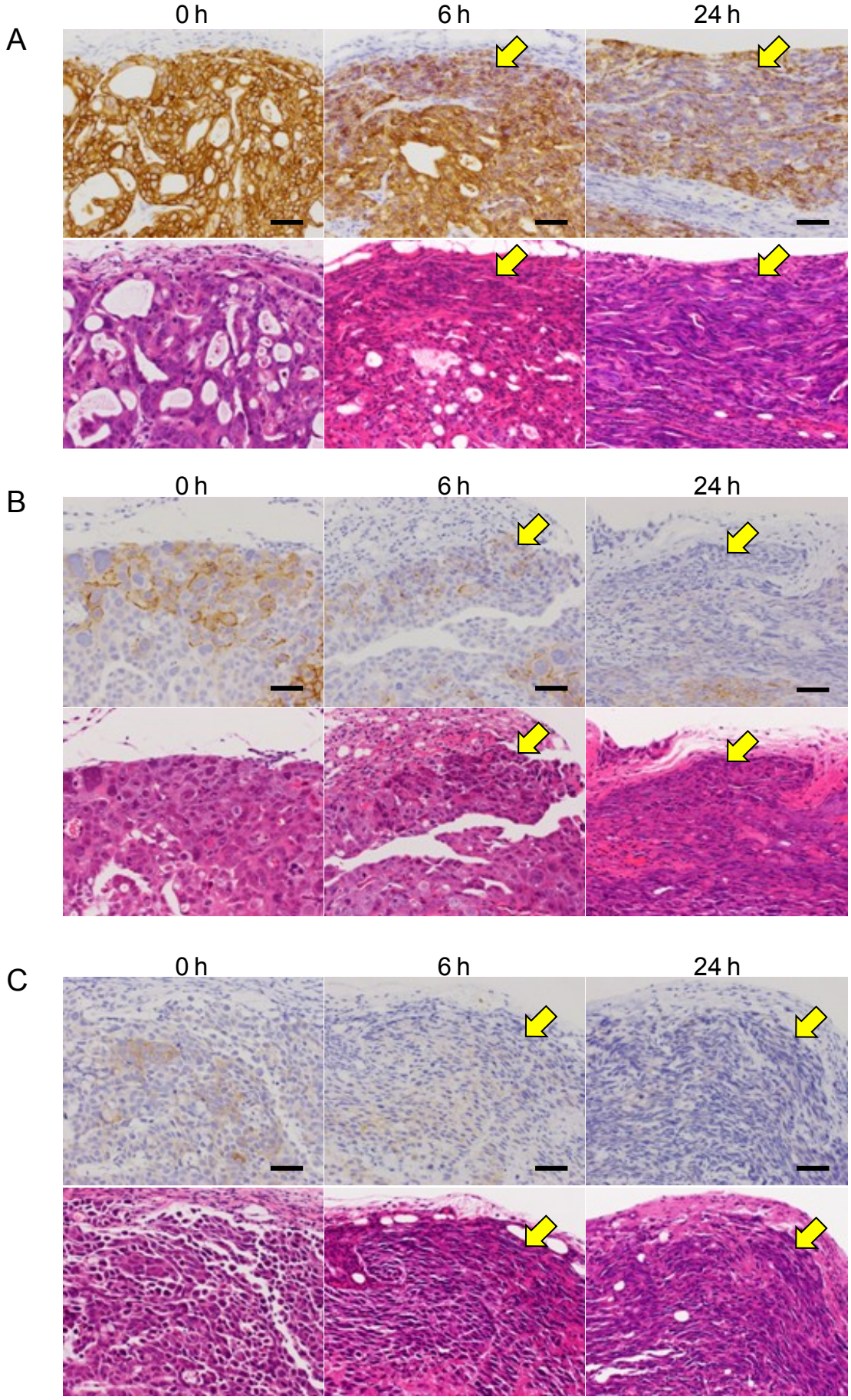
A
0 h
6 h
24 h
B
0 h
6 h
24 h
C
0 h
6 h
24 h

◂ **Figure 1. Effect of time to fixation on IHC staining for HER2 in tumor tissue periphery.** Tumor tissue specimens of (A) NCI-N87, (B) SCH, or (C) SNU-16 were collected and allowed to stand for 0, 6, or 24 h before fixing with 10% NBF for 24 h. Upper panels: HER2 IHC staining. Lower panels: hematoxylin-eosin staining. Arrows: shrunk and decreased-staining intensity areas. − represents 50 mm.

Results

IHC and FISH status of tumor tissues used

Three tumor tissues with different HER2 status were used in this study. The HER2 status of these tumor tissues were assessed by IHC and FISH, using specimens fixed with 10% NBF for 24 hours immediately after the resection of the tumors. The IHC scores for NCI-N87, SCH, SNU-16 were 3+, 2+, 1+, and HER2/CEP17 ratios by FISH were 8.4, 2.3, 1.4, respectively (Table 1).

Effect of time to fixation and fixation time on IHC staining for HER2

Firstly, the author examined the effect of time to fixation and length of fixation on IHC staining for HER2 in NCI-N87, SCH, and SNU-16 tumor tissues. Leaving specimens for 6 or 24 hours before fixation at room temperature promoted shrinkage in the tumor tissue periphery and decreased immunostaining intensity at the shrinkage area in tumors from all of the cell lines irrespective of HER2 status and fixation time (Fig. 1A, and Tables 2 and 3). In SCH or SNU-16 tumors, leaving the specimens for 24 hours before fixation also induced autolysis and decreased the number of stained cells in the center of tumor tissues (Fig. 2 and Table 3). As a result, the total staining intensity and total staining area was decreased in these two tumors. In SCH tumors, a decrease of the HER2 IHC score to 1+ was observed in two of three specimens left for 24 hours and then fixed for 24 hours (Table 2).

Secondly, the author examined the effect of fixation time on IHC staining for HER2. In NCI-N87 specimens from tumors with a HER2 IHC 3+ score, there was no change in HER2 IHC score (Fig. 3A and Table 2). However, in SCH or SNU-16 specimens from tumors with HER2 IHC 2+ or 1+ scores, the scores were decreased to 1+ or 0, respectively, in one of three or one of two specimens by fixing for 10 days even when fixation was started immediately after the tumor collection (Fig. 3B and 3C, and Table 2). Moreover, in SNU-16

Table 2 Effect of fixation conditions on HER2 IHC score in human gastric cancer xenografted tumors

Time to fixation	NCI-N87				SCH				SNU-16			
	Fixation time				Fixation time				Fixation time			
	24 h	5 d	7 d	10 d	24 h	5 d	7 d	10 d	24 h	5 d	7 d	10 d
0 h	3+	3+	3+	3+	2+ [a]	2+ [a]	2+ [a]	1+/2+	1+	1+	1+	0/1+
6 h	3+	3+	3+	3+	2+	2+/3+	2+	2+	1+	1+	1+	0/1+
24 h	3+	3+	3+	3+	1+/2+	1+ [a]	1+/2+	1+/2+	1+	0/1+	1+	0

HER2 IHC was performed by HercepTest™.
The tests were performed in duplicate for NCI-N87 and SNU-16, in triplicate or duplicate ([a]) for SCH. If the test results of duplicate sample were different, both values were indicated.

Table 3 Effect of fixation conditions on the detailed histological assessment of HER2 IHC staining in human gastroc cancer xenografted tumors

Time to fixation	NCI-N87				SCH				SNU-16			
	Fixation time				Fixation time				Fixation time			
	24 h	5 d	7 d	10 d	24 h	5 d	7 d	10 d	24 h	5 d	7 d	10 d
0 h	–	–	–	–	– [g]	– [g]	– [g]	–/+	–	+	+	+/++
6 h	±	±	±	±	–/±	±	–/±	–/±	±	±/+	+	+/++
24 h	±	±/+	±/+	±	+	+	±/+	±/+	+	+/++	+	++/+++

Histological assessment on the decrease in staining was performed in terms of the following criteria and judged in a comprehensive manner: a) tumor periphery shrinkage (dry), b) decrease of staining intensity at shrinkage area, c) autolysis, d) decrease in positive cells, e) decrease of total staining intensity, f) decrease of total staining area. –: no change, ±: very slightly decreased, +: slightly decreased, ++: moderately decreased, +++: markedly decreased
The assessments were performed in duplicate for NCI-N87 and SNU-16, in triplicate or duplicate ([g]) for SCH. If the results of duplicate or triplicate sample were different, all results were indicated.

tumor specimens which were left for 24 hours before fixation, prolonged fixation time (10 day-fixation) promoted the decrease of HER2 staining intensity at the shrunk area and a decrease in HER2-positive cells (Table 3). HER2 IHC scores for these specimens were 0 in all specimens (two of two) (Table 2).

Effect of time to fixation and fixation time on FISH results

The author also investigated whether delay to formalin fixation or prolonged fixation time affects FISH results. SCH specimens in which time to fixation and fixation time were i) 0 h and 24 h, ii) 0 h and 10 days, iii) 6 h and 24 h, iv) 24 h and 24 h, or v) 24 h and 10 days, were assessed by FISH (HER2/CEP17 ratio). The mean of the

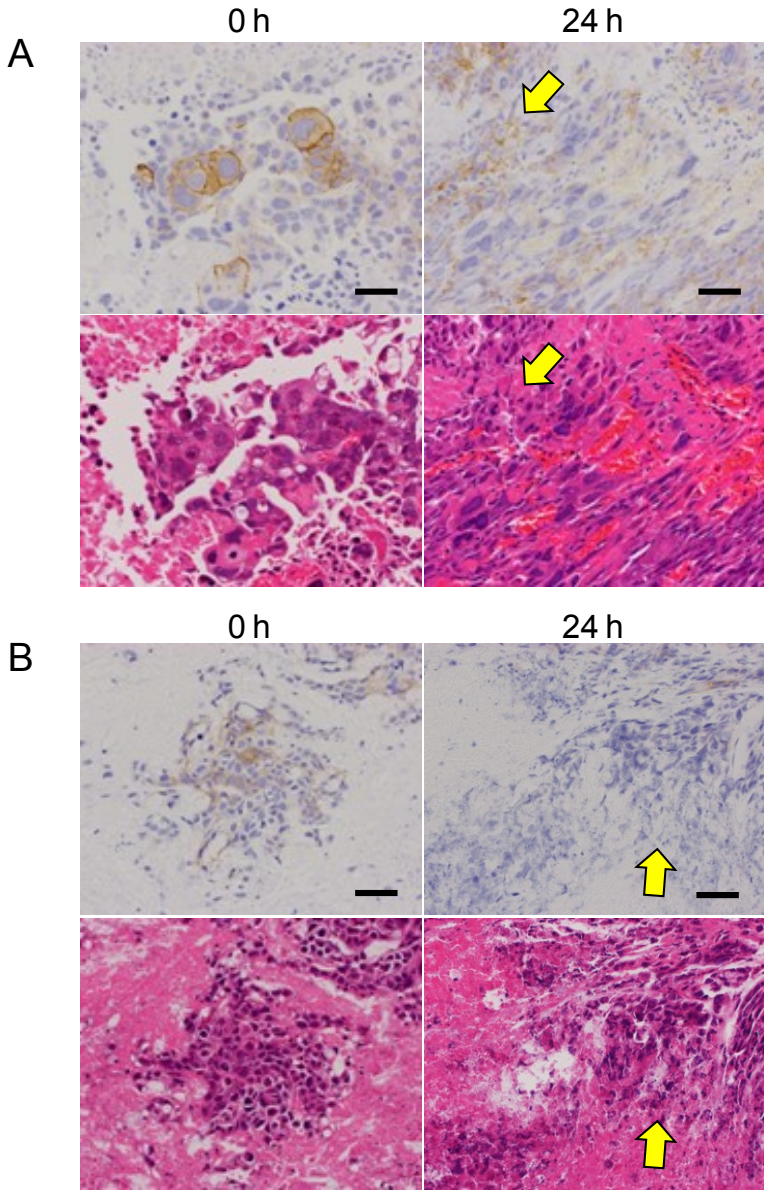

Figure 2. Effect of time to fixation on IHC staining for HER2 in tumor tissue centre. Tumor tissue specimens of (A) SCH and (B) SNU-16 were collected and allowed to stand for 0 or 24 h before fixing with 10% NBF for 24 h. Upper panels: HER2 IHC staining. Lower panels: hematoxylin-eosin staining. Arrows: advanced autolysis areas. – represents 50 mm.

HER2/CEP17 ratios of specimens of i), ii), iii), iv), and v) were 2.3, 2.6, 1.3, 1.2, and 1.1, respectively, suggesting that prolonged fixation time did not affect the FISH results but delay to fixation strongly reduced the FISH score (Table 4).

Effect of fixative type on IHC staining for HER2

The type of fixative used for the preparation of specimens may be another important factor that affects the concordance of HER2 testing results. Therefore, the author next examined the effect of fixative type on IHC staining for HER2. In this experiment, firstly, the author used the specimens of SCH tumor (HER2 IHC score 2+)

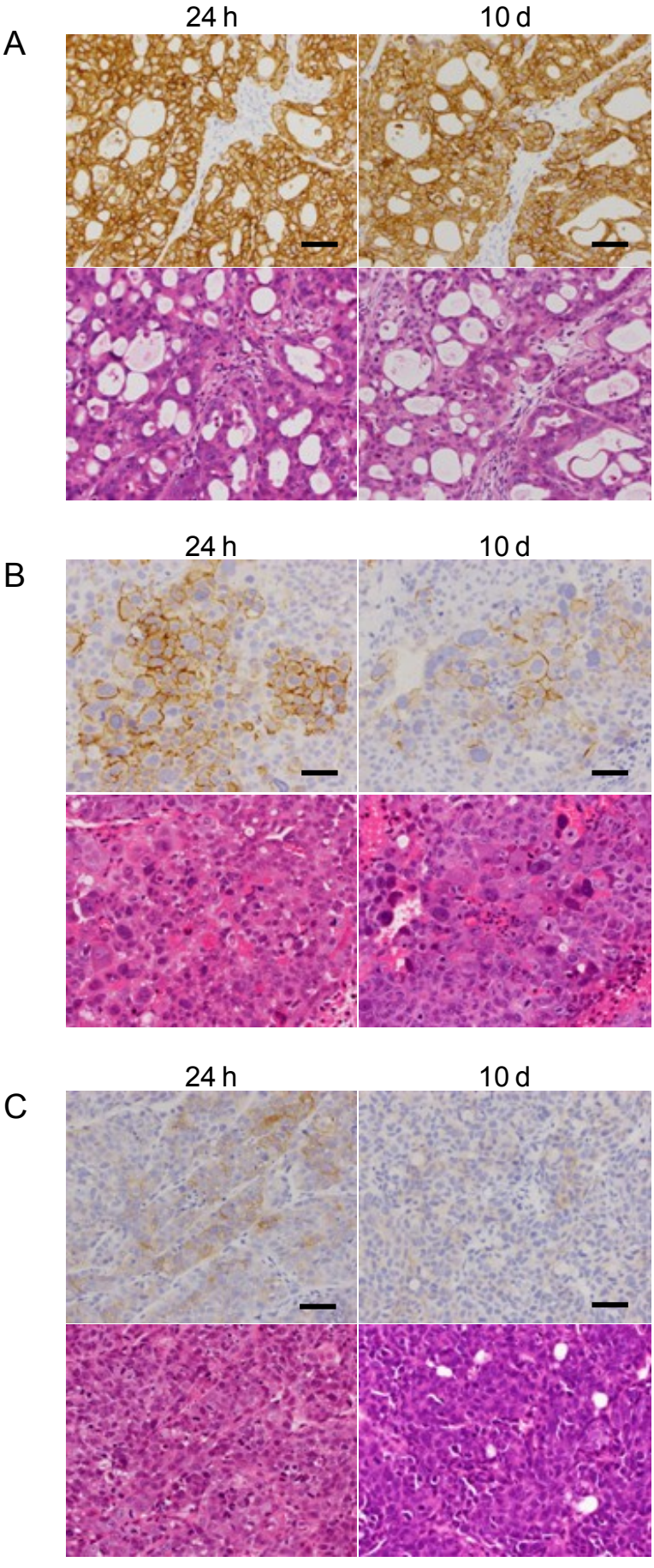

Figure 3. Effect of fixation time on IHC staining for HER2. Tumor tissue specimens of (A) NCI-N87, (B) SCH, and (C) SNU-16 were collected and immediately fixed with 10% NBF for 24 h or 10 days . Upper panels: HER2 IHC staining. Lower panels: hematoxylin-eosin staining. − represents 50 mm.

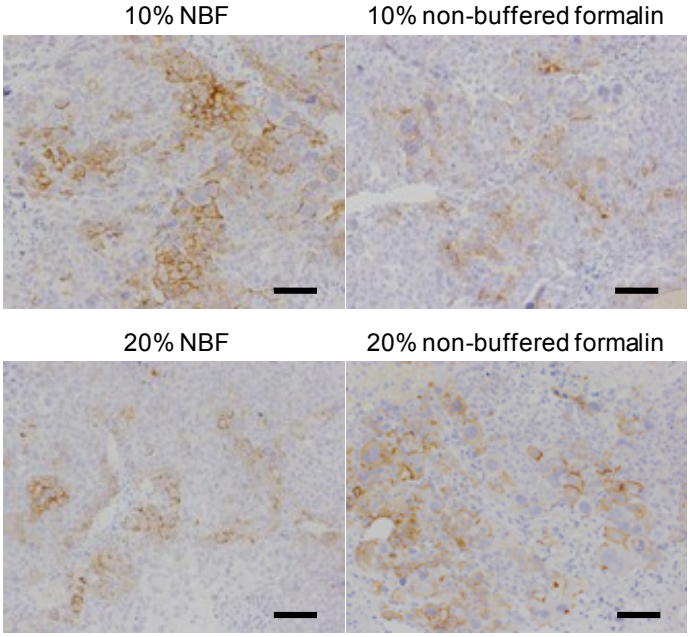

Figure 4. Effect of fixative type on IHC staining for HER2. SCH tumor tissues were collected and immediately fixed with 10% NBF, 20% NBF, 10% non-buffered formalin, or 20% non-buffered formalin for 24 h. – represents 100 mm.z

Table 4 Effect of fixation conditions on HER2 FISH in SCH xenografted tumors

Time to fixation	Fixation time	HER2/CEP17 ratio (FISH)
0 h	24 h	2.3
0 h	10 d	2.6
6 h	24 h	1.3
24 h	24 h	1.2
24 h	10 d	1.1

because, in clinical, specimens judged as HER2 IHC score 2+ are considered as equivocal and recommended to conduct FISH test in order to make a final diagnosis for trastuzumab application. Therefore, it makes sense to examine whether fixative type affect the result of HER2 IHC test in tumor tissue specimens of HER2 IHC score 2+. For this purpose, the author used 10% NBF, 20% NBF, 10% and 20% non-buffered formalin. The tumor tissues were fixed with each fixative immediately after collecting. Fixing with 20% NBF, 10% non-buffered formalin or 20% non-buffered formalin for 24 hours reduced the staining intensity of HER2 and reduced the HER2 IHC score from 2+ to 1+ in one of three specimens compared to fixing with 10% NBF (Fig 4 and Table 5). When tumor tissues were fixed for 10 days, the reduction in HER2 staining intensity was more apparent and an HER2 IHC score reduction was observed in two of three specimens in 20% NBF and 10% non-buffered formalin, and in three of three specimens in 20% non-buffered formalin (Table 5). These results indicate that all formalin fixatives used

Table 5 Effect of fixative type on HER2 IHC staining and histological assessment in SCHxenografted tumors

Fixation time	Evaluation	Fixatives			
		10% NBF	10% non-buffered formalin	20% NBF	20% non-buffered formalin
24 h	HER2 IHC score[a]	2+	1+/2+	1+/2+	1+/2+
	Histological assessment / decrease in staining[b]	–	–/+	–/+	–/+
10 d	HER2 IHC score[a]	2+	1+/2+	1+/2+	1+
	Histological assessment / decrease in staining[b]	–	–/+	–/+	+

[a]: HER2 IHC was performed by HercepTest™.
[b]: Histological assessment on the decrease in staining was performed in terms of the following criteria and judged in a comprehensive manner: a) autolysis, b) decrease in positive cells, c) decrease of total staining intensity, d) decrease of total staining area. –: no change, ±: very slightly decreased, +: slightly decreased, ++: moderately decreased, +++: markedly decreased.
The tests and assessments were performed in triplicate. If the test results of triplicate sample were different, all results were indicated.

Table 6 Effect of fixative type on HER2 IHC staining and histological assessment in NCI-N87 xenografted tumors

Fixation time	Evaluation	Fixatives			
		10% NBF	10% non-buffered formalin	20% NBF	20% non-buffered formalin
24 h	HER2 IHC score	3+	3+	3+	3+
	Histological assessment / decrease in staining	–	–	–	–
10 d	HER2 IHC score	3+	3+	3+	3+
	Histological assessment / decrease in staining	–	–	–	–

Histological assessment on the decrease in staining was performed in terms of the following criteria and judged in a comprehensive manner: a) autolysis, b) decrease in positive cells, c) decrease of total staining intensity, d) decrease of total staining area. －: no change, ±: very slightly decreased, ＋: slightly decreased, ++: moderately decreased, +++: markedly decreased.
The tests and assessments were performed in duplicate.

other than 10% NBF could negatively affect the results of HER2 IHC staining in tumors with HER2 IHC score 2+. Secondly, the author examined the effect of fixative type on HRE2 IHC staining using specimens of NCI-N87 tumor (HER2 IHC score 3+) in the same way as above. As a result, the author found that all of the four fixatives did not affect the results of HER2 IHC staining in both 24 hours- and 10 days-fixation (Table 6).

Discussion

In breast cancer, ASCO/CAP issued guidelines to standardize fixation for increased HER2 testing accuracy. In addition, many investigations into the optimal conditions for accurate HER2 testing have been conducted(14-17). Delay to formalin fixation after specimen collection and extended fixation times may affect HER2 testing results. Several reports have shown the effect of time to fixation, fixation time, or fixative type on IHC or FISH for HER2. Khoury et al reported that more than a 1 hour delay to formalin fixation negatively affected the HER2 IHC and FISH results (15). On the other hand, Moatamed et al showed that ischemic time (with a delay in fixation of 4 days at 4°C) , fixation time (0–168 hours), and fixative type did not significantly alter HER2 IHC and FISH results (17). Thus, even in breast cancer, it may be considered that more studies are required to determine the most appropriate procedure for HER2 testing which can be applied in every laboratory. Needless to say, it is also important in gastric cancer to assess HER2 status accurately and reliably. However, there are no reports which analyze the formalin fixing conditions on HER2 testing in gastric cancer. In the present study, the author investigated how the fixation conditions of specimens affected HER2 IHC and FISH results using paraffin-embedded gastric cell line xenografted specimens prepared using various fixation conditions. To prepare the specimens in guideline-recommended conditions, the author made paraffin-embedded specimens in accordance with HER2 testing guidelines defined by the Trastuzumab pathological advisory board for gastric cancer.

In the present study, leaving specimens at room temperature for more than 6 hours before fixation led to shrinkage at the tumor periphery and decreased the staining intensity at the shrinkage area in all of the tumors assessed, irrespective of HER2 status. However, a decrease in HER2 IHC score was observed only in SCH specimens with a 24-hour delay to fixation. However, HER2/CEP17 ratio of FISH in SCH was decreased from 2.3 to 1.3 if the tumor sample was left at room temperature for only 6 hours before fixation. In breast cancer, it has been reported that a delay to formalin fixation affects FISH results but not IHC scores (15). Therefore, the author would expect that FISH results would be more vulnerable to delayed fixation than IHC in gastric cancer specimens.

With regard to fixation time, prolonged fixation did not affect the HER2 IHC scores of NCI-N87 tumors

(HER2 3+ score) (Table 2). However, in the specimens where HER2 scores were 2+ (SCH) or 1+ (SNU-16), prolonged fixation reduced the HER2 IHC score (Table 2). These results corresepond well to the report of Hashizume et al (14) who showed that prolonged fixation affects HER2 IHC score in 2+ or 1+ breast cancer specimens. These results suggest that considerable attention should be paid to the time from excision to fixation and fixation time of tumor tissues in gastric cancer as well as breast cancer.

The present study using several types of fixatives showed that with fixatives other than 10% NBF IHC staining of HER2 in SCH (IHC score 2+) was reduced. The author also examined the effect of fixatives in NCI-N87 (IHC score 3+), however, there were no differences in staining between fixatives. Staining of specimens which moderately express HER2 protein may therefore be affected more easily by the type of fixative used compared to staining of specimens with HER2 high expression. In the present study, the author did not examine the effect of fixative type on FISH results. This is because, for gastric cancer, IHC testing is recommended as a first examination for HER2 followed by confirmative testing by FISH for IHC score 2+ specimens.

In the clinical setting, it is important to take unique HER2 staining characteristics into consideration when standardizing HER2 testing in gastric cancer. One is the heterogeneity defined as <30% of tumor cells staining positive or only focal staining of tumor cells (12, 18) . Gastric cancer exhibits heterogeneity in up to 30% of HER2-positive cases (18). The other consideration is that HER2-positive gastric carcinomas are usually of the gland-forming, intestinal type and may show incomplete, basolateral, or lateral membranous staining (19). In the present study, the author used xenografted tumors from mouse models as specimens which did not reflect the heterogeneity or other staining features of human gastric cancer. Therefore, in clinical cases, the impact of the formalin fixing condition on the result of IHC staining or FISH for HER2 may not be the same as in the present study. Further study is required in clinical setting.

In conclusion, the results of the present study indicate that the delay to fixation and length of fixation, may affect the HER2 IHC score in a gastric cancer model. Non-buffered formalin or high concentrations of NBF may also affect IHC results. These results highlight how it is of critical importance to optimize the sample preparation conditions for HER2 testing in gastric cancer.

References

1. Yarden Y, Sliwkowski MX. Untangling the ErbB signalling network. Nat Rev Mol Cell Biol. 2001;2:127-37.

2. Borg A, Tandon AK, Sigurdsson H, Clark GM, Ferno M, Fuqua SA, et al. HER-2/neu amplification predicts poor survival in node-positive breast cancer. Cancer Res. 1990;50:4332-7.

3. Parkes HC, Lillycrop K, Howell A, Craig RK. C-erbB2 mRNA expression in human breast tumours: comparison with c-erbB2 DNA amplification and correlation with prognosis. Br J Cancer. 1990;61:39-45.

4. Slamon DJ, Clark GM, Wong SG, Levin WJ, Ullrich A, McGuire WL. Human breast cancer: correlation of relapse and survival with amplification of the HER-2/neu oncogene. Science. 1987;235:177-82.

5. Ross JS, McKenna BJ. The HER-2/neu oncogene in tumors of the gastrointestinal tract. Cancer Invest. 2001;19:554-68.

6. Bang YJ, Van Cutsem E, Feyereislova A, Chung HC, Shen L, Sawaki A, et al. Trastuzumab in combination with chemotherapy versus chemotherapy alone for treatment of HER2-positive advanced gastric or gastro-oesophageal junction cancer (ToGA): a phase 3, open-label, randomised controlled trial. Lancet. 2010;376:687-97.

7. Sauter G, Lee J, Bartlett JM, Slamon DJ, Press MF. Guidelines for human epidermal growth factor receptor 2 testing: biologic and methodologic considerations. J Clin Oncol. 2009;27:1323-33.

8. Roche PC, Suman VJ, Jenkins RB, Davidson NE, Martino S, Kaufman PA, et al. Concordance between local and central laboratory HER2 testing in the breast intergroup trial N9831. J Natl Cancer Inst. 2002;94:855-7.

9. Reddy JC, Reimann JD, Anderson SM, Klein PM. Concordance between central and local laboratory HER2 testing from a community-based clinical study. Clin Breast Cancer. 2006;7:153-7.

10. Perez EA, Suman VJ, Davidson NE, Martino S, Kaufman PA, Lingle WL, et al. HER2 testing by local, central, and reference laboratories in specimens from the North Central Cancer Treatment Group N9831 intergroup adjuvant trial. J Clin Oncol. 2006;24:3032-8.

11. Wolff AC, Hammond ME, Schwartz JN, Hagerty KL, Allred DC, Cote RJ, et al. American Society of

Clinical Oncology/College of American Pathologists guideline recommendations for human epidermal growth factor receptor 2 testing in breast cancer. Arch Pathol Lab Med. 2007;131:18-43.

12. Hofmann M, Stoss O, Shi D, Buttner R, van de Vijver M, Kim W, et al. Assessment of a HER2 scoring system for gastric cancer: results from a validation study. Histopathology. 2008;52:797-805.

13. Fujimoto-Ouchi K, Sekiguchi F, Yasuno H, Moriya Y, Mori K, Tanaka Y. Antitumor activity of trastuzumab in combination with chemotherapy in human gastric cancer xenograft models. Cancer chemotherapy and pharmacology. 2007;59:795-805.

14. Hashizume K, Hatanaka Y, Kamihara Y, Kato T, Hata S, Akashi S, et al. Interlaboratory comparison in HercepTest assessment of HER2 protein status in invasive breast carcinoma fixed with various formalin-based fixatives. Appl Immunohistochem Mol Morphol. 2003;11:339-44.

15. Khoury T, Sait S, Hwang H, Chandrasekhar R, Wilding G, Tan D, et al. Delay to formalin fixation effect on breast biomarkers. Mod Pathol. 2009;22:1457-67.

16. Tong LC, Nelson N, Tsourigiannis J, Mulligan AM. The effect of prolonged fixation on the immunohistochemical evaluation of estrogen receptor, progesterone receptor, and HER2 expression in invasive breast cancer: a prospective study. Am J Surg Pathol. 2011;35:545-52.

17. Moatamed NA, Nanjangud G, Pucci R, Lowe A, Shintaku IP, Shapourifar-Tehrani S, et al. Effect of ischemic time, fixation time, and fixative type on HER2/neu immunohistochemical and fluorescence *in situ* hybridization results in breast cancer. Am J Clin Pathol. 2011;136:754-61.

18. Ruschoff J, Nagelmeier I, Baretton G, Dietel M, Hofler H, Schildhaus HU, et al. [Her2 testing in gastric cancer. What is different in comparison to breast cancer?]. Pathologe. 2010;31:208-17.

19. Ruschoff J, Hanna W, Bilous M, Hofmann M, Osamura RY, Penault-Llorca F, et al. HER2 testing in gastric cancer: a practical approach. Mod Pathol. 2012;25:637-50.

Chapter IV: Biomarkers for antitumor activity of bevacizumab in gastric cancer models

Introduction

Vascular endothelial growth factor (VEGF), a diffusible glycoprotein produced by normal and neoplastic cells, is an important regulator of physiologic and pathologic angiogenesis. Increased VEGF levels in serum or tumor tissue have been reported to correlate with poor survival; therefore, efficacy of anti-VEGF therapy is expected in clinical application(1, 2).

Bevacizumab is a humanized monoclonal antibody to human VEGF that inhibits VEGF-mediated angiogenesis in many types of tumors. Although bevacizumab improves progression-free survival (PFS) in these cancers, it is not effective for all patients. Predictive markers of bevacizumab efficacy have been assessed in many clinical trials(3), however, no validated biomarker is available to predict bevacizumab efficacy and identify the patients who could benefit from bevacizumab. Therefore, it is important to investigate the biomarker of bevacizumab efficacy from the phase of clinical development for other cancer types.

Gastric cancer is one of the most malignant cancers and second leading cause of cancer death in the world (4). The incidence is reportedly highest in Asia, South America, and Southern Europe(5). Increased levels of VEGF expression have been found in gastric cancers as well as in tumors of lung, breast, thyroid, gastrointestinal tract, kidney, bladder, ovary, cervix, and pancreas, angiosarcomas and glioblastomas(6, 7). A previous report suggests the possibility of VEGF as a prognostic factor of gastric cancer(8). Therefore, bevacizumab may also be effective against gastric cancers (9). In the present study, the relationship between the efficacy of bevacizumab, selected biomarkers in gastric cancers and various histological types of gastric cancer has been examined.

Materials and methods

Test agents

Bevacizumab was provided by F. Hoffman-La Roche (Nutley, NJ, USA) as a liquid and diluted with saline. Human immunoglobulin G (HuIgG) was purchased from MP Biomedicals, Inc. (Aurora, OH, USA) and was reconstituted with water and diluted with saline.

Animals

Male 5-week-old BALB/c-nu/nu mice (CAnN.Cg-Foxn1<nu>/CrlCrlj nu/nu) were obtained from Charles River Japan (Yokohama, Japan). All animals were allowed to acclimatize and recover from shipping-related stress for one week prior to the study. The health of the mice was monitored by daily observation. Chlorinated water and irradiated food were provided ad libitum, and the animals were kept in a controlled light-dark cycle (12h-12h). Animal procedures were approved by the Institutional Animal Care and Use Committee at Chugai Pharmaceutical Co., Ltd..

Cell lines and culture conditions

Nine human gastric cancer cell lines and two human colorectal cancer cell lines were used in the present study. MKN-45 and MKN-28 were purchased from Immuno-Biochemical Laboratories Co., Ltd. (Fujioka, Japan). NCI-N87, SCH, and HUVEC were obtained from the American Type Culture Collection (Rockville, MD, USA), the Japan Health Science Foundation (Osaka, Japan), and KURABO (Osaka, Japan), respectively. MKN-45 was maintained in TIL Media medium (Immuno-Biochemical Laboratories) supplemented with 10% (v/v) FBS, and MKN-28, NCI-N87, and SCH were maintained in RPMI-1640 supplemented with 10% (v/v) FBS at 37°C under 5% CO_2. HUVEC was maintained in HuMedia-EG2 (KURABO) at 37°C under 5% CO_2. Cell lines 4-1ST, SC-08-JCK, SC-09-JCK, SC-10-JCK and COL-16-JCK were purchased from the Central Institute for Experimental Animals (Yokohama, Japan). GXF97 and CXF280 were kindly provided by Prof. H. H. Fiebig (University of Freiberg, Freiberg, Germany). 4-1ST, SC-08-JCK, SC-09-JCK, SC-10-JCK, GXF97 and CXF280 were maintained in BALB/c-nu/nu mice by subcutaneous (sc) inoculation of pieces of the tumor tissue.

***In vivo* tumor growth inhibition studies**

Each mouse was inoculated sc into the right flank with either 5×10^6 cells/mouse of human gastric cancer cell line MKN-45, MKN-28, NCI-N87 or SCH, or an 8-mm^3 piece of 4-1ST, SC-08-JCK, SC-09-JCK, SC-10-JCK, GXF97 or CXF280 tumor tissue. Several weeks after tumor inoculation, the mice were randomly allocated to control and treatment groups. The administration of anticancer agents was started when tumor volumes reached approximately 0.2 to 0.3 cm^3. To evaluate the antitumor activity of the test agents, tumor volume and body weight were measured twice a week. Tumor volumes (V) were estimated from the equation $V = ab^2/2$, where a and b are tumor length and width, respectively. The percentage of tumor growth inhibition (TGI%) was calculated as described previously(10).

Treatment of animals

Bevacizumab was administered intraperitoneally (ip) once a week for 3 weeks.

Histological classification by hematoxylin-eosin staining

Xenograft tumor tissues were collected, formalin-fixed, and paraffin-embedded. Slide specimens were prepared by sectioning the tissue and staining with hematoxylin-eosin stain. The histological classification was determined according to the *Japanese Classification of Gastric Carcinoma* (13th Edition, June 1999, Japanese Gastric Cancer Association).

IHC, and gene amplification of HER2

HER2 protein expression and HER2 gene amplification in tumors were examined by IHC using HercepTest® and FISH using Pathvysion® respectively as described previously(11).

Measurement of microvessel density in tumor tissues

Microvessel density (MVD) in tumor tissue was evaluated immunohistochemically using a monoclonal anti-mouse CD31 antibody (rat anti-mouse CD31 monoclonal antibody, clone MEC 13.3; BD Biosciences, NJ, USA). Tumor samples were collected 24 h, 96 h or 21 days after bevacizumab administration.

Immunohistochemical staining was performed as described previously(12). MVD (%) was calculated from the ratio of the CD31-positive staining area to the total observation area in the viable region. Three to six fields per section (0.4856 mm^2 each) were randomly analyzed, excluding necrotic areas. Positive staining areas were calculated using imaging analysis software (Win Roof; Mitani Corporation, Fukui, Japan).

Quantification of human or mouse VEGF and other angiogenic proteins in tumor tissues and mouse serum

Blood and tumor samples were taken when tumors had reached a volume of approximately 0.3 to 0.5 cm^3. Blood serum was immediately retrieved and tumors were immediately frozen in liquid nitrogen and stored at -80°C. Tumor samples were homogenized in PBS containing 0.05% Tween 20 and centrifuged (4°C, 10,000 × g, 20 min.). The resultant supernatant was used for the assays. Human VEGF, placental growth factor (P*l*GF), interleukin-8 (IL-8) and basic fibroblast growth factor (bFGF) were quantified using Quantikine® ELISA kits (R&D Systems, Minneapolis, MN, USA). Human VEGF165b was quantified using the DuoSet® ELISA Development System (R&D Systems). Mouse VEGF was quantified using a Mouse VEGF Assay Kit (Immuno-Biochemical Laboratories). Total protein levels in the samples were quantified using a DC protein assay kit (BioRad Laboratories, Hercules, CA, USA).

VEGF genotyping

DNA was extracted from the cultured cells. VEGF polymorphisms (-2578, -1154, -634 and 936 on VEGF genomic DNA) were genotyped with two fluorescent hybridization probes using LightCycler™ software. Briefly, the analysis is based on PCR amplification of the region surrounding the polymorphism sites, followed by slowly melting off the polymorphism-covering hybridized probe while continuously detecting the fluorescence. Melting off the hybridized probe from its target sequence causes the fluorescent signal to disappear, and this allows a narrow and reproducible estimation of the melting-point temperature. Subtle differences in melting points between a completely matched hybrid duplex and a duplex with a single nucleotide mismatch are detectable using LightCycler.

HUVEC pVEGFR2 assay

Tumor samples were homogenized in HuMedia-EB2 (KURABO) and centrifuged (4°C, 10,000 × g, 20 min). The supernatant was retrieved and used as the assay medium. VEGF concentration in the samples was measured as described above. HUVEC was seeded at a density of 3×10^5 cells/well into 6-well plates in HuMedia-EG2 and incubated for one day at 37°C under 5% CO_2. After that, the medium was changed to a serum-starved medium (HuMedia-EB2 containing 0.5 % FBS). After overnight incubation, the medium was changed to an assay medium which had been pre-treated with bevacizumab or human IgG at 37°C for 30 min. After 5-min incubation at 37°C under 5% CO_2, the plates were immediately placed on ice and the cells washed with PBS. The cells were then lysed with ice-cold lysis buffer #9 (R&D systems). Lysates were centrifuged at 14,000 × g for 20 min at 4°C. The pVEGFR2 was detected using western blot method and DuoSet IC® ELISA Development System (R&D Systems). For western blot, antibodies against VEGFR2 and pVEGFR2 (Tyr1175) (#2479 and #2478 respectively, Cell Signaling Tschnology, Beverly, MA, USA) were used as the first antibodies. The proteins were detected by horseradish peroxidase-conjugated secondary antibodies (Santa Cruz Biotechnology, Santa Cruz, CA, USA) and visualized using ECL plus (GE Healthcare Life Science, Buckinghamshire, UK).

Statistical analysis

The statistical analysis was carried out using a SAS preclinical package (SAS Institute, Inc., Tokyo, Japan).

Results

Sensitivity to bevacizumab in human gastric cancer xenograft models.

The author examined the antitumor activity of bevacizumab in the MKN-45 human gastric xenograft model. Bevacizumab showed significant antitumor activity against MKN-45 tumors at doses ranging from 1.25 mg/kg to 20 mg/kg (Fig. 1A). On day 22 (21 days after starting treatment), tumor growth inhibition rates (TGI%) were 62%, 76%, and 79% at doses of 1.25, 5, and 20 mg/kg, respectively. The maximum effective dose was 5 mg/kg. Then the author investigated 5 mg/kg of bevacizumab antitumor activity against human gastric cancer xenografts of various

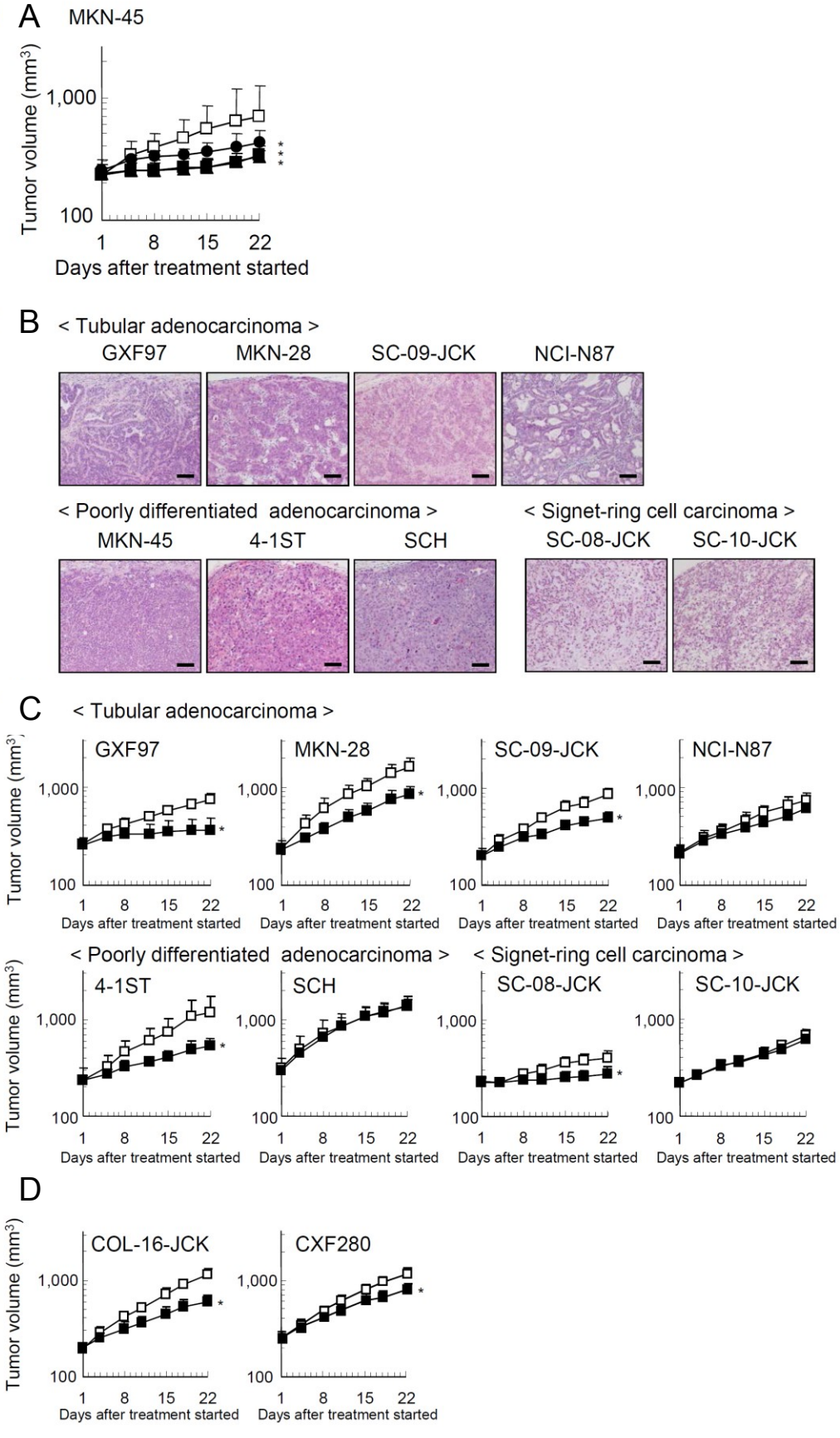
A
MKN-45
Tumor volume (mm3)
1,000
100
1
8
15
22
Days after treatment started
B
< Tubular adenocarcinoma >
GXF97
MKN-28
SC-09-JCK
NCI-N87
< Poorly differentiated adenocarcinoma >
MKN-45
4-1ST
SCH
< Signet-ring cell carcinoma >
SC-08-JCK
SC-10-JCK
C
< Tubular adenocarcinoma >
GXF97
MKN-28
SC-09-JCK
NCI-N87
< Poorly differentiated adenocarcinoma >
4-1ST
SCH
< Signet-ring cell carcinoma >
SC-08-JCK
SC-10-JCK
D
COL-16-JCK
CXF280

◂**Figure 1. Antitumor activity of bevacizumab as a single agent in human gastric cancer xenograft models.** A, Mice bearing MKN-45 tumors were randomly divided into groups and HuIgG or bevacizumab (1.25, 5, 20 mg/kg) was administered intraperitoneally, once a week for 3 weeks. □: human IgG 20 mg/kg, ●: bevacizumab1.25 mg/kg, ■: bevacizumab 5 mg/kg, ▲: bevacizumab 20 mg/kg. B, Differentiation degree of each tumor was determined by hematoxylin-eosin staining. C, Antitumor activity of bevacizumab (5 mg/kg) was evaluated in various types of gastric cancer xenograft models: GXF97, MKN-28, NCI-N87, 4-1ST, SCH, SC-08-JCK, SC-09-JCK, SC-10-JCK. □: human IgG 20 mg/kg, ■: bevacizumab 5 mg/kg. D, Antitumor activity of bevacizumab (5 mg/kg) was evaluated in two colorectal cancer xenograft models, COL-16-JCK and CXF280. □: human IgG 20 mg/kg, ■: bevacizumab 5 mg/kg. Data points are mean + SD of tumor volume (mm^3). Statistically significant differences were shown as *: $P < 0.05$ vs. control group by Wilcoxon test. (n = 5 - 7/group)

degrees of differentiation as shown in Figure 1B. Bevacizumab showed significant antitumor activity in GXF97, MKN-28, 4-1ST, SC-08-JCK and SC-09-JCK, with TGI% values on day 22 of 78%, 56%, 68%, 75%, and 55%, respectively. Meanwhile, bevacizumab did not show significant antitumor activity in NCI-N87, SCH and SC-10-JCK, with TGI% values on day 22 of 21%, 3% and 11%, respectively (Fig. 1C). The author also tested the antitumor activity of bevacizumab against two colorectal tumors, COL-16-JCK and CXF280, as the control because bevacizumab is approved for clinical use in colorectal cancers, and the author found the TGI% to be 59% and 40%, respectively (Fig. 1D). The degree of antitumor activity of bevacizumab in the gastric cancer models was comparable to that in the colorectal cancer models. No weight loss (>20%) was observed for any of the doses tested in either model (data not shown).

Histological types of tumor tissues.

The degree of differentiation among the tumors was examined by using hematoxylin-eosin staining (Fig. 1B). GXF97, MKN-28, SC-09-JCK, and NCI-N87 were categorized as tubular adenocarcinoma, known as a well differentiated type. MKN-45, 4-1ST and SCH were categorized as poorly-differentiated adenocarcinoma and all of them were solid-type. SC-08-JCK and SC-10-JCK were categorized as signet-ring cell carcinoma. There was no correlation between the efficacy of bevacizumab and the degree of differentiation of the tumors, and bevacizumab showed antitumor activity against every differentiation type of tumor the author tested as shown in figure 1.

HER2 status of tumor tissues.

HER2 status of tumor tissues which the author examined bevasizumab sensitivity was shown in Table 1. There

Table. 1 HER2 expression in gastrointestinal cancer cell lines

	HER2 status	
Cell line	IHC	FISH
NCI-N87	2+	8.4
4-1ST	3+	5.3
SCH	2+	2.0
SC-09-JCK	0	1.2
SC-10-JCK	0	1.2
MKN-45	0	1.1
MKN-28	0	1.0
SC-08-JCK	0	1.0
GXF97	0	0.9

HER2 protein expression and HER2 gene amplification in tumors were examined by IHC using HercepTest™ and FISH using Pathvysion® respectively.

also no relevancy between the efficacy of bevacizumab and the HER2 status, as shown by the observation that the HER2-positive tumor 4-1ST was sensitive to bevacizumab but HER2-positive tumors NCI-N87, and SCH were insensitive to bevacizumab.

Expression of human VEGF.

There is a possibility that the level of expression of human VEGF in tumor tissue is involved in the efficacy of bevacizumab, because bevacizumab is an anti-human VEGF monoclonal antibody. The author quantified the expression level of human VEGF and VEGF165b in several gastric and colorectal tumor tissues (Fig.2A). The author found that human VEGF was hardly expressed in bevacizumab-insensitive tumors SCH and NCI-N87 but, in the insensitive tumor SC-10-JCK, human VEGF was expressed. VEGF165b is reported to be an anti-angiogenic factor(13) and thus, could inhibit bevacizumab activity. However, it was not expressed to any extent in the tumors the author investigated. Therefore, the effect of VEGF165b was considered to be negligible in the examined tumor models. Angiogenic human VEGF was more significantly expressed in bevacizumab-sensitive tumors compared with bevacizumab-insensitive tumors (Fig. 2B, $p=0.0485$). The correlation coefficient (r^2) between TGI% and the log concentration of human VEGF per mg protein in tumor tissue was 0.5312. The author also quantified the expression level of mouse VEGF in the tumors, but the correlation coefficient between TGI% and mouse tumor

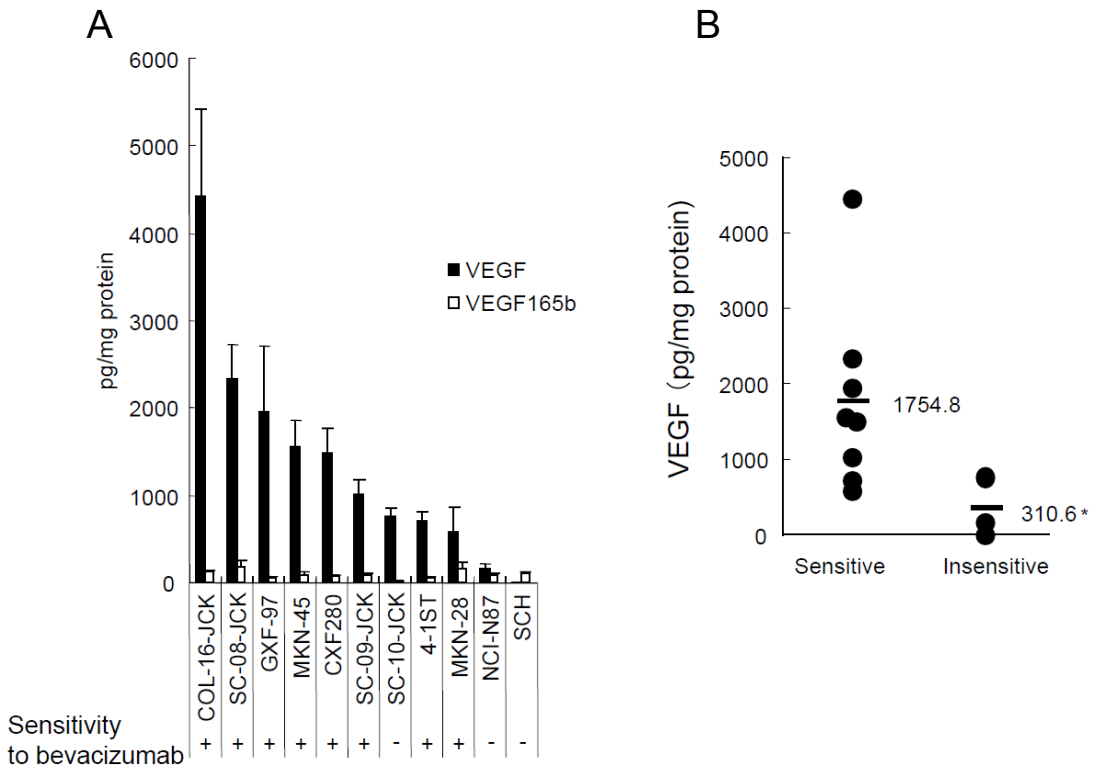

Figure 2. Expression of human VEGF proteins in tumor tissues of gastric and colorectal cancer xenograft models. A, The level of human VEGF (black bar) and VEGF165b (open bar) protein in bevacizumab-sensitive and bevacizumab-insensitive tumor tissues was quantified by ELISA (n = 4/group). B, The quantity of VEGF was compared between the two groups. The averages were shown as bars and numeric values. *: $P < 0.05$ vs. sensitive group by Wilcoxon test.

VEGF was not observed (r^2=0.0098). The author also quantified human and mouse VEGF in serum, but the level of expression was below the limit of detection (<31.25 pg/mL).

Polymorphisms of VEGF.

In clinical breast cancer patients, the efficacy of bevacizumab is reported to correlate to the status of VEGF polymorphism, the -2578A allele. Hence, the author tried to examine the correlation of VEGF polymorphisms and efficacy, but statistical analysis could not be done because the A/A allele was only observed in the MKN-45 tumor. The level of VEGF in MKN-45 was not high, even though the -2578 allele exists in the VEGF promoter (Table 2).

Bioactivity of VEGF in SC-10-JCK.

The author examined whether the VEGF expressed in SC-10-JCK was bioactive. Tumor tissue lysates of two bevacizumab-sensitive models, GXF97 (high VEGF expression) and 4-1ST (VEGF level equivalent to SC-10-JCK),

Table. 2 VEGF polymorphisms in gastrointestinal cancer cell lines

	Genotype			
	Polymorphic site			
Cell line	-2578	-1154	-634	936
MKN-45	A/A	A/A	G/G	T/T
4-1ST	C/A	G/A	G/G	C/C
GXF97	C/A	G/A	C/G	C/C
MKN-28	C/C	G/A	C/C	C/C
SC-09-JCK	C/C	G/A	G/G	C/C
SC-08-JCK	C/C	G/A	C/C	T/T
NCI-N87	C/A	G/A	G/G	C/C
SC-10-JCK	C/A	G/A	G/G	C/T
SCH	C/C	G/A	C/G	C/C

VEGF polymorphisms (-2578, -1154, -634 and 936 on VEGF genomic DNA) were examined by using LightCycler™.

and one bevacizumab-insensitive model, SC-10-JCK, with or without bevacizumab, were added to HUVEC, and the phosphorylation level of VEGFR2 in HUVEC was tested by western blot (Fig. 3A). VEGF levels of the lysates of GXF97, 4-1ST and SC-10-JCK were 24.7, 8.0 and 4.7 ng/mL respectively. VEGF derived from bevacizumab-sensitive tumors (GXF97 and 4-1ST) phosphorylated VEGFR2. The VEGF diluted to 4.7 ng/mL (a concentration equal to SC-10-JCK-derived VEGF) still phosphorylated VEGFR2. All phosphorylation of VEGFR2 by VEGF from bevacizumab-sensitive tumors was reduced by bevacizumab. On the other hand, SC-10-JCK-derived VEGF did not phosphorylate VEGFR2 both in western blot and ELISA (Fig. 3B). These results suggest that the VEGF in SC-10-JCK was not bioactive.

Anti-angiogenic activity of bevacizumab.

The author also examined changes in MVD in bevacizumab-sensitive and -insensitive tumors after bevacizumab treatment using CD31-staining (Fig. 4A). In the bevacizumab-sensitive tumor models, GXF97 and SC-08-JCK, a significant decrease of MVD was observed at 96 h after single-treatment of bevacizumab and at 21 days after the 3-week treatment (Figs. 4B and C). On the other hand, MVD had not changed at any time point after

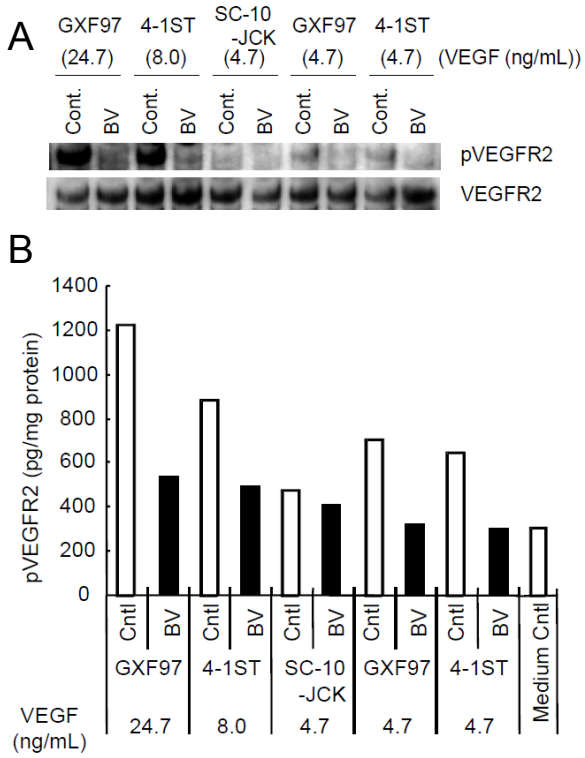

Figure 3. Differences in the bioactivity of human VEGF in bevacizumab-sensitive tumors and bevacizumab-insensitive tumor SC-10-JCK. The bioactivity of VEGF in tumors was determined by the VEGFR2 phosphorylation of HUVEC treated with tumor tissue homogenate administered with bevacizumab or human IgG using western blot (A) and ELISA (B). Each VEGF level in the homogenate was shown in figure 3A and B.z

bevacizumab treatment in the bevacizumab-insensitive tumor models, SC-10-JCK and SCH (Fig. 4D and E). The decrease of MVD was corresponded to the antitumor activity of bevacizumab, but was detected earlier than the decrease of tumor volume (Fig. 4F-I). The author also examined the change in MVD in the GXF97 tumor samples at the lower dose (1 mg/kg), at which bevacizumab had not shown efficacy on day 22 (Fig. 4J). In correlation with the efficacy of bevacizumab, MVD had not changed in GXF97 tumor tissue 96 h after bevacizumab treatment at the low dose. Therefore the author considered that bevacizumab showed antitumor activity by inhibiting tumor angiogenesis.

Other angiogenic factors as the bevacizumab resistance factor in tumor tissues.

The MVD results after bevacizumab treatment suggested that angiogenic factors other than VEGF are involved in angiogenesis in bevacizumab-insensitive tumors. Therefore, the author investigated the expression levels of angiogenic factors bFGF, IL-8 and P*l*GF in tumor tissues, all of which are reported to be angiogenic factors for tumors (Table 3). Each one as a single factor did not significantly correlate with bevacizumab efficacy (Fig. 5A). However, the VEGF/bFGF ratio in bevacizumab-insensitive tumors was significantly lower than that in bevacizumab-sensitive tumors (1.30% vs. 12.4%, Fig. 5B, p=0.0242).

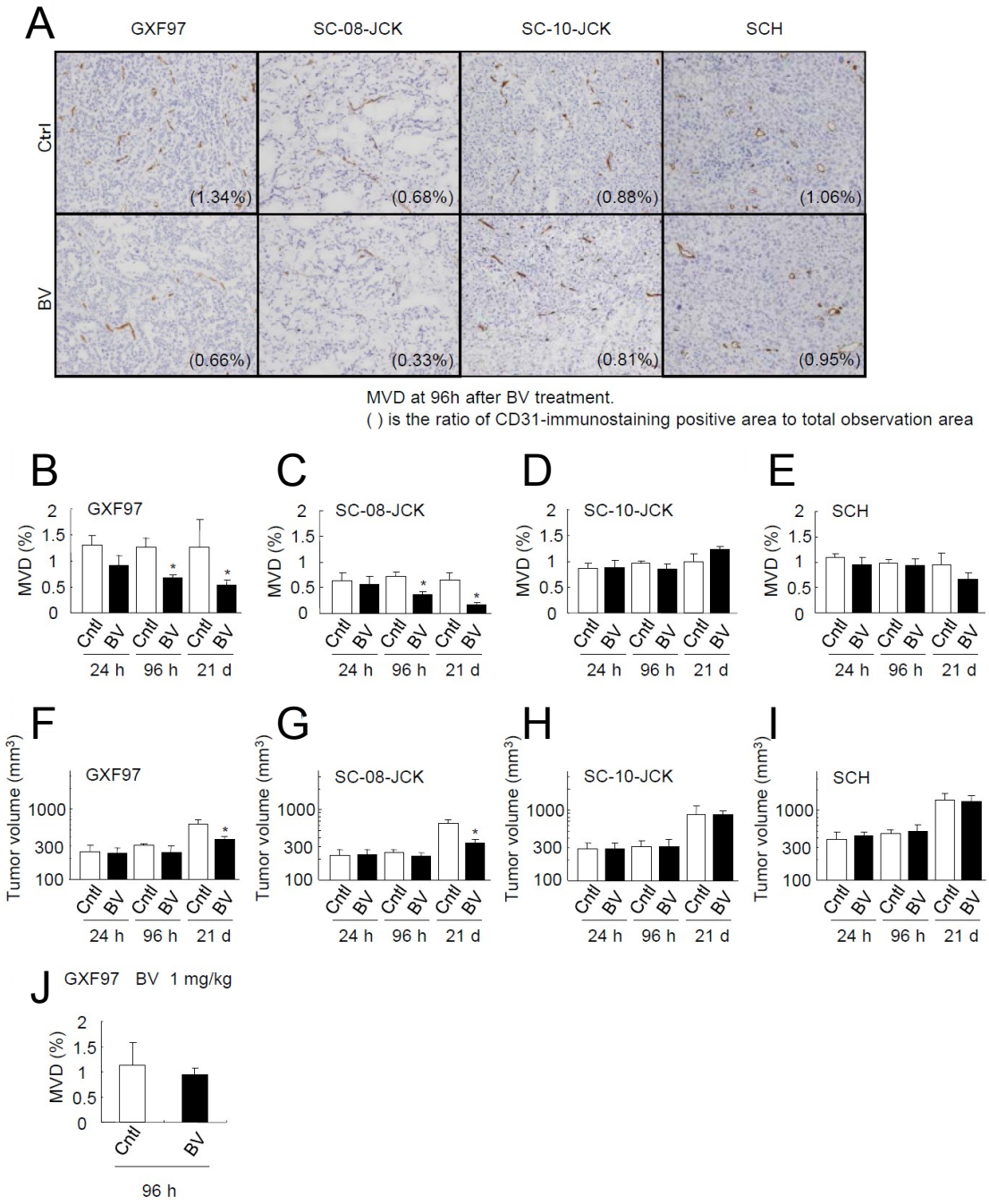

Figure 4. Change in MVD after bevacizumab treatment. A, CD31 immunostaining in tumor tissue at 96 h after treated with HuIgG (Ctrl) and bevacizumab (BV) in GXF97, SC-08-JCK, SC-10-JCK and SCH models. B-E, The MVD in tumor tissue was determined by calculating the ratio of CD31-immunostaining positive area to the total observation area at 24 h, 96 h and 21 days (21 d) after bevacizumab treatment (n = 3-6/group). F-I, Tumor volumes were measured on the day of MVD evaluation. (J) MVD after treatment of bevacizumab at 1 mg/kg was evaluated in GXF97 (n = 4). *: $P < 0.05$ vs. control group by Wilcoxon test.

Discussion

Gastric cancer has long been classified according to degree of differentiation and histopathologic type.

Table. 3 Expression of angiogenic factors in gastrointestinal cancer cell lines

Cell line	Sensitivity to bevacizumab	VEGF	PlGF	IL-8	bFGF
COL-16-JCK	+	4430 ± 991	<15.6	360 ± 171	268 ± 75.3
SC-08-JCK	+	2330 ±402	<15.6	<31.3	145 ± 25.9
GXF97	+	1950 ± 753	<15.6	362 ± 134	107 ± 63.6
MKN-45	+	1560 ± 310	<15.6	65.9 ± 9.38	183 ± 43.0
CXF280	+	1480 ± 290	<15.6	<31.3	77.6 ± 16.5
SC-09-JCK	+	1020 ± 163	<15.6	165 ± 60.3	151 ± 13.3
4-1ST	+	706 ± 106	<15.6	<31.3	87.7 ± 5.47
MKN-28	+	577 ± 285	16.4 ± 8.22	<31.3	200 ± 27.8
SC-10-JCK	-	760 ± 80.2	<15.6	198 ± 96.5	231 ± 105
NCI-N87	-	171 ± 52.5	<15.6	34.4 ± 10.8	1090 ± 328
SCH	-	<31.3	1210 ± 205	<31.3	38.4 ± 18.6

Mean ± SD (pg/mg protein)

The expression of human VEGF, PlGF, IL-8 and bFGF in tumor tissues were examined by ELISA.

Recently, HER2 expression has been included as a classification method in response to the positive results of a phase III study showing that addition of trastuzumab to a combination of capecitabine (or 5FU) and CDDP in patients with HER2-overexpressing gastric cancers prolonged overall survival(14). In light of this, the author attempted to clarify the types of gastric cancers for which bevacizumab would be effective. The author used human cancer xenograft models developed by inoculating human gastric cancer cells into T-cell–deficient mice to investigate the efficacy of bevacizumab. Human VEGF secreted from human cancer cells is known to have an effect on mouse endothelial cells and results in angiogenesis in xenograft tumor tissues. In MKN-45, bevacizumab showed significant antitumor activity, although the dose dependency was not strong. A low dose of bevacizumab (1.25 mg/kg) was sufficient to produce antitumor activity. The author examined the antitumor activity of bevacizumab in 9 human gastric cancer xenograft models of various degrees of differentiation, tumor types, and HER2 expression. However, the sensitivity of the gastric cancer models to bevacizumab was found to be unrelated to the histological type or the HER2 status of the tumors. The antitumor activity of bevacizumab in the gastric cancer xenograft models was similar to that observed in colorectal cancer(15), for which bevacizumab has shown survival and clinical benefit.

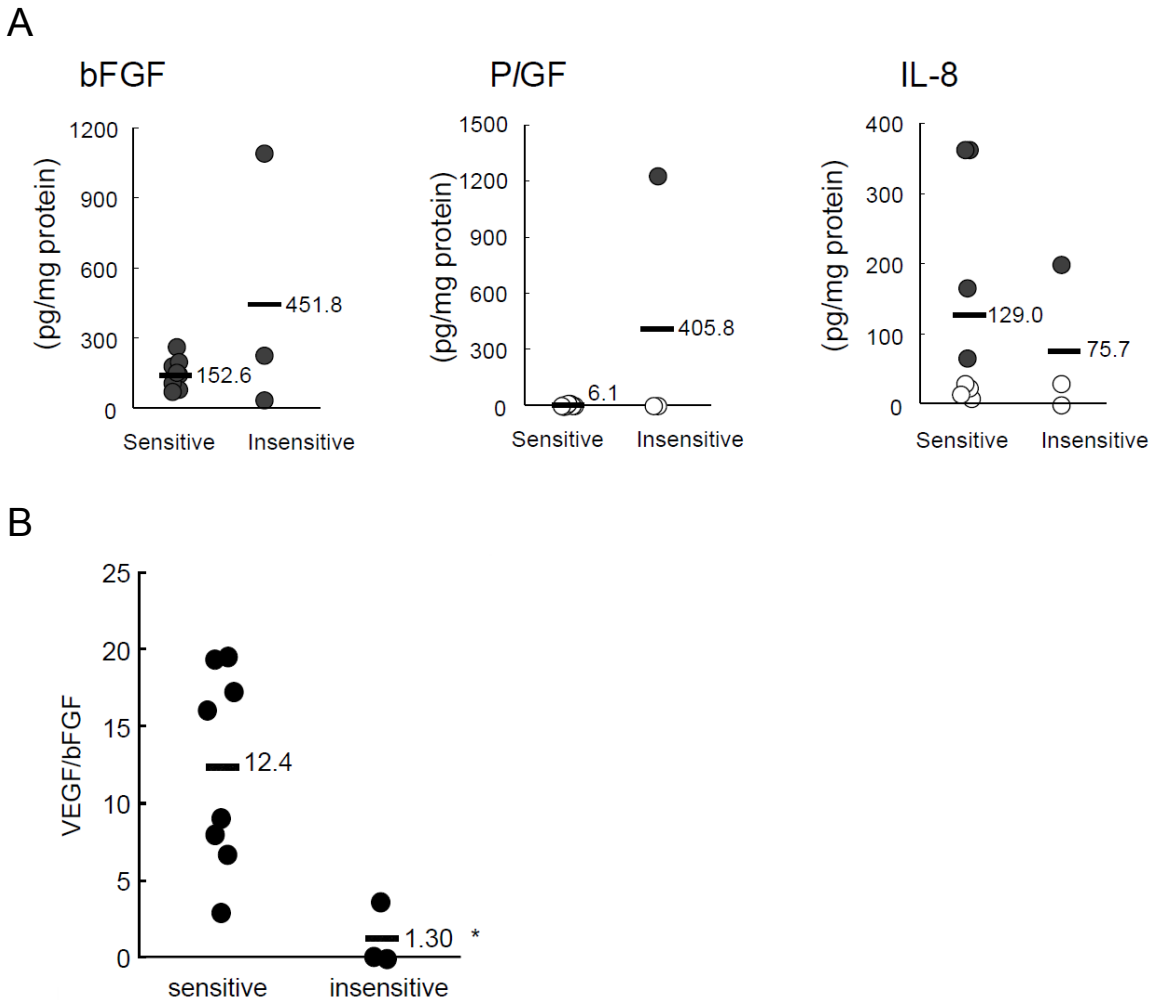

Figure 5. Expression of human bFGF protein in tumor tissues of gastric and colorectal cancer xenograft models. A, The level of human bFGF, PlGF, and IL-8 proteins in tumor tissues sensitive (9 models) or insensitive (3 models) to bevacizumab was quantified by ELISA ($n = 4$). Open circle means less than the detection limit of ELISAs. The averages were shown as bars and numeric values. B, The ratio of VEGF to bFGF was compared between the two groups. *: $P < 0.05$ vs. sensitive group by Wilcoxon test.

Next, the author examined other biomarker candidates of bevacizumab efficacy using sensitive and insensitive gastric tumor models. Because VEGF is the molecular target of bevacizumab, the tumor level of VEGF is thought to influence the sensitivity to bevacizumab. Tumor VEGF levels were significantly lower in the xenograft models insensitive to bevacizumab than in the sensitive models; however, mouse tumor VEGF showed no differences between sensitive and insensitive tumors. Human and mouse blood VEGF were lower than the detection limit in these models, and thus they were of little concern. In the SC-10-JCK model, in spite of VEGF expression, bevacizumab did not exhibit efficacy. To clarify the role of VEGF as a biomarker candidate of bevacizumab sensitivity, the author investigated subtypes of VEGF in more detail. Various isoforms of VEGF are known such as

the reportedly anti-angiogenic VEGF, VEGF165b(13). VEGF165b binds to bevacizumab(16) . In this study, VEGF165b exhibited 100% cross-reactivity to VEGF ELISA (data not shown) so we thought that VEGF165b expression would be high in SC-10-JCK. However, the level of VEGF165b was low in the SC-10-JCK model. Additionally, VEGF165b expression was low in all of the tumor tissues the author examined. In the gastrointestinal models tested, VEGF165b is not a concern. Because bevacizumab binds to all angiogenic isoforms of VEGF, such as VEGF121, VEGF165, and VEGF189(17), identification of these isoforms is not necessary. In clinical breast cancer treatment, polymorphisms of VEGF have been found to correlate with the efficacy of the bevacizumab and paclitaxel combination(18). The survival time of patients with the 2578 AA allele or 1154 A allele of VEGF was longer than that of others. However, VEGF 2578 and 1154 of SC-10-JCK were CA and GA, respectively, and the type of allele was the same as with the sensitive tumors 4-1ST and GXF97. The VEGF allele did not distinguish sensitivity to bevacizumab in these models. Next, to clarify whether the VEGF of SC-10-JCK had biological activity, the effect of a tumor homogenate of SC-10-JCK on the induction of VEGFR phosphorylation on HUVEC was examined. The tumor homogenate of SC-10-JCK did not have phosphorylation activity in contrast to that of 4-1ST or GXF97. Furthermore, the MVD in the SC-10-JCK xenograft model treated with bevacizumab was not reduced, indicating that the VEGF of SC-10-JCK did not show angiogenic activity. These results suggest the possibility of existence of non-active VEGF in tumors.

The author attempted to clarify both the biomarker for and the mechanisms of bevacizumab. The inhibition of MVD in tumor tissue is reported to be a major mechanism of bevacizumab efficacy, and so the author compared MVD inhibition with efficacy in bevacizumab-sensitive and -insensitive tumor models. The existence of MVD inhibition corresponded with antitumor efficacy. In the present study, the MVD inhibition prior to antitumor efficacy was shown, and MVD inhibition was found to be a mechanism of bevacizumab efficacy. This results indicated that other angiogenic factors except for VEGF are involved in biomarkers for bevacizumab resistance. The author examined tumor bFGF, IL-8 and P*l*GF, all of which are reported to be angiogenic factors for tumors(19-21). When the author compared the ratio of bFGF to VEGF with bevacizumab efficacy to clarify the extent of the role of VEGF in angiogenesis, the ratio of VEGF to bFGF in bevacizumab-insensitive tumors was clearly lower than that in bevacizumab-sensitive tumors. It is thought that an intimate cross-talk of bFGF and

VEGF family is exist during angiogenesis and bFGF increases neuroplin-1, a co-receptor for VEGF, expression in human vascular smooth muscle cell that in turn enhance the effect of VEGF on cell migration and promote neovascularizaion(22). In the present study, the author did not examine the bioactivity of bFGF in the bevacizumab insensitive tumors. It is necessary to investigate the effect of bFGF on VEGF-dependent angiogenesis and on its inhibition by bevacizumab in the future. Neither VEGF/PlGF nor VEGF/IL-8 showed significant results (data not shown). P*l*GF has been reported to form a homodimer or heterodimer with VEGF and bind the resulting VEGFR in angiogenesis(23). However, the cell lines the author examined did not express P*l*GF, except for SCH, so the author examined the relationship between P*l*GF and bevacizumab in SCH *in vitro*. HUVEC growth induction with a P*l*GF/VEGF heterodimer was inhibited by bevacizumab (data not shown), suggesting that the number of heterodimers of P*l*GF and VEGF would also be a biomarker for bevacizumab sensitivity. Further examination is needed. P*l*GF homodimers did not show HUVEC growth induction, and the author did not examine the effect of bevacizumab on HUVEC growth.

Some reports have indicated that bevacizumab exhibits direct cell growth inhibition against tumor cells(24, 25). However, in the gastric cancer cell lines the author examined, no direct antitumor activity was observed in spite of the growth inhibition shown by bevacizumab in the xenograft model of the same cancer cell line (data not shown).

In the present study of gastric cancer treatment, the author found that levels of VEGF and the VEGF/bFGF ratio have a close correlation with sensitivity to bevacizumab in the tested cell lines. There was no correlation between sensitivity to bevacizumab and the histological classification according to the degree of differentiation or HER2 status of the tumor cells. Clinical evidence is expected.

References

1. Kuroi K, Toi M. Circulating angiogenesis regulators in cancer patients. Int J Biol Markers. 2001;16:5-26.

2. Poon RT, Fan ST, Wong J. Clinical implications of circulating angiogenic factors in cancer patients. J Clin Oncol. 2001;19:1207-25.

3. Jubb AM, Harris AL. Biomarkers to predict the clinical efficacy of bevacizumab in cancer. Lancet Oncol. 2010;11:1172-83.

4. Jemal A, Bray F, Center MM, Ferlay J, Ward E, Forman D. Global cancer statistics. CA Cancer J Clin. 2011;61:69-90.

5. Kamangar F, Dores GM, Anderson WF. Patterns of cancer incidence, mortality, and prevalence across five continents: defining priorities to reduce cancer disparities in different geographic regions of the world. J Clin Oncol. 2006;24:2137-50.

6. Ferrara N, Davis-Smyth T. The biology of vascular endothelial growth factor. Endocr Rev. 1997;18:4-25.

7. von Marschall Z, Cramer T, Hocker M, Burde R, Plath T, Schirner M, et al. De novo expression of vascular endothelial growth factor in human pancreatic cancer: evidence for an autocrine mitogenic loop. Gastroenterology. 2000;119:1358-72.

8. Kido S, Kitadai Y, Hattori N, Haruma K, Kido T, Ohta M, et al. Interleukin 8 and vascular endothelial growth factor -- prognostic factors in human gastric carcinomas? Eur J Cancer. 2001;37:1482-7.

9. Maeda K, Kang SM, Onoda N, Ogawa M, Sawada T, Nakata B, et al. Expression of p53 and vascular endothelial growth factor associated with tumor angiogenesis and prognosis in gastric cancer. Oncology. 1998;55:594-9.

10. Fujimoto-Ouchi K, Sekiguchi F, Tanaka Y. Antitumor activity of combinations of anti-HER-2 antibody trastuzumab and oral fluoropyrimidines capecitabine/5'-dFUrd in human breast cancer models. Cancer chemotherapy and pharmacology. 2002;49:211-6.

11. Fujimoto-Ouchi K, Sekiguchi F, Yasuno H, Moriya Y, Mori K, Tanaka Y. Antitumor activity of trastuzumab in combination with chemotherapy in human gastric cancer xenograft models. Cancer chemotherapy

and pharmacology. 2007;59:795-805.

12. Yanagisawa M, Yorozu K, Kurasawa M, Nakano K, Furugaki K, Yamashita Y, et al. Bevacizumab improves the delivery and efficacy of paclitaxel. Anticancer Drugs. 2010;21:687-94.

13. Woolard J, Wang WY, Bevan HS, Qiu Y, Morbidelli L, Pritchard-Jones RO, et al. VEGF165b, an inhibitory vascular endothelial growth factor splice variant: mechanism of action, *in vivo* effect on angiogenesis and endogenous protein expression. Cancer Res. 2004;64:7822-35.

14. Bang YJ, Van Cutsem E, Feyereislova A, Chung HC, Shen L, Sawaki A, et al. Trastuzumab in combination with chemotherapy versus chemotherapy alone for treatment of HER2-positive advanced gastric or gastro-oesophageal junction cancer (ToGA): a phase 3, open-label, randomised controlled trial. Lancet. 2010;376:687-97.

15. Yanagisawa M, Fujimoto-Ouchi K, Yorozu K, Yamashita Y, Mori K. Antitumor activity of bevacizumab in combination with capecitabine and oxaliplatin in human colorectal cancer xenograft models. Oncol Rep. 2009;22:241-7.

16. Varey AH, Rennel ES, Qiu Y, Bevan HS, Perrin RM, Raffy S, et al. VEGF 165 b, an antiangiogenic VEGF-A isoform, binds and inhibits bevacizumab treatment in experimental colorectal carcinoma: balance of pro- and antiangiogenic VEGF-A isoforms has implications for therapy. Br J Cancer. 2008;98:1366-79.

17. Kim KJ, Li B, Houck K, Winer J, Ferrara N. The vascular endothelial growth factor proteins: identification of biologically relevant regions by neutralizing monoclonal antibodies. Growth Factors. 1992;7:53-64.

18. Schneider BP, Wang M, Radovich M, Sledge GW, Badve S, Thor A, et al. Association of vascular endothelial growth factor and vascular endothelial growth factor receptor-2 genetic polymorphisms with outcome in a trial of paclitaxel compared with paclitaxel plus bevacizumab in advanced breast cancer: ECOG 2100. J Clin Oncol. 2008;26:4672-8.

19. Presta M, Dell'Era P, Mitola S, Moroni E, Ronca R, Rusnati M. Fibroblast growth factor/fibroblast growth factor receptor system in angiogenesis. Cytokine Growth Factor Rev. 2005;16:159-78.

20. Waugh DJ, Wilson C. The interleukin-8 pathway in cancer. Clin Cancer Res. 2008;14:6735-41.

21. De Falco S, Gigante B, Persico MG. Structure and function of placental growth factor. Trends Cardiovasc Med. 2002;12:241-6.

22. Korc M, Friesel RE. The role of fibroblast growth factors in tumor growth. Curr Cancer Drug Targets. 2009;9:639-51.

23. Autiero M, Waltenberger J, Communi D, Kranz A, Moons L, Lambrechts D, et al. Role of PlGF in the intra- and intermolecular cross talk between the VEGF receptors Flt1 and Flk1. Nat Med. 2003;9:936-43.

24. Liang Y, Hyder SM. Proliferation of endothelial and tumor epithelial cells by progestin-induced vascular endothelial growth factor from human breast cancer cells: paracrine and autocrine effects. Endocrinology. 2005;146:3632-41.

25. Kim SJ, Seo JH, Lee YJ, Yoon JH, Choi CW, Kim BS, et al. Autocrine vascular endothelial growth factor/vascular endothelial growth factor receptor-2 growth pathway represents a cyclooxygenase-2-independent target for the cyclooxygenase-2 inhibitor NS-398 in colon cancer cells. Oncology. 2005;68:204-11.

Conclusions

Although cancer treatment has been greatly improved by molecular-targeted agents including antibodies, numerous problems persist. To conquer cancer, it is necessary to develop therapies that are more effective by improving the administered agents and patient selection. In the present study, the author has focused on anticancer antibodies and investigated: I) the treatment after disease progression during trastuzumab therapy; II) new anti-HER2 treatments for gastric cancer; III) formalin fixing conditions for HER2 testing, which determine whether trastuzumab will be a beneficial option for patients; and IV) a predictive marker for bevacizumab, to maximize the potential of antibodies against tumors.

In Chapter I, the author established *in vivo* trastuzumab PD models, in which trastuzumab monotherapy ceases to have antitumor activity during the treatment. The mechanisms of PD with trastuzumab are considered to involve both reversible changes in the gene expression profiles in tumor tissues and a decrease of ADCC activity in the host. These results demonstrate that trastuzumab shows antitumor activity in combination with taxanes or capecitabine, even though it showed no antitumor activity as a monotherapy, thereby suggesting the clinical relevance of treatment with trastuzumab as a combination therapy beyond PD.

In Chapter II, the author first investigated the usefulness of pertuzumab in combination with trastuzumab as a new therapy for HER2 over-expressing gastric cancer. The author demonstrated the significantly enhanced efficacy of pertuzumab combined with trastuzumab through the potentiation of cell-growth inhibition, apoptosis activity, cell-killing activity by ADCC, and anti-angiogenic activity. This study suggests the clinical benefit of combination therapy with pertuzumab and trastuzumab for patients with HER2-positive gastric cancers. The author also examined the combination therapy of pertuzumab and T-DM1 for HER2-positive gastric cancers as a further new potential therapy, and suggested that T-DM1 in combination with pertuzumab shows significant antitumor activity by increasing AKT-signal inhibition and ADCC. These results show the potential of the combination therapy of two different anti-HER2 drugs for HER2-positive gastric cancers.

In Chapter III, the author examined the impact of formalin fixing conditions on HER2 IHC and FISH in xenografted tumor tissues in order to show how it is of critical importance to optimize the sample preparation

conditions for HER2 testing in gastric cancer. The time to and length of fixation of tumor specimens could affect HER2 IHC and FISH scores. The fixative used could affect IHC results.

In Chapter IV, the author attempted to identify predictive markers for efficacy of bevacizumab in gastric cancer patients by using bevacizumab-sensitive and insensitive tumor models. VEGF levels and VEGF/bFGF ratios in tumors were related to the bevacizumab sensitivity of the xenografts tested. Further clinical investigation into useful predictive markers for bevacizumab sensitivity is warranted.

The results of these studies enhance the potential of antibody drugs for antitumor therapy and might lead to maximizing the value of antibody drugs against tumors.

List of publications

Kaori Fujimoto-Ouchi, Fumiko Sekiguchi, Kaname Yamamoto, Masatoshi Shirane, Yoriko Yamashita, and Kazushige Mori

Preclinical study of prolonged administration of trastuzumab as combination therapy after disease progression during trastuzumab monotherapy

Cancer Chemotherapy Pharmacology 66(2), 69-76 (2009)

Yoriko Yamashita-Kashima, Shigeyuki Iijima, Keigo Yorozu, Koh Furugaki, Mitsue Kurasawa, Masateru Ohta, and Kaori Fujimoto-Ouchi

Pertuzumab in combination with trastuzumab shows significantly enhanced antitumor activity in HER2-positive human gastric cancer xenograft models

Clinical Cancer Research 17(15), 5060-5070 (2011)

Yoriko Yamashita-Kashima, Kaori Fujimoto-Ouchi, Keigo Yorozu, Mitsue Kurasawa, Mieko Yanagisawa, Hideyuki Yasuno and Kazushige Mori

Biomarkers for antitumor activity of bevacizumab in gastric cancer models

BMC Cancer 12:37 (2012)

Yoriko Yamashita-Kashima, Sei Shu, Naoki Harada, and Kaori Fujimoto-Ouchi

Enhanced antitumor activity of trastuzumab emtansine (T-DM1) in combination with pertuzumab in a HER2-positive gastric cancer model

Oncol Reports 3, 1087-1093 (2013)

Yoriko Yamashita-Kashima, Sei Shu, Keigo Yorozu, Kaoru Hashizume, Yoichiro Moriya, Kaori Fujimoto-Ouchi, and Naoki Harada

Importance of formalin fixing conditions for HER2 testing in gastric cancer: immunohistochemical staining and fluorescence *in situ* hybridization

Gastric Cancer in press

Related publications

Mieko Yanagisawa, Kaori Fujimoto-Ouchi, Keigo Yorozu, Yoriko Yamashita, and Kazushige Mori

Antitumor activity of bevacizumab in combination with capecitabine and oxaliplatin in human colorectal cancer xenograft models

Oncol Reports 2, 241-247 (2009)

Mieko Yanagisawa, Keigo Yorozu, Mitsue Kurasawa, Kohnosuke Nakano, Koh Furugaki, Yoriko Yamashita, Kazushige Mori, and Kaori Fujimoto-Ouchi

Bevacizumab improves the delivery and efficacy of paclitaxel

Anticancer Drugs 7, 687-94 (2010)

Toru Kawamoto, Kazunori Ishige, Melanie Thomas, Yoriko Yamashita-Kashima, Sei Shu, Nobuyuki Ishikura, Shunichi Ariizumi, Masakazu Yamamoto, Kunihiko Kurosaki, and Junichi Shoda

Overexpression and Gene Amplification of EGFR, HER2, and HER3 in Biliary Tract Carcinomas, and the Possibility for Therapy with the HER2-Targeting Antibody Pertuzumab

J Gastroenterol in press

Acknowledgements

The author deeply thanks Professor Kazumitsu Ueda (Kyoto University), who provided an opportunity for the author to receive her doctorate. The author also greatly appreciates his helpful support and critical review of the manuscript.

The author greatly appreciates Associate Professor Noriyuki Kioka (Kyoto University) for his valuable advice and review.

The author greatly appreciates Drs. Kaori Fujimoto-Ouchi, Kazushige Mori, Naoki Harada, and Yoichiro Moriya (Chugai Pharmaceutical Co., Ltd.) for critical suggestions and advice regarding all experiments and their support regarding this requirement of the dissertation.

The author also thanks all of her co-workers at Chugai Pharmaceutical Co., Ltd., for their support.

Sep. 2014

Yoriko Yamashita-Kashima